ISSN 2658-3518

LIMNOLOGY & FRESHWATER BIOLOGY

2018, № 2

> abiotic and biotic water components;
> ecosystem-level studies;
> systematics and aquatic ecology;
> paleolimnology and environmental histories;
> laboratory experiments and modeling

Limnology and Freshwater Biology 2018 (2): 98-102 DOI:10.31951/2658-3518-2018-A-2-98

Original Article

ISSN 2658-3518
LIMNOLOGY FRESHWATER BIOLOGY
www.limnolfwbiol.com

Comrapative analysis of inverted sequences of noncoding region in the mitochondrial DNA of the Baikal sponges (Fam. Lubomirskiidae)

Maikova O.O. [1,*], Balakshin D.D.[1,2], Belikov S.I.[1]

[1] *Limnological Institute, Siberian Branch of the Russian Academy of Sciences, Ulan-Batorskaya Str., 3, Irkutsk, 664033, Russia*
[2] *Irkutsk State University, Sukhe-Batora Str., 5, 664011, Russia*

ABSTRACT. In recent years, mitochondrial DNA (mtDNA) has been used to solve many phylogenetic problems at different taxonomic levels. Previously, the nucleotide sequences of the mitochondrial genomes of the Baikal endemic sponge species of the Lubomirskiidae family have been identified. Their phylogenetic links are still being actively studied, and their systematics is considered to be not definitive. In order to study the mechanisms of speciation and evolution of mtDNA, special attention is paid to the investigations of noncoding DNA. We have studied the characteristics of the organization of the intergenic mtDNA regions in the Baikal sponges on the example of the longest region between the tRNATyr and tRNAIle genes of the species *L. baicalensis*, *S. papyracea*, *R. echinata*, and *B. intermedia profundalis*. A comparative analysis of the sequences has shown the presence of secondary structures represented by individual hairpins and complex multilevel structures. Based on a comparative analysis of secondary structures, we have suggested their role as both regulative elements and potential mobile elements. We have determined the continuity of these structures among representatives of different genera of the Lubomirskiidae family. The highest similarity in their distribution and localization was found in phylogenetically related species of the Baikal sponges.

Keywords: sponges, Lake Baikal, mitochondrial DNA, intergenic regions, secondary-structure elements

1. Introduction

The Baikal endemic sponges (the Lubomirskiidae family) are a bouquet of closely related species that diverged from cosmopolitan sponges approximately 10 million years ago (Maikova et al., 2015). To date, 14 species of the Lubomirskiidae family have been described, but so far their systematics is not definitive and requires further research (Efremova, 2001; 2004; Itskovich et al., 2017). In the past few years, sequences of the mitochondrial genome have been used to resolve the phylogenetic relationships of the Baikal sponges at various taxonomic levels.

Previously, the nucleotide sequences of the mitochondrial genomes of the Baikal endemic species *Lubomirskia baicalensis, Swartchewskia papyracea, Rezinkovia echinata*, and *Baikalospongia intermedia profundalis* were identified (Lavrov, 2010; Lavrov et al., 2012). Based on the nucleotide sequences of 14 protein-coding genes, a phylogenetic analysis of the Baikal sponges was performed. The analysis showed that the mitochondrial DNA (mtDNA) of the Baikal sponges evolves at different rates. The nucleotide substitution rate in the protein-coding genes of the species *S. Papyracea* was twice higher relative to other species of the Lubomirskiidae family (Maikova et al., 2015). There were also different nucleotide substitution rates in different regions of the mitochondrial DNA. The accumulation of single substitutions in intergenic regions was four times higher than in protein-coding genes (Maikova et al., 2012). The causes of the different nucleotide substitution rates in different species and different mtDNA regions of the Baikal sponges are still unknown.

The evolution of mitochondrial genome of sponges has been well studied at high taxonomic levels. The presence of several common features characterize mitochondrial genomes in sponges of the Demospongiae class: minimally modified genetic code, the presence of several additional genes, conservatism of transport RNA (tRNA), and many noncoding regions. However, there were also significant genomic changes, mainly, in gene

*Corresponding author.
E-mail address: maikova@lin.irk.ru (O.O. Maikova)

rearrangement, number of tRNA genes and noncoding DNA. The length of mitochondrial DNA in most sponges of the class Demospongiae varied within 16-25 kbp (Wang and Lavrov, 2008; Gazave et al., 2010). The longest mitochondrial genome of Demospongiae was found in the Baikal endemic family Lubomirskiidae dominated by the species *L. Baicalensis*, approximately 30 kbp (Lavrov, 2010). The variability in the length of the mitochondrial DNA in the Baikal sponges is mainly an elongation of noncoding sequences, which comprise from 28.6 to 33.6 % of the total size of genome compared to 2-24 % in cosmopolitan and marine sponges (Wang and Lavrov, 2008). Direct and inverted repeats comprised the intergenic mtDNA regions in the Baikal sponges. For example, *L. Baicalensis* contained approximately 160 secondary structures, hairpins (Lavrov, 2010), *S. papyracea* – 97 such structures, *B. intermedia profundalis* – 96, and *R. Echinata* – 144 (Lavrov et al., 2012). Other Demospongiae representatives also contained such secondary structures, but the nature of their occurrence and distributions, as well as their functions remain unknown (Erpenbeck et al., 2009). Stable secondary structures were found in some sponges of the class Demospongiae, which repeatedly occured in different phylogenetic lines during evolution. For example, *S. domuncula* had approximately 700 direct repeats with a predominant length of 12-15 bp, 100 inverted repeats (the longest repeat was 44 bp) and 100 palindromes. In *Vaceletia* sp., intergenic regions contained inverted repeats of considerable length (up to 339 bp). Such repeats were found in different regions. A + T-pairs comprised more than 90 % in these long repeats. In *Igernella notabilis* (Demospongiae, Keratosa), intergenic regions also contained AT-rich inverted repeats, which can form double and triple secondary elements. However, the mitochondrial DNA of most representatives of the class Demospongiae, which have intergenic regions with a length varying from 340 to 2134 bp, either cannot contain inverted repeats at all, or have short GC-rich hairpins. A comparative analysis of intergenic mtDNA regions in most Demospongiae sponges showed that the introduction and distribution of hairpin elements among sponges is uneven, i.e. some sponge families are more susceptible to their introduction (Keratosa and Myxospongiae), and others – less (Hexactinellida and Homoscleromorpha) (Lukic-Bilela et al., 2008; Erpenbeck et al., 2009; Lavrov, 2010).

Noncoding DNA plays a great role in the functioning of the entire genome. The inverted repeats in the noncoding mitochondrial DNA can contribute to intramolecular recombination and are involved in various regulatory processes, including replication and transcription (Ling et al., 2011; Kolesnikov and Gerasimov, 2012). Unlike the bilaterian animals, most non-bilaterian animals do not have a common control region for regulating replication and transcription of the mitochondrial DNA, and regulatory elements are distributed over intergenic regions (Lavrov and Pett, 2016). Probably, the accumulation of inverted repeats in the future may result in gene rearrangements and other significant structural transformations of the genome.

In order to study the distribution mechanisms of inverted repeats in noncoding mitochondrial DNA of Baikal sponges, we have carried out a comparative analysis of sequences of one of the longest regions located between the $tRNA^{Tyr}$ and $tRNA^{Ile}$ genes in representatives of all four genera of the Lubomirskiidae family. The length of the studied intergenic region varied from 300 bp in *E. fluviatilis* (Spongillidae) to 600 bp in *L. fusifera* (Lubomirskiidae), and these changes were associated with the presence of indels. Previously, based on the nucleotide sequences of this region, we performed a phylogenetic analysis. It showed that some of these indels were species-specific, and the sequences of the intergenic region appeared to be suitable for studying phylogenetic relationships of closely related sponges of the Lubomirskiidae family (Maikova et al., 2012).

2. Materials and methods

For a comparative analysis of noncoding mtDNA regions located between the $tRNA^{Tyr}$ and $tRNA^{Ile}$ genes, we used previously published sequences of the mitochondrial genomes for the species *L. baicalensis, S. papyracea, R. Echinata*, and *B. intermedia profundalis* (Lavrov et al., 2012). The sequences were aligned using the MAFFT v.6.240 and BioEdit programs. Pairwise distances based on indels of the noncoding regions using Jukes-Cantor (Jukes and Cantor, 1969) method, were determined using MEGA 4.0.

Inverted repeats were found using Unipro UGENE software (http://ugene.unipro.ru/index.html). The secondary elements were constructed at 4° C and visualized using Mfold webserver (version 3.2) (Zuker, 2003) and Vienna RNA package (RNAfold, RNAalifold) (Hofacker, 2003).

3. Results and discussion

We have carried out a detailed study of the characteristics of organization and distribution of secondary structures in the Baikal sponges on the example of the mtDNA region between the $tRNA^{Tyr}$ and $tRNA^{Ile}$ of four species of the Baikal sponges, *Lubomirskia baicalensis, Swartchewskia papyracea, Rezinkovia echinata*, and *Baikalospongia intermedia profundalis*, which mitochondrial genomes were published previously (Lavrov, 2010; Lavrov et al., 2012). To name the hairpins, we used their previous classification, in which they are divided into 9 families, H1-H9 (Lavrov, 2010).

Modelling of the potential secondary structure of the nucleotide sequence has shown that all studied species form complex elements: individual hairpins (Fig. 1) and complex multilevel elements (Fig. 2). We have indicated a specific occurrence of some hairpins that form stable clusters. For instance, the structures H3 and H4 are mainly observed together and resemble double hairpin elements (Fig. 2) found by Paquin with co-authors (Paquin et al., 2000) in the mitochondrial DNA of *Allomyces macrogynus* fungi, which were described as mobile elements.

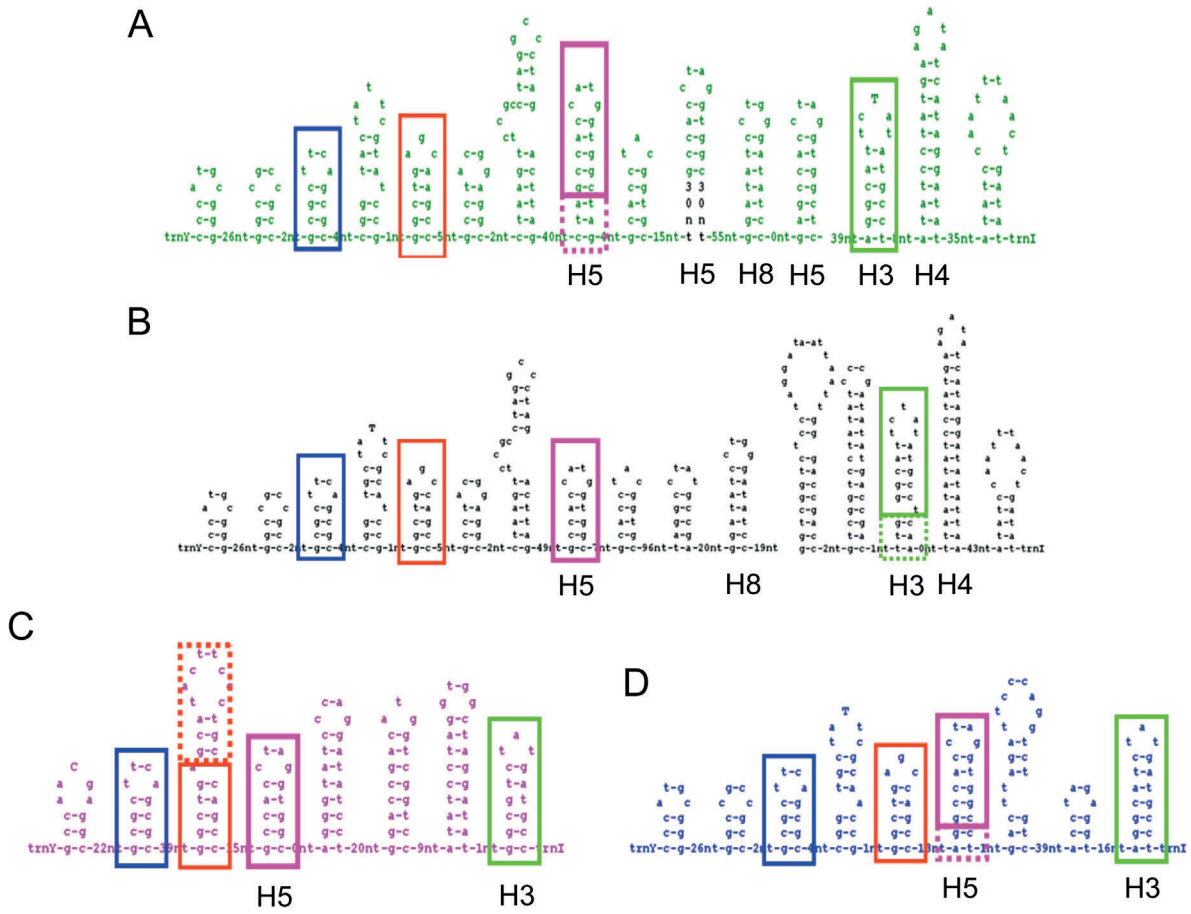

Fig. 1. Potential secondary elements located in the region of the mitochondrial DNA between the $tRNA^{Tyr}$ and $tRNA^{Ile}$ genes: A – *L. baicalensis*, B – *R. echinata*, C – *S. papyracea*, and D – *B. intermedia profundalis*.

In the studied intergenic region, we have found one conservative (marked in blue) and three homologous hairpins (Nos. 1-3, marked in red, pink and green, respectively). Notably, the conservative hairpin and homologous hairpin No.1 have been found for the first time. *L. baicalensis* and *R. echinata* have another common AT-rich H4-element. Homologous hairpins differ in insertion or deletion of complementary base pairs. The sequences of *L. baicalensis* and *R. echinata* have the highest similarity in the number and distribution of hairpins in the region between $tRNA^{Tyr}$ and $tRNA^{Ile}$ genes. At the same time, *R. echinata* and *S. Papyracea* show the highest similarity in the region between $tRNA^{Ile}$ и $tRNA^{Met}$ genes.

Three homologous and one conservative hairpins in all four species have GC-clusters increasing their GC-content. Table 1 shows the GC-content of these hairpins (excluding the nucleotide composition of the loops).

Using the data on the presence or absence of hairpins, we have determined the genetic distances of two intergenic regions between four studied species of the Baikal sponges. We observed minimal differences between *L. baicalensis* and *S. papyracea* (90%). Therefore, the example of two intergenic regions shows the general tendency of the maximum similarity of *L. baicalensis* and *R. echinata* in distribution and localization of secondary elements in the noncoding mitochondrial DNA. This can be explained by the presence of the common ancestor for these two species, which phylogenetic reconstructions confirm based on the nucleotide sequences of 14 protein-coding genes of the mitochondrial DNA (Maikova et al., 2015).

The presence of both, identical hairpins in all sponges of the Lubomirskiidae family and unique hairpins in certain species, may indicate their repeated introduction into the mitochondrial genome of the Baikal sponges during evolution. Interestingly, in the Baikal sponges, like in different Demospongiae representatives, the bulk of secondary elements found in the intergenic mtDNA regions have increased GC-content, which can reach 100 % (Gazave et al., 2010). This can also indicate the continuity of these structures at high taxonomic levels.

The presence of hairpins conservative in the nucleotide sequence and localization among representatives of different genera of closely related Baikal sponges suggests that they can have functional load.

Similar hairpins with GC-clusters were characterized as recombination sites in fungi (Paquin et al., 2000). This assumption is also supported by the fact that homologous hairpins vary significantly in loops, hence, they cannot be involved in various regulatory processes, such as the regulation of transcription. At the same time, the existence of conservative and homologous secondary elements in closely related sponge

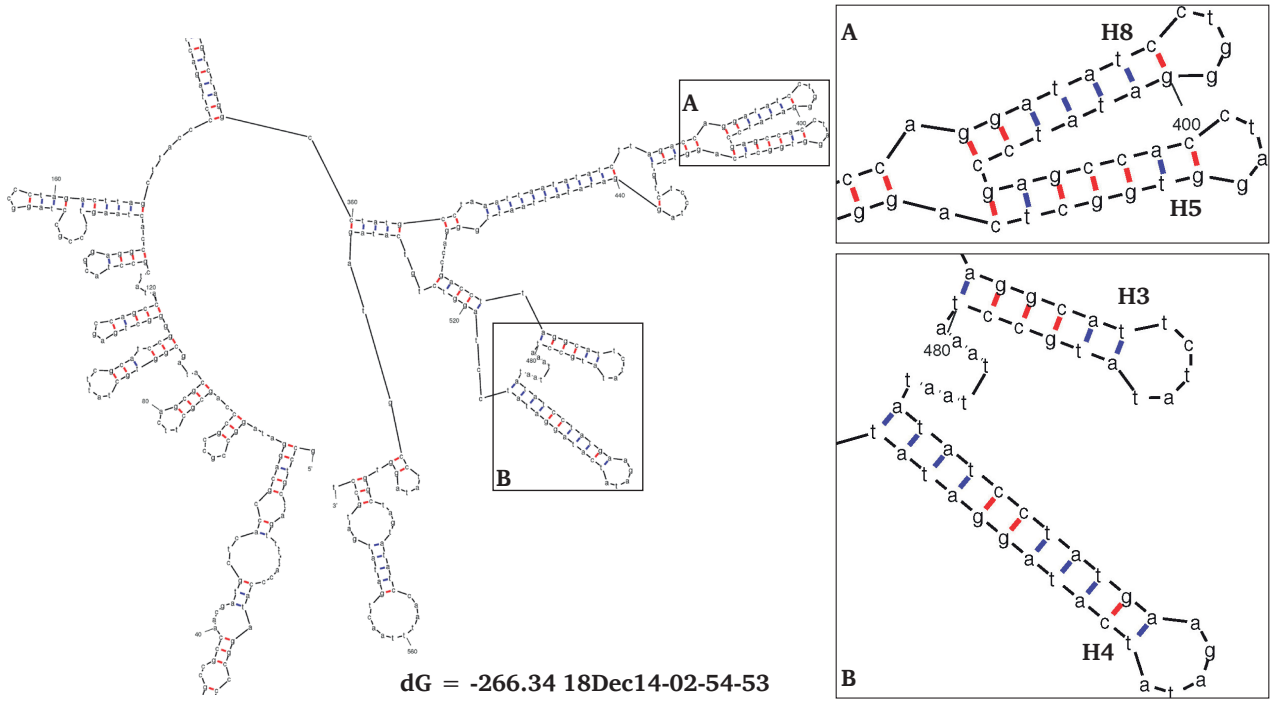

Fig. 2. Fragment of the sequence secondary structure from the mitochondrial DNA region of *L. baicalensis* located between the $tRNA^{Tyr}$ and $tRNA^{Ile}$ genes: A – possible combination of H8 and H5 hairpins, but not conservative in the mitochondrial DNA of the Baikal sponges, B – secondary structure conservative in the mitochondrial DNA of the Baikal sponges consisting of H3 and H4 hairpins.

species indicates a possible exchange of genetic material between them (Paquin et al., 2000; Erpenbeck et al., 2009).

4. Conclusions

Search and comparative analysis of inverted repeats has identified interesting features. Firstly, the mitochondrial DNA of the Baikal sponges has a large number of inverted repeats capable of forming hairpins, which is unusual for sponges. Secondly, we have found the continuity of these structures among representatives of different genera of the Lubomirskiidae family. The genetically closest species have shown the highest similarity in their distribution and localization. We have indicated that secondary elements are single and double hairpins similar to those of some other organisms in the mitochondrial DNA, where they are regarded as mobile elements. The results obtained within this study allow us to have a deeper insight into not only mechanisms of explosive speciation of closely related species of the Baikal sponges, but also the evolution of the mitochondrial genome in general.

Acknowledgments

The study was performed within the framework of the LIN SB RAS State task No. 0345-2016-0002 (AAAA-A16-116122110066-1) “Molecular ecology and evolution of living systems of the Central Asia under global ecological changes”.

References

Efremova S.M. 2001. Sponges (Porifera). In: Timoshkin O.A. (Ed.), Index of animal species of Lake Baikal fauna and its catchment area. Novosibirsk, pp. 179–192. (in Russian)

Efremova S.M. 2004. Novel genus and novel species of the Lubomirskiidae Rezvoj, 1936 sponge family. In: Timoshkin O.A. (Ed.), Index of animal species of Lake Baikal fauna and

Table 1. GC-content of secondary structures shown in four species of the Baikal sponges in the region between the $tRNA^{Tyr}$ and $tRNA^{Ile}$ genes. The colours correspond to those shown in Fig. 1.

Species	Conservative hairpin (blue)	Homologous hairpin No. 1 (red)	Homologous hairpin No. 2 (pink)	Homologous hairpin No. 3 (green)
L. baicalensis	100%	80%	62.5%	50%
R. echinata	100%	80%	80%	50%
S. papyracea	100%	75%	80%	66.6%
B. int. prof.	100%	80%	71.4%	57%

its catchment area. Novosibirsk, pp. 1261–1278. (in Russian)

Erpenbeck D., Voigt O., Wörheide G. et al. 2009. The mitochondrial genomes of sponges provide evidence for multiple invasions by Repetitive Hairpin-forming Elements (RHE). BMC Genomics 10: 1–14. DOI: 10.1186/1471-2164-10-591

Gazave E., Lapebie P., Renard E. et al. 2010. Molecular phylogeny restores the supra-generic subdivision of homoscleromorph sponges (Porifera, Homoscleromorpha). PLoS ONE 5: 12. e14290. DOI: 10.1371/journal.pone.001429

Hofacker I.L. 2003. Vienna RNA secondary structure server. Nucleotide Acids Research 31: 3429–3431. DOI: 10.1093/nar/gkg599

Itskovich V., Kaluzhnaya O., Veynberg Y. et al. 2017. Endemic Lake Baikal sponges from deep water. 2: Study of the taxonomy and distribution of deep-water sponges of Lake Baikal. Zootaxa 4236: 335–342. DOI: 10.11646/zootaxa.4236.2.8

Jukes T.H., Cantor C.R. 1969. Evolution of protein molecules. In: Munro H.N. (Ed.), Mammalian Protein Metabolism. New York, pp. 21–123.

Kolesnikov A.A., Gerasimov E.S. 2012. Diversity of mitochondrial genome organization. Biochemistry 77: 1424–1435. DOI: 10.1134/S0006297912130020

Lavrov D.V. 2010. Rapid proliferation of repetitive palindromic elements in mtDNA of the endemic Baikalian sponge *Lubomirskia baicalensis*. Molecular Biology and Evolution 27: 757–760. DOI: 10.1093/molbev/msp317

Lavrov D.V., Maikova O.O., Pett W. et al. 2012. Small inverted repeats drive mitochondrial genome evolution in Lake Baikal sponges. Gene 505: 91–99. DOI: 10.1016/j.gene.2012.05.039

Lavrov D.V., Pett W. 2016. Animal mitochondrial DNA as we do not know it: mt-genome organization and evolution in nonbilaterian lineages. Genome Biology and Evolution 8: 2896–2913. DOI: 10.1093/gbe/evw195

Ling W., Xuming Z., Liuwang N. 2011. Organization and variation of mitochondrial DNA control region in pleurodiran turtles. ZOOLOGIA 28: 495–504. DOI: 10.1590/S1984-46702011000400011

Lukic-Bilela L., Brandt D., Pojskic N. et al. 2008. Mitochondrial genome of *Suberites domuncula*: Palindromes and inverted repeats are abundant in non-coding regions. Gene 412: 1–11. DOI: 10.1016/j.gene.2008.01.001

Maikova O.O., Stepnova G.N., Belikov S.I. 2012. Variations in noncoding sequences of the mitochondrial DNA in sponges from family Lubomirskiidae. Doklady Biochemistry and Biophysics 442: 46–48. DOI: 10.1134/S1607672912010140

Maikova O., Khanaev I., Belikov S. et al. 2015. Two hypotheses of the evolution of endemic sponges in Lake Baikal (Lubomirskiidae). Journal of Zoological Systematics and Evolutionary Research 53: 175–179. DOI: 10.1111/.jzs.12086

Paquin B., Laforest M.-J., Lang B.F. 2000. Double-hairpin elements in the mitochondrial DNA of Allomyces: Evidence for Mobility. Molecular Biology and Evolution 17: 1760–1768. DOI: 10.1093/oxfordjournals.molbev.a026274

Wang X., Lavrov D.V. 2008. Seventeen new complete mtDNA sequences reveal extensive mitochondrial genome evolution within the Demospongiae. PLoS ONE 3: 1–11. DOI: 10.1371/journal.pone.0002723

Zuker M. 2003. Mfold web server for nucleic acid folding and hybridization prediction. Nucleic Acids Research 31: 3406–3415. DOI: 10.1093/nar/gkg595

Limnology and Freshwater Biology 2018 (2): 103-106 DOI:10.31951/2658-3518-2018-A-2-103

Short communication

ISSN 2658-3518
LIMNOLOGY FRESHWATER BIOLOGY
www.limnolfwbiol.com

Representatives of Diplomonadida in fishes of East Siberia

Denikina N.N., Nebesnykh I.A., Kondratov I.G.*, Khanaev I.V., Dzyuba E.V.

Limnological Institute, Siberian Branch of the Russian Academy of Sciences, Ulan-Batorskaya Str., 3, Irkutsk, 664033, Russia

ABSTRACT. In this study, we analyze the diversity of flagellated protozoa Diplomonadida, which are parasites in the digestive system of animals, in fishes of East Siberia. We have developed a method to diagnose the presence of DNA of Diplomonadida representatives, in particular, of *Spironucleus barkhanus*, in the analyzed samples. In our previous studies, we used molecular genetic methods to analyze salmonids of East Siberia for the presence of diplomonads and to determine the infection. The analysis of genetic diversity of diplomonads in the fishes of the genera *Coregonus* and *Thymallus* revealed the presence of one species, *S. barkhanus*. However, in addition to a cosmopolitan genotype widespread among Holarctic salmonids, in *C. migratorius* and *C. lavaretus baicalensis*, we have found a new genotype obviously different from those registered previously. Probably, *S. barkhanus* of this genotype is endemic for Lake Baikal. To determine a probable parasite exchange between *C. migratorius* and other fish species in the pelagic zone of Lake Baikal, we performed a screening of near-shore pelagic and pelagic cottoid fish for the presence of *S. barkhanus*. The analysis did not indicate the presence of DNA of *S. barkhanus* in the studied samples. We suppose the presence of other diplomonads species in endemic cottoid fish different from *S. barkhanus*.

Keywords: molecular genetic methods, Lake Baikal, *Coregonus, Thymallus, Comephorus, Cottocomephorus*

Diplomonadida are the flagellated protozoa that for many years have been considered the most primitive of eukaryotes, since they lack the typical mitochondria, peroxisomes and the Golgi apparatus (Keeling and Doolittle, 1997). The discovery of several varieties of mitochondria in Diplomonadida revealed that their cells were secondarily simplified, and these protists cannot be an intermediate stage in the formation of organelles in the general scheme of the evolutionary history of eukaryotes (Jerlstrom-Hultqvist et al., 2013). The order Diplomonadida includes the genera *Spironucleus, Hexamita*, *Trepomonas*, *Trimitus*, *Enteromonas*, *Octomitus*, and *Giardia* (Kolisko et al., 2008). The species *Hexamita* are mostly free-living anaerobic organisms inhabiting bottom sediments. At the same time, other taxa are almost purely commensals and pathogens, which usually inhabit the digestive system of mammals, birds, reptiles, amphibians, arthropods, molluscs, and fishes (Williams et al., 2011).

Diplomonads are of special interest for veterinary and agricultural organisations due to the severe pathologies that they cause in bred animals. Species of the genus *Spironucleus* are of particular attention, since they can cause devastating episodes of systemic infections in both ornamental and commercial fishes. These ubiquitous flagellates are found in cold, temperate and tropic waters and can infect a wide range of freshwater and marine fishes, as well as molluscs and crustaceans (Noga, 2010). The fish industry (and aquaculture in general) is becoming increasingly important in the world, since the natural fish stocks are depleted. At the same time, fishes and other objects of aquaculture are especially susceptible to outbreaks of diseases caused by diplomonads. For instance, *Spironucleus salmonicida* Jorgensen & Sterud, 2006 caused massive episodes of systemic infections in the farm-raised *Salmo salar* Linnaeus, 1758 and *Oncorhynchus tshawytscha* (Walbaum, 1792) (Kent et al., 1992; Poppe and Mo, 1993). The life cycle of diplomonads is direct and includes the stage of mobile parasitic trophozoite, which is generally followed by a stage of cysts. Infection rate is extremely high, especially in aquaculture, which also leads to a significantly high risk of host death.

The biology and ecology of species of the genus *Spironucleus* are poorly investigated in many aspects, including specific hosts, geographic ranges, transmission mechanisms, and pathogenicity of different species. Lack of knowledge is a serious limitation in disease control, since it impedes an accurate diagnosis and identification of the infection source. These obstacles are primarily associated with difficult detection of the genera and species of the order Diplomonadida,

*Corresponding author.
E-mail address: kondratovig@mail.ru (I.G. Kondratov)

which also explains the confusion in the nomenclature. The descriptions of the diplomonads are incomplete. Morphological studies using scanning and transmission microscopy often do not allow accurate identification of species. For example, *Spironucleus barkhanus* Sterud, Mo, & Poppe, 1998 has been described for a long time as eukaryotic organism of two morphologically similar types (nonpathogenic freshwater and pathogenic marine) (Sterud et al., 1998). Based only on the molecular genetic analysis, the representatives of this pathogenic genotype were described as a new species (*S. salmonicida*). Subsequently, the gene sequences of the small subunit ribosomal DNA were determined for all known species of diplomonads isolated from fishes and belonging to the genus *Spironucleus*: *S. barkhanus*, *S. salmonicida*, *S. salmonis*, *S. torosa*, and *S. vortens*. Previously, they were studied by ultrastructure analysis (Jørgensen and Sterud, 2006). Therefore, molecular genetic analysis plays a key role in detection and a correct identification of diplomonads in fishes.

Despite the relatively high level of knowledge about animals of Lake Baikal and water bodies of East Siberia, data on the species composition of parasitic protozoa are still fragmentary and incomplete. Previously, representatives of the genus *Hexamita* were described by morphological characteristics in *Coregonus migratorius* (Georgi, 1775), *Thymallus baicalensis* Dybowski, 1874, *Thymallus brevipinnis* Svetovidov, 1931, *Leuciscus baicalensis* (Dybowski, 1874), *Lota lota* (Linnaeus, 1758), and endemic cottoid fish: *Batrachocottus multiradiatus* Berg, 1907, *Batrachocottus nikolskii* (Berg, 1900), *Cottocomephorus grewingkii* (Dybowski, 1874), and *Limnocottus bergianus* (Taliev, 1935) (Zaika, 1965; Pronin, 2001; Pugachev, 2001; Rusinek, 2007).

Nucleotide sequences of a gene fragment of the small subunit ribosomal RNA were obtained in the study of the microbiota from the intestinal tract of *T. baicalensis* from the Angara River. These sequences were identical to *S. barkhanus* from *Thymallus thymallus* (Linnaeus, 1758) and *Salvelinus alpinus* (Linnaeus, 1758) (Belkova et al., 2008; 2009). Based on the sequences obtained, a diagnostic system was developed allowing detection of diplomonads and determination of their species (genotype).

In this study, we performed molecular genetic studies by standard methods: DNA was extracted using a DNA-Sorb-B kit according to the manufacturer's instructions (Ampli-Sens, Moscow); PCR was carried out in a standard reaction mixture.

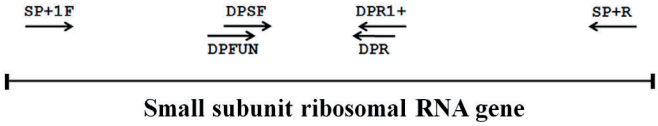

Fig. 1. Schematic arrangement of primers on the gene sequence of the small subunit rRNA

The regions conservative for eukaryotes (DpFun-DpR) served as primer to diagnose the presence of DNA of diplomonads. At the same time, the difference in the length of the observed gene fragment in diplomonads (~450 bp) and other eukaryotic organisms (~630 and more) provided the specificity of the target amplicons. Gene fragments of the small subunit rRNA of *S. barkhanus* were amplified using species-specific primers developed and tested in this study (Table 1, Fig. 1).

Using the developed diagnostic system, we determined infection in the representatives of the genera *Coregonus* and *Thymallus* (Denikina et al., 2011; 2016; 2017).

The representatives of the genus *Thymallus* occupy a large area of unconnected basins of the Palaearctic and Nonarctic rivers and lakes. Analysis of fish of the genus *Thymallus* from water bodies of East Siberia and Mongolia has shown an obvious trend in infection of graylings *S. barkhanus* in the catchment area of the Angara River: the minimum in Lake Khubsugul (38.5 %), the significant amount in the Barguzin River and Lake Baikal (80.0 and 85.2 %, respectively) and the maximum in the Angara River (100 %) (Denikina et al., 2011).

The genus *Coregonus* in water bodies of south-eastern Siberia is represented by species that occupy different ecological niches and have different food strategies. *S. barkhanus* infection rate in *C. migratorius* varies from 29.3 to 76.2 %. *Coregonus lavaretus baicalensis* Dybowski, 1874 is slightly infected (10-20%). The infection rate of *Coregonus* species in the Barguzin River was 12.5 %, in the tributaries of the Lena River is even lower. Therefore, habitat conditions, food preferences, behaviour and morphological features of the jaw structure are the determining factors of infection (Denikina et al., 2016).

Analysis of the genetic diversity of diplomonads in fish of the genera *Coregonus* and *Thymallus* revealed

Table 1. Primer pairs used in the study

Direct primer sequence	Reverse primer sequence	Amplicon length (bp)
DPFUN 5'-GCCAGCAGCCGCGGTAATTCC	DPR 5'-AGCCGCAGACTCCAC**R**TCT	450
DPSF 5'- CAGCCGCGGTAATTCCGACAC	DPR1 + 5'- AGCCGCAGACTCCACGTCTGGTGG	450
DPSF 5'- CAGCCGCGGTAATTCCGACAC	Sp + R 5'-GCAGCCTTGTTACGACTTCTCC	984
Sp + 1F 5'-GCCATGCATGCCTATGTGTAGAC	DpR1 + 5'- AGCCGCAGACTCCACGTCTGGTGG	881

the presence of a single species of *S. barkhanus*. At the same time, along with the cosmopolitan genotype, which is widespread in salmonid fish of Holarctic, in *C. migratorius* and *C. lavaretus baicalensis* we found a new genotype significantly different from all previously recorded ones. *S. barkhanus* of this genotype is likely to be endemic for Lake Baikal (Denikina et al., 2016; 2017).

To identify a possible parasite exchange between *C. migratorius* and other fish species in the pelagic zone of Lake Baikal, we screened the coastal-pelagic and pelagic cottoid fish for the presence of *S. barkhanus*. To investigate the infestation of endemic species of cottoid fish, we collected the material from 25 May to 15 June 2011 throughout the entire water area of Lake Baikal. The fishes were collected with an RK-15/30 midwater trawl at different depths. In total, we investigated 27 specimens of *Comephorus dybowski* Korotneff, 1905, 5 specimens of *Comephorus baicalensis* (Pallas, 1776), 11 specimens of *Cottocomephorus inermis* (Jakowlew, 1890), 58 specimens of *Cottocomephorus grewingkii* (Dybowskii, 1874), and 60 specimens of *Cottocomephorus alexandrae* Taliev, 1935 (Table 2, Fig. 2).

The necessity of these experiments was due to the following circumstances. i) Along with *C. migratorius*, five endemic Cottoidei species inhabit the open pelagic zone of Lake Baikal: pelagic species (*C. baicalensis* and *C. dybowski*) and three benthopelagic species of the genus *Cottocomephorus* (*C. inermis, C. grewingkii* and *C. alexandrae*). The habitats of these species coincide with those of *C. migratorius* in the winter and spring period. ii) The food spectra of these species are similar with the food spectrum of *C. migratorius* in the feeding period and includes zooplankton: *Epischura baikalensis* Sars, 1900 and *Macrohectopus branickii* (Dybowsky, 1874). iii) *T. baicalensis* inhabit the coastal zone of Lake Baikal, where bentopelagic cottoid fish spawn. There is evidence of the finding of *Hexamita* in *C. grewingkii* (Zaika, 1965). Since species determined in 1965 is rather ambiguous considering the revised classification, and the indicated localization (the intestine and gallbladder) corresponds to *S. barkhanus*, the analysis was necessary. All above-mentioned ecological features of cottoid fish inhabiting the pelagic zone of the lake suggest that they have diplomonads, which were previously found in *T. baicalensis* and *C. migratorius*. However, the analysis did not reveal the presence of *S. barkhanus* in the studied DNA samples. The presence of *Hexamita* in *C. grewingkii* (Zaika, 1965) and the absence of *S. barkhanus* in our samples can be explained by the fact that the fish studied differed greatly. Most likely, in (Zaika, 1965) fish for parasitological analysis were collected from the coastal zone of Lake Baikal. *C. grewingkii* is the most numerous representative of the shallow water ichthyocenosis. Within a species, three spawning populations (schools) are distinguished at different times: March, May, and August (Taliev, 1955; Koryakov, 1972). Multi-layer rocky grounds in the coastal zone of the lake serve for *C. grewingkii* as a substrate for spawning. In schools of *C. grewingkii* spawning at different times, the incubation period for the development of clutches

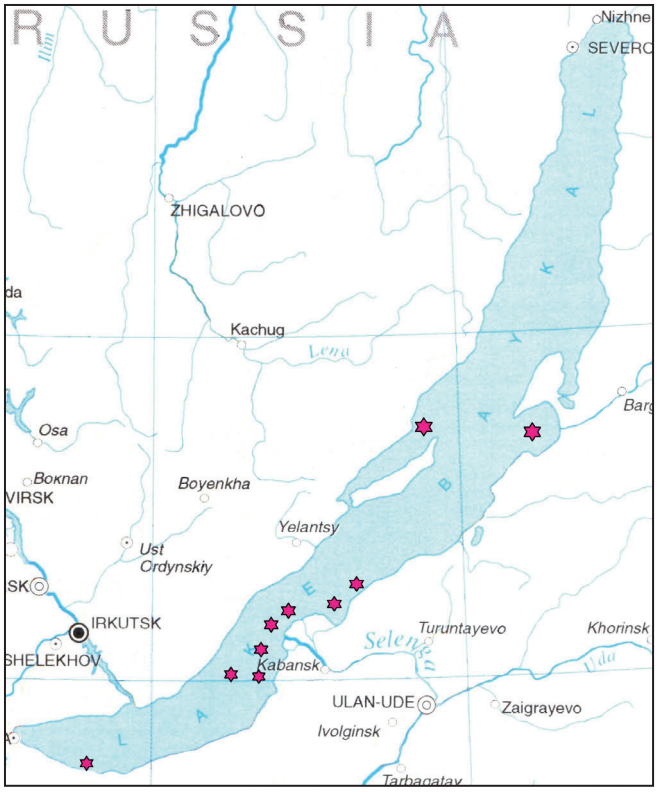

Fig. 2. Schematic sample collection map, May-June 2011

Table 2. Specimens of cottoid fish, Lake Baikal May-June 2011

Trawl coordinates	Fish species	Quantity, specimen
51°51’17”N 104°37’39”E	*C. dybowski*	5
	C. baicalensis	3
52°03’67”N 106°02’15”E	*C. dybowski*	5
52°08’94”N 105°81’32”E	*C. baicalensis*	2
	C. alexandrae	10
	C. inermis	3
52°25’46”N 106°02’41”E	*C. grewingkii*	10
52°46’53”N 106°67’59”E	*C. dybowski*	5
52°58’42”N 106°97’38”E	*C. inermis*	1
53°43’39”N 108°68’59”E	*C. inermis*	3
53°46’57”N 107°60’67”E	*C. inermis*	3
52°38’64”N 106°18’06”E	*C. alexandrae*	30
	C. grewingkii	20
	C. inermis	1
52°31’85”N 106°05’97”E	*C. grewingkii*	28
	C. alexandrae	20
	C. dybowski	12

ranges from 20 to 80-90 days depending on spawning season and temperature conditions during the development of eggs. Male protects the clutch from the moment of spawning to the appearing of larvae. Most males die after the period of clutch protection. This zone is the main feeding ground for the *T. baicalensis*, which infection rate reaches 85.2 %. We assumed that *C. grewingkii* samples with *Hexamita* (Zaika, 1965) were collected in the spawning area. Therefore, we did not detect *S. barkhanus* in the open pelagic zone of the lake in the fattening *C. grewingkii* specimens. It is also likely that diplomonads in salmonid and cottoid fish were attributed to the same species by mistake, since previous data by (Zaika, 1965) were obtained using methods of light microscopy. In this case, cottoid fish may have other diplomonads species than *S. barkhanus*. This assumption requires additional studies.

Acknowledgments

This research was supported by the State Project No. 0345–2016–0002.

References

Belkova N.L., Dzyuba E.V., Sukhanova E.V. 2008. Molecular-genetic detection of a nonpathogenic genotype of *Spironucleus barkhanus* (Diplomonadida: Hexamitidae) in the black Baikal grayling (*Thymallus arcticus baicalensis* Dybowski, 1874). Biology Bullutin 35: 219–221. DOI: 10.1134/S1062359008020179

Belkova N.L., Dzyuba E.V., Sukhanova E.V. 2009. Molecular-genetic identification of the intestinal microflora and protozoa of the baikalian fish. In: Timoshkin O.A. (Ed.), Index of animal species inhabiting Lake Baikal and its catchment area. Vol. 2. Novosibirsk: Nauka. (In Russian)

Denikina N.N., Nebesnykh I.A., Sukhanova E.V. et al. 2011. Development and approbation of detection method of the Diplomonadida order for the fish infection research. Biologicheskiye nauki Kazakhstana [Biological sciences of Kazakhstan] 4: 28–33. (in Russian)

Denikina N., Nebesnykh I., Maikova O. et al. 2016. Genetic diversity of Diplomonadida in fish of the genus *Coregonus* from East Siberia. Acta Parasitologica 61: 299–306. DOI: 10.1515/ap-2016-0040.

Denikina N.N., Nebesnykh I.A., Belkova N.L. et al. 2017. The genetic diversity of the Diplomonadida and the infection of the genera *Coregonus* and *Thymallus* of Eastern Siberia. Map № 144.4. In: Plusnin V.M. (Ed.), Ecological atlas of the Baikal region. [http://atlas.isc.irk.ru] (In Russian)

Jerlstrom-Hultqvist J., Einarsson E., Xu F. et al. 2013. Hydrogenosomes in the diplomonad *Spironucleus salmonicida*. Nature communications 4: 2493. DOI: 10.1038/ncomms3493 |www.nature.com/naturecommunications

Jørgensen A., Sterud E. 2006. The marine pathogenic genotype of *Spironucleus barkhanus* from farmed salmonids redescribed as *Spironucleus salmonicida* n. sp. Journal of Eukaryotic Microbiology 53: 531–541. DOI: 10.1111/j.1550-7408.2006.00144.x

Keeling P.J., Doolittle W.F. 1997. Widespread and ancient distribution of a noncanonical genetic code in Diplomonads. Molecular Biology and Evolution 14: 895–901. DOI: 10.1093/oxfordjournals.molbev.a025832

Kent M.L., Ellis J., Fournie J.W. et al. 1992. Systemic hexamitid infection in seawater pen-reared chinook salmon. Diseases of Aquatic Organisms 14: 81–89. DOI: 10.3354/dao014081

Kolisko M., Cepicka I., Hampl V. et al. 2008. Molecular phylogeny of diplomonads and enteromonads based on SSU rRNA, alpha- tubulin and HSP90 genes: Implications for the evolutionary history of the double karyomastigont of diplomonads. BMC Evolutionary Biology 8: 205. DOI: 10.1186/1471-2148-8-205

Koryakov E.A. 1972. Pelagic sculpins of Baikal. Moscow: Nauka. (In Russian)

Noga E.J. 2010. Fish disease- diagnosis and treatment. 2nd edition. Wiley-Blackwell.

Poppe T., Mo T.A. 1993. Systemic, granulomatous hexamitosis of farmed Atlantic salmon: interactions with wild fish. Fisheries Research 17: 147–152. DOI: doi.org/10.1016/0165-7836(93)90014-X

Pronin N.M. 2001. Polymastigotes (Mastigophora: Polymastigota). In: Timoshkin O.A. (Ed.), Index of animal species inhabiting Lake Baikal and its catchment area. Vol. 1. Novosibirsk: Nauka. (In Russian)

Pugachev O.N. 2001. Catalog of parasites in freshwater fish of Northern Asia. Protozoa. Saint Petersburg: ZIN RAS. (In Russian)

Rusinek O.T. 2007. Fish parasites of Lake Baikal (fauna, communities, zoogeography and historical background). Moscow: KMK Scientific Press Ltd. (In Russian)

Sterud E., Mo T.A., Poppe T.T. 1998. Systemic spironucleosis in sea-farmed Atlantic salmon *Salmo salar*, caused by *Spironucleus barkhanus* transmitted from feral Arctic char *Salvelinus alpinus*? Diseases of Aquatic Organisms 33: 63–66. DOI: 10.3354/dao033063

Taliev D.N. 1955. Baicalian sculpins (Cottoidei). Moscow-Leningrad: Publishing House of the USSR Academy of Sciences. (In Russian)

Williams C., Lloyd D., Poynton S. et al. 2011. *Spironucleus* species: economically-important fish pathogens and enigmatic single-celled Eukaryotes. Journal of Aquaculture Research and Development S2-13. DOI: dx.doi.org/10.4172/2155-9546.

Zaika V.E. 1965. Parasitofauna of Lake Baikal fishes. Moscow: Nauka. (In Russian)

Limnology and Freshwater Biology 2018 (2): 107-112 DOI:10.31951/2658-3518-2018-A-2-107

Original Article

ISSN 2658-3518
LIMNOLOGY FRESHWATER BIOLOGY
www.limnolfwbiol.com

The diversity of hydras (Cnidaria: Hydridae) in the Baikal region

Peretolchina T.E.*, Khanaev I.V., Kravtsova L.S.

Limnological Institute, Siberian Branch of the Russian Academy of Sciences, Ulan-Batorskaya Str., 3, Irkutsk, 664033, Russia

ABSTRACT. We have studied the fauna of *Hydra* in the waters of the Baikal region using morphological and molecular genetic methods. By the external morphological features of the structure of the polyp and the microscopic study of nematocysts, we have identified four species belonging to three different genetic groups: "oligactis group" (*Hydra oligactis*, *H. oxycnida*), "braueri group" (*H. circumcincta*) and "vulgaris group" (*H. vulgaris*). Molecular phylogenetic analysis has confirmed the species status of the hydras studied. The intraspecific genetic distances between the Baikal and European hydras are 1.5–4.2% and 0.4–2.7% of the substitutions in COI and ITS1–5.8S–ITS2 markers, respectively, while, interspecific distances for different species significantly exceed intraspecific and amount to 9.8 – 16.1% and 6.4 – 32.1% of substitutions for the markers COI and ITS1–5.8S–ITS2, respectively. The temperature regime of the water and the availability of food resources, which play a key role in the reproduction of hydras, determine the habitats of the identified species. The research performed has replenished the regional fauna with species whose findings were previously considered presumptive or doubtful. The first record of *H. vulgaris* in the artificial reservoir near the Angara River (Lake Kuzmikhinskoye) will help to clarify the distribution of this species.

Keywords: Baikal region, *Hydra*, nematocysts, molecular phylogenetic analysis

1. Introduction

Hydra is a member of the ancient phylum Cnidaria, class Hydrozoa, order Hydroida, family Hydridae. Genus *Hydra* comprises 15 species (Jankowski et al., 2008), five of them are found in Europe: *Hydra viridissima* Pallas, 1766, *H. circumcincta* Schulze, 1914, *H. oligactis* Pallas, 1766, *H. vulgaris* Pallas, 1766 and *H. oxycnida* Schulze, 1914 (Schuchert, 2010).

There have been no detailed studies of the fauna of the cnidarians in Lake Baikal. According to available literature data, four species of freshwater hydroids of the genus *Hydra* were recorded in Lake Baikal: *H. baikalensis*, *H. oligactis* and, rarely, *H. circumcincta*, *H. oxycnida* (= *H. oxycnidoides* sensu Shultze, 1927) (Kozhov, 1962; Stepanyants et al., 2003; 2006). Gajewskaja supposed the existence of *H. vulgaris* in Lake Baikal (Gajewskaja, 1933); however, subsequent researchers never found *H. vulgaris*, as well as *H. oxycnida*, and doubted their presence in the lake. In the "Index of animal species inhabiting Lake Baikal and its catchment area", only two species are mentioned: *H. oligactis* and *H. baikalensis* (Stepanyants and Anokhin, 2001).

The aim of this work was to study the diversity of the fauna of the hydroids in the Baikal region using morphological and molecular genetic methods.

2. Materials and methods

Hydras were collected at depths of 1 to 18 meters by a scuba diver and with hands: 1) along the littoral zone of Lake Baikal; 2) in Posolsky Sor. Hydras together with aquatic plants were also collected by hands from lakes Zama (near Lake Baikal) and Kuzmikhinskoye (the artificial reservoir near the Angara River) at depths of 0.5 m (Fig. 1). Typically, representatives of *Hydra* were brought live to the laboratory, but some samples were fixed in 80% ethanol in the field.

The nematocysts of *Hydra* representatives (stenoteles, desmonemes holotrichous and atrichous isorhizas) were photographed using Olympus CX22 microscope with 1000-fold magnification under oil immersion. Morphometric measurements of holotrichous isorhizas and stenoteles were carried out with the Image-Pro program (Table 1). Hydras specimens were identified according to keys provided by Schuchert (2010) and Anokhin (2002).

DNA was extracted from a single live or fixed specimen according to the protocol described by Doyle and Dickson (1987). Gene fragments of mitochondrial cytochrome c oxidase subunit I (COI) and internal transcribed spacer 1 – 5.8S ribosomal DNA – internal transcribed spacer 2 (ITS1–5.8S–ITS2) were amplified in PCR using the primers listed in Table 2. The PCR

*Corresponding author.
E-mail address: tatiana.peretolchina@gmail.com (T.E. Peretolchina)

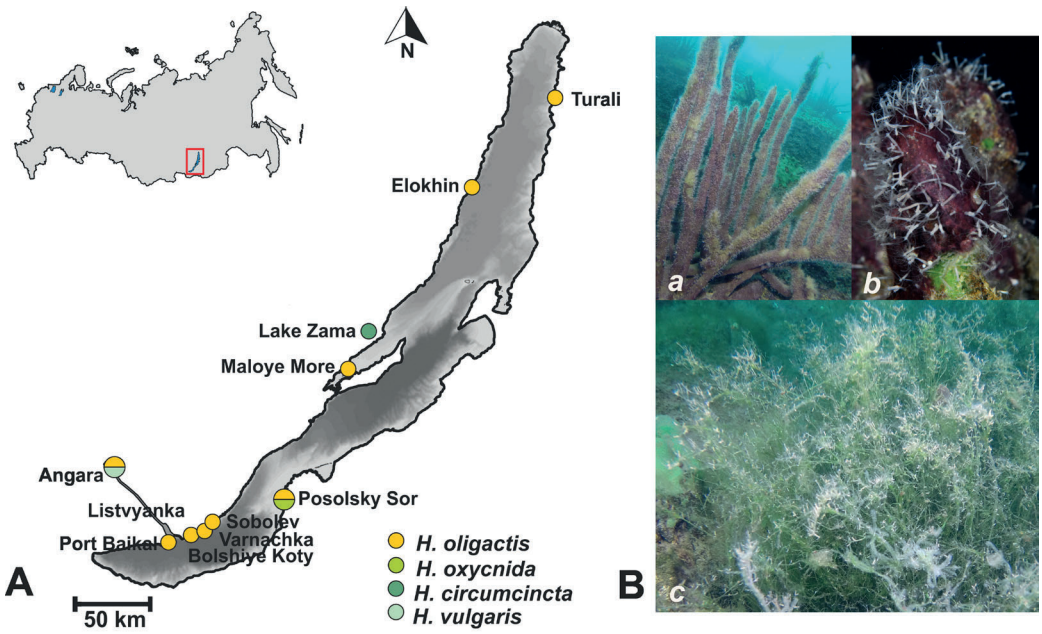

Fig. 1. A – Sampling sites of *Hydra*; B – photos of massively growing *H. oligactis* on the dying Porifera (*a, b*) and on the filamentous algae (*c*) (photos by I.V. Khanaev)

amplification conditions for both molecular markers were as follows: denaturation at 94 ºC for 5 min, 30 cycles at 94 ºC for 30 sec, 50 ºC for 45 sec, 72 ºC for 2 min, and a final elongation step at 72 ºC for 10 min. Direct sequencing of forward sequences was performed in Research and Production Company SYNTOL (Russia) using an ABI 3130 automated sequencer.

The DNA sequences obtained were edited in BioEdit v.7.2.5 (Hall, 2011) and aligned using ClustalW (Thompson et al., 1994) and MAFFT v.6.240 (Katoh et al., 2002). Resulting COI alignment was translated to check for the absence of stop codons. To confirm species identity, we compared our sequence dataset with the published ortholog sequences from other members of *Hydra* and analyzed genetic distances using Mega v.6 (Table 3) (Tamura et al., 2013).

Phylogenetic analysis was performed using MrBayes v.3.2 (Ronquist and Huelsenbeck, 2003). The dataset consisted of eight combined COI + ITS1–5.8S–ITS2 sequences: four sequences of hydra specimens produced for this study and four ones of specimens belonging to European species: *H. circumcincta* (GU722853, GU722669), *H. oligactis* (GU722868, GU722691), *H. vulgaris* (GU722918, GU722744) and *H. oxycnida* (GU722876, GU722690) (Martínez et al., 2010) retrieved from GenBank. To estimate the posterior probabilities of the phylogenetic tree, we used 15,000,000 generations of Metropolis-coupled Markov chain Monte Carlo simulation (two runs with four chains). We used the jModelTest v.2.1 (Darriba et al., 2012) to determine the substitution models for the three genes separately. The best-fit model for phylogenetic analysis in each case was GTR + I + G. We constructed a majority-rule (50%) consensus tree following 25% burn-in of all sampled trees to allow likelihood values to reach stationary equilibrium.

3. Results and discussion

All *Hydra* samples collected were identified by external morphology of polyps and microscopic examination of their nematocysts as *H. oligactis*, *H. oxycnida* ("oligactis group"), *H. circumcincta* ("brauneri group") and *H. vulgaris* ("vulgaris group") (Fig. 2).

The consensus tree topology (Fig. 3) based on combined sequence data (COI and ITS1–5.8S–ITS2) have confirmed that hydras from the Baikal region belong to four species: *H. circumcincta*, *H. oligactis*, *H. vulgaris* and *H. oxycnida*. The intra-specific distances of hydras from the Baikal region and Europe do not exceed 5% that indicate species level of the samples studied (Martínez et al., 2010; Schwentner and Bosch,

Table 1. The nematocysts sizes of different species of *Hydra* from the Baikal region

Species	holotrichous isorhiza							stenotele						
	width, μm			length, μm			n	width, μm			length, μm			n
	x ± m	min	max	x ± m	min	max		x ± m	min	max	x ± m	min	max	
H. oligactis	4.2 ± < 0.1	3.1	5.2	8.8 ± 0.1	7.4	11.4	100	9.6 ± 0.1	9.1	9.9	12.9 ± 0.2	12.2	13.6	8
H. oxycnida	4.2 ± 0.1	3.9	4.8	10.1 ± 0.2	8.9	11.4	15	11.8 ± 0.2	10.7	12.8	20.3 ± 0.5	18.0	22.8	9
H. circumcincta	5.8 ± 0.1	4.9	6.7	8.6 ± 0.1	7.5	9.4	29	11.6 ± 0.5	10.6	12.6	13.6 ± < 0.1	13.5	13.6	3
H. vulgaris	4.7 ± 0.1	4.2	5.2	10.2 ± 0.2	7.9	12.4	19	12.6 ± 2.2	9.9	25.6	16.4 ± 2.6	11.6	31.9	7

x- mean, m – standard error of mean, min and max – limits, n – number of measurements

Table 2. Primers used in this study

Gene	Primer	Reference
COI	LCO1490: 5'-GGT CAA CAA ATC ATA AAG ATA TTG G-3' HCO2198: 5'-TAA ACT TCA GGG TGA CCA AAA AAT CA-3'	Folmer et al. (1994)
ITS1–5.8S–ITS2	ITS1 (f): 5'-TCC GTA GGT GAA CCT GCG G-3' ITS4 (r): 5'- TCC TCC GCT TAT TGA TAT GC-3	White et al. (1990)

2015). Inter-specific distances varied from 9.8% to 16.1% between COI sequences and from 6.4% to 32.1% between ITS1–5.8S–ITS2 sequences for different species of *Hydra* (Table 3). Large genetic distances between hydras belonging to different genetic groups determined by ITS1–5.8S–ITS2 marker can be explained by presence of indels obtained after alignment.

Below are the ecological and morphological characteristics of the studied species (the description of the species based on morphological characters according to Schuchert (2010) and measurements of nematocysts (Table 1)):

Phylum Cnidaria Verrill, 1865
Subphylum Medusozoa Peterson, 1979
Class Hydrozoa Owen, 1843
Subclass Hydroidolina Collins 2000
Order Anthoathecata Cornelius, 1992
Family Hydridae Dana, 1846

Hydra oligactis Pallas, 1766, syn.: *Hydra fusca* Linnaeus, *Hydra roeselii* Haacke, *Hydra rhaetica* Asper, *Hydra rhistica* Asper, *Pelmatohydra oligactis* Schulze.

Description. The Baikal *Hydra* is large, typically with 5–7 long tentacles and a more or less distinct pedicel. The cnidome includes four types of nematocysts: stenoteles, holotrichous isorhizas, atrichous isorhizas and desmonemes (Fig. 2E–H). Holotrichous isorhizas are elongated, with a length/width ratio of approximately 2, and with thread-forming longitudinal irregular coils inside the capsule. Other types of nematocysts are of a size and shape typical of hydras. Sexes are strictly separated, no sex change, the onset of gametogenesis stops vegetative budding.

Distribution. Lake Baikal: Port Baikal, Ulanovo, Listvennichny Bay, Bolshie Koty, Varnachka, Sobolev Cape, Turali Cape, Elokhin Cape, Mukhor Bay, Posolsky Sor; Lake Kuzmikhinskoye (Artificial reservoir near the Angara River). This species is also widespread and common on the entire European continent, including the British Isles and Iceland as well as Russia and North America (Hyman, 1930; Holstein, 1995; Stepanyants et al., 2006).

Hydra oxycnida Schulze, 1914, syn.: *Hydra oxycnidoides* Schulze, 1927, *Hydra pirardi* Brien, 1961.

Description. Very large dark brown *Hydra* without pedicel, stenoteles are markedly ovoid (Fig 2D), width/length ratio is 0.6, and upper part is characteristically pointed. Holotrichous isorhizas are ovoid to oval, the length/width ratio is >2 (Fig. 2B), there is shaft in intact capsule thread in 3-4 oblique or transverse coils in the upper part of capsule. Tentacles are 7-8, rarely 6-11, relatively short, extended and reaching only 1/4 to 1/3 of body length, polyp buds form tentacles simultaneously. Sexes are strictly separated, no sex change, the onset of gametogenesis stops vegetative budding and nematocyst production.

Distribution. Lake Baikal (Posolsky Sor). Additionally, it occurs in Russia (Holstein, 1995) and is common in Northern Europe (Schuchert, 2010).

Hydra circumcincta Schulze, 1914, syn.: *Hydra braueri* Bedot, 1912, *Hydra stellata* Schulze, 1914, *Hydra ovata* Boecker, 1920, *Hydra graysoni*.

Description. Small *Hydra* with short tentacles, no pedicel, holotrichous isorhizas are ovoid (Fig. 2K), the length/width ratio is <1.5, there is thread in 3-4 distinct coils in the upper part of capsule, stenoteles are ovoid (Fig. 2L), with two size classes, the width/length ratio is approximately 0.85. Hypostome is conical, below hypostome there are usually six tentacles, sometimes five tentacles, tentacles are shorter than hydranth body (ratio $<$ 0.5), held horizontally. Contracted hydranths are with star-shaped tentacle crown. Vegetative multiplication is by buds, which are relatively basal, tentacles of buds are formed simultaneously, usually six in number. Vegetative and sexual reproduction can occur simultaneously. Sexual reproduction is as hermaphrodites, sometimes proterandric.

Distribution. Lake Zama (near Lake Baikal). They are also found in Russia, Japan, North America

Table 3. Pairwise *p*-distances between COI (below diagonal) and ITS1–5.8S–ITS2 (above diagonal) for different species of *Hydra*. Intra-specific pairwise *p*-distances are in bold.

	H. oxycnida	***H. oligactis***	***H. vulgaris***	***H. circumcincta***
H. oxycnida	**0.015 (0.004)**	0.064	0.205	0.317
H. oligactis	0.098	**0.018 (0,007)**	0.214	0.321
H. vulgaris	0.123	0.122	**0.042 (0.026)**	0.251
H. circumcincta	0.161	0.158	0.132	**0.036 (0.027)**

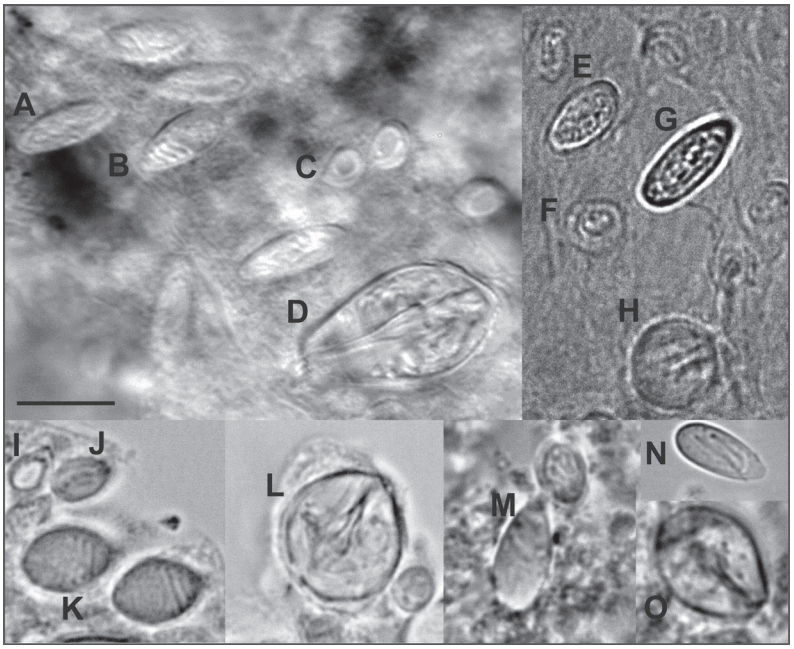

Fig. 2. Nematocysts of different *Hydra* species: A–D – *H. oxycnida*; E–H – *H. oligactis*; I–L – *H. circumcincta*; M–O – *H. vulgaris*. A, E, J, N – atrichous isorhizas; C, F, I – desmonemes; B, G, K, M – holotrichous isorhizas; D, H, L, O – stenoteles. Scale bar is 10 μm.

(Heitkamp, 1986; Holstein, 1995; Stepanyants et al., 2006) and in Europe, including the British Isles, except for Iceland (Schuchert, 2010).

Hydra vulgaris Pallas, 1766, syn.: *Hydra grisea* Linnaeus, 1767, *Hydra vulgaris aurantiaca* Ehrenberg, 1838, *Hydra trembleyi* Haacke, 1879.

Description. Medium sized *Hydra*, extended hydranth is usually 3-6 mm, may reach sizes of up to 15 mm, with 6-8 long tentacles, without algal symbionts, no or indistinct pedicel, holotrichous isorhizas are oblong, the length/width ratio is >2, thread is in 4-5 oblique or transverse coils the in upper part of capsule, stenotele width/length ratio is approximately 0.78 (Fig. 2M, O). Vegetative multiplication is by buds located in lower third of the body, usually there are only 1-2 buds, rarely 3-4, initial four tentacles of buds are formed more or less simultaneously, later more tentacles develop, and, thus, tentacles are transiently of unequal length. Vegetative and sexual reproduction can occur simultaneously. Sexual reproduction of gonochoristic and hermaphroditic animals is very rare. In hermaphrodites, male and female gonads are mixed, and are not in separate regions.

Distribution. Lake Kuzmikhinskoye (Artificial reservoir near the Angara River). In Russia, it was found in the Far East (Stepanyants et al., 2006). It also inhabits the entire European continent and the British Isles (Schuchert, 2010).

Currently, among the hydras listed above, in open Lake Baikal only *H. oligactis* occurs, mass growth of which has been observed in the last decade (Fig. 1B). Representatives of this species are capable of very intense budding: 10–20 young polyps that have not yet budded are found on one maternal specimen (Stepanyants et al., 2003; Tökölyi et al., 2016). For this reason, *H. oligactis* became the most widespread representative of freshwater cnidaria in almost all continental waters. Previously, representatives of hydras were found in small numbers in the coastal zone of Lake Baikal. The first record of the mass development of *H. oligactis* was in the 2000s (Stepanyants et al., 2003). Now, it is abundant along the open coasts of all three basins of Lake Baikal. In the last decade, the blooming of filamentous algae (*Spirogyra*, *Ulotrix* and others) and the trend towards a more widespread distribution of invasive species, in particular, *Elodea canadensis*, have been observed in Lake Baikal (Kravtsova et al., 2010). In addition, mass death of the endemic species of *Porifera* (Denikina et al., 2016; Khanaev et al., 2018) is currently observed. On the contrary, representatives of *Hydra* acquire a significant role along the open coasts of Lake Baikal.

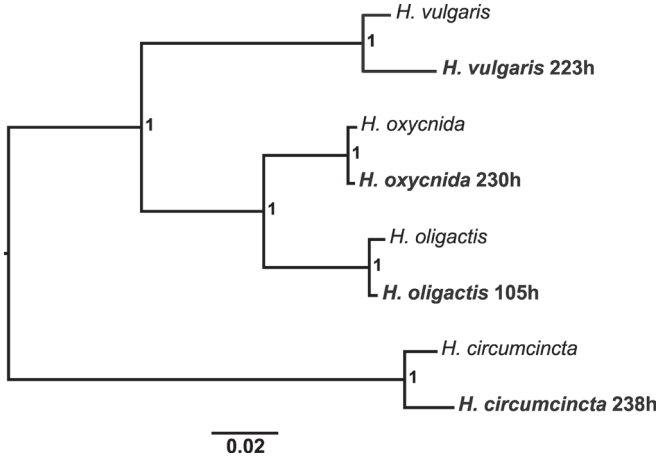

Fig. 3. Combined COI and ITS1–5.8S–ITS2 phylogenetic tree. Haplotypes of hydras from the Baikal region are in bold

According to the literature data, the temperature optimum for sexual reproduction of *H. oligactis* is 10–12

°C, and for vegetative budding is 18–22 °C (Littlefield, 1991). The water temperature in the surface layer of the coastal zone of the Lake Baikal in summer does not exceed 16 °C (Timoshkin et al., 2018). Despite the fact that the water temperature in Baikal is slightly lower than the temperature optimum for vegetative reproduction, *H. oligactis* exhibits intensive budding and develops along the open coasts of the lake in all three basins.

Due to the global climate change since the early 70s of the past century, an increase in air temperature has been observed in the Baikal region during all seasons of the year, especially in winter, as well as an increase in the duration of the ice-free period of Lake Baikal and warming of its surface waters (in May–September) by 1 °C (Shimaraev et al., 2002). However, such increase in temperature hardly contributes to the mass distribution of other *Hydra* species in open Baikal, in particular, *H. oxycnida*, *H. circumcincta* and *H. vulgaris*.

Rare species *H. oxycnida* was found in 2015 together with *H. oligactis* on the leaves of *Potamogeton perfoliatus* in the coastal zone of Lake Baikal, Posolsky Sor, where the temperature of water during the summer may reach 24°C (Kozhov, 1947). Despite the existing water exchange between Posolsky Sor and open Baikal, *H. oxycnida* has not been observed yet outside this area, unlike *H. oligactis*. Perhaps, the rare records of *H. oxycnida*, even in the coastal zone, are due to not only environmental conditions but also the biological features of this species, which are the lower rate of budding during the vegetative reproduction than in *H. oligactis* (Schuhert, 2010).

The habitats of other representatives of *Hydra* are confined to shallow water bodies located in areas adjacent to Lake Baikal. *H. circumcincta* lives in Lake Zama near Lake Baikal. The maximum depth of Zama is 1.5 m (average is 1 m); bottom sediments are sand with detritus and pebble covered with silt. The water in the lake is yellowish; the temperature in August is 18.4 °C. There are thickets of *Potamogeton* and *Ceratophylum*; Copepoda (77,000 specimens/m^2), Rotatoria (52,000 specimens/m^2) and Cladocera (20,000 specimens/m^2) dominate in zooplankton (Koryakov et al., 1977). The abundance of food for hydras is also an important factor influencing the biological characteristics of the species as well as temperature. The availability of food resources plays a key role in the change of the reproduction strategy of hydras (Kaliszewicz and Lipinska, 2013).

In 2018, *H. vulgaris* was found in the Baikal region for the first time in Lake Kuzmikhinskoye located near the Angara River, downstream dam. This is an artificial reservoir created during the construction of the Irkutsk Hydroelectric Power Station in 1950. The lake has a length of 430 m, a width of 145 m and a maximum depth of 2.7 m (Kamaltynov and Kamaltynov, 2000). Bottom sediments in the lake consist of silted sand with pebbles and plant detritus; occasionally fragments of marble rocks are found. The summer water temperature in the lake is over 20 °C. *Elodea canadensis* dominates among the aquatic plants. Apparently, the temperature regime in Lake Kuzmihinskoye corresponds to those in the water bodies of Europe and the Far East.

Conclusions

Thus, in the Baikal region, the fauna of hydras is represented by typical inhabitants of freshwater bodies of northern latitudes. The morphological and molecular genetic analysis of the hydras from the Baikal region water bodies studied allowed us to uniquely identify four species: *H. oligactis*, *H. oxycnida*, *H. circumcincta* and *H. vulgaris*. In open part and in the coastal zone of Lake Baikal, only representatives of the "oligactis group" were found: *H. oligactis* and *H. oxycnida*. The regional fauna of the hydra has been replenished with species whose findings were previously considered presumptive or doubtful. The record of *H. vulgaris* in the Baikal region makes the species area less fragmented since it was previously found only in water bodies of Europe and the Far East.

Acknowledgements

We thank Dr. Tatiana Y. Sitnikova, Ivan A. Nebesnykh and Yuriy A. Yuschuk for their assistance in collecting material. This study was supported by the governmentally funded project No. 0345–2016–0004 (*AAAA-A16-116122110060-9*).

References

Adams J., Greenwood P. J., Naylor C.J. 1987. Evolutionary aspects of environmental sex determination. International Journal of Invertebrate Reproduction and Development 11: 123–136. DOI: 10/1080/01688170.1987.10510273.

Anokhin B. 2002. Redescription of the endemic Baikalian species *Pelmatohydra baikalensis* (Cnidaria: Hydrozoa, Hidridae) and assessment of the hydra fauna of Lake Baikal. Annales zoologici 52: 195–200.

Darriba D., Taboada G.L., Doallo R. et al. 2012. jModelTest 2: more models, new heuristics and parallel computing. Nature methods 9: 772. DOI: 10.1038/nmeth.2109

Denikina N.N., Dzyuba E.V., Bel'kova N.L. et al. 2016. The first case of disease of the sponge *Lubomirskia baicalensis*: investigation of its microbiome. Biology Bulletin 43: 263–270. DOI: 10.1134/S106235901603002X

Doyle J.J., Dickson E. 1987. Preservation of plant samples for DNA restriction endonuclease analysis. Taxon 36: 715-722.

Folmer O., Black M., Hoeh W. et al. 1994. DNA primers for amplification of mitochondrial cytochrome c oxidase subunit I from diverse metazoan invertebrates. Molecular Marine Biology and Biotechnology 3: 294–299.

Gajewskaja N. 1933. Ecology, morphology and systematics of the infusoria of Lake Baikal. Zoologica 85: 1–29. (In German)

Hall T. 2011. BioEdit: an important software for molecular biology. Green Earth Research Foundation Bulletin of Bioscience 2: 60–61.

Holstein T. 1995. Cnidaria: Hydrozoa. In: Schwoerbel J. and Zwick P. (Eds.), Freshwater fauna of Central Europe, Cnidaria: Hydrozoa / Kamptozoa. Stuttgart, pp. 1–142. (In German)

Hyman L. H. 1930. Taxonomic studies on the *Hydra* of North America. II. The characters of *Pelmatohydra oligactis* Pallas. Transactions of the American microscopical Society

49: 322–333. DOI: 10.2307/3222161

Jankowski T., Collins A.G., Campbell R.D. 2008. Global diversity of inland water cnidarians. Hydrobiology 595: 35–40. DOI: 10.1007/s10750-007-9001-9

Kaliszewicz A., Lipińska A. 2013. Environmental condition related reproductive strategies and sex ratio in hydras. Acta Zoologica (Stockholm) 94: 177–183. DOI: 10.1111/j.1463-6395.2011.00536.x

Kamaltynov R.M., Kamaltynov P.R. 2000. Crawfish colonization of the basins near Irkutsk City. In: Third International Vereshchagin Baikal Conference, pp. 103.

Katoh K., Misawa K., Kuma K. et al. 2002. MAFFT: A novel method for rapid multiple sequence alignment based on fast Fourier transform. Nucleic Acids Research 30: 3059–3066.

Khanaev I.V., Kravtsova L.S., Maikova O.O. et al. 2018. Current state of the sponge fauna (Porifera: Lubomirskiidae) of Lake Baikal: Sponge disease and the problem of conservation of diversity. Journal of Great Lakes Research 44: 77–85. DOI: 10.1016/j.jglr.2017.10.004

Koryakov E.A., Glazunov I.V., Vilisova I.K. 1977. Coastal lakes of Lake Baikal until its stabilization. In: Florensov N.A. (Ed.), Limnology of the coastal zone of Lake Baikal. Novosibirsk, pp. 4–44. (in Russian)

Kozhov M.M. 1947. The animal world of Lake Baikal. Irkutsk: Ogiz. (in Russian)

Kozhov M.M. 1962. Biology of Lake Baikal. Moscow: Nauka. (in Russian)

Kravtsova L.S., Izhboldina L.A., Mekhanikiva I.V. et al. 2010. Naturalization of *Elodea canadensis* Mich. in Lake Baikal. Russian Journal of Biological Invasions 1: 162–171. DOI: 10.1134/S2075111710030045 (in Russian)

Littlefield C.L. 1986. Sex determination in hydra: control by a subpopulation of interstitial cells in *Hydra oligactis* males. Developmental Biology 117: 428–434.

Martínez D.E., Iñigues A.R., Percell K.M. et al. 2010. Phylogeny and biogeography of *Hydra* (Cnidaria: Hydridae) using mitochondrial and nuclear DNA sequences. Molecular Phylogenetics and Evolution 57: 403–410. DOI: 10.1016/j.ympev.2010.06.016

Ronquist F., Huelsenbeck J.P. 2003. MrBayes 3: Bayesian phylogenetic inference under mixed models. Bioinformatics 19: 1572–1574. DOI: 10.1093/bioinformatics/btg180.

Schuchert P. 2010. The European athecate hydroids and their medusae (Hydrozoa, Cnidaria): Capitata part 2. Revue suisse de Zoologie 3: 440–449.

Schwentner M., Bosch T.C.G. 2015. Revisiting the age, evolutionary history and species level diversity of the genus Hydra (Cnidaria: Hydridae). Molecular Phylogenetics and Evolution 91: 41–55. DOI: 10.1016/j.ympev.2015.05.013

Shimaraev M.N., Kuimova L.N., Sinyukovich V.N. 2002. On evidence of global climate changes at Lake Baikal in the XX century. Doklady Earth Science 383: 397–400.

Stepanyants S.D., Anokhin B.A. 2001. Hydrozoa (Cnidaria: Hydrida). In: Timoshkin O.A. (Ed.), Index of animal species inhabiting Lake Baikal and its catchment area. Volume 1, Book 1. Novosibirsk, pp. 193–194. (in Russian)

Stepanyants S.D., Kuznetsova V.G., Anokhin B.A. 2003. Hydra: from Abraam Tramble until our days. Moscow-Saint-Petersburg: Association of scientific publications KMK. (in Russian)

Stepanyants S.D., Anokhin B.A., Kuznetsova V.G. 2006. Cnidarian fauna of relict Lakes Baikal, Biwa and Khubsugul. Hidrobiologia 568: 225–232. DOI: 10.1007/s10750-006-0310-1

Tamura K., Stecher G., Peterson D. et al. 2013. MEGA6: molecular evolutionary genetics analysis version 6.0. Molecular Biology and Evolution 30: 2725–2729. DOI: 10.1093/molbev/mst197

Thompson J.D., Higgins D.G., Gibson T.J. 1994. ClustalW: improving the sensitivity of progressive multiple sequence alignment through sequence weighting, positionspecific gap penalties and weight matrix choice. Nucleic Acids Research 22: 4673–4680.

Timoshkin O.A., Moore M.V., Kulikova N.N. et al. 2018. Groundwater contamination by sewage causes benthic algal outbreaks in the littoral zone of Lake Baikal (East Siberia). Journal of Great Lakes Research 44: 230–244. DOI: 10.1016/j.jglr.2018.01.008

Tökölyi J., Bradács F., Hóka N. et al. 2016. Effects of food availability on asexual reproduction and stress tolerance along the fast–slow life history continuum in freshwater hydra (Cnidaria: Hydrozoa). Hydrobiologia 766: 121–133.

White T.J., Bruns T., Lee S. et al. 1990. Amplification and direct sequencing of fungal ribosomal RNA genes for phylogenetics. In: Innis M.A., Gelfand D.H., Sninsky J.J., White T.J. (Eds.), PCR Protocols: A Guide to Methods and Applications. NY Acad. Press, pp. 315–322.

Limnology and Freshwater Biology 2018 (2): 113-121 DOI:10.31951/2658-3518-2018-A-2-113

Original Article

ISSN 2658-3518
LIMNOLOGY FRESHWATER BIOLOGY
www.limnolfwbiol.com

Phenetic relationships and diagnostic features of sculpins of the genus *Asprocottus* (Scorpaeniformes: Cottoidea)

Bogdanov B.E.*

Limnological Institute, Siberian Branch of the Russian Academy of Sciences, Ulan-Batorskaya Str., 3, Irkutsk, 664033, Russia

ABSTRACT. Aimed at the study of phenetic and taxonomic relationships of Baikal endemic sculpins of the genus *Asprocottus* Berg 1906, the author has carried out a morphometric investigations by 11 meristic and 29 plastic characters as well as analyzed nonmetric features: coloration peculiarities of specimens, form and location of bony spinelets on the integuments, morphology of the sensory system organs and the number of preopercular spines. The results of the study have confirmed the validity of seven species: *A. herzensteini*, *A. abyssalis, A. intermedius*, *A. korjakovi, A. parmiferus, A. platycephalus*, and *A. pulcher*. Based on the revision of the diagnostic features, the author proposes the new key to determine species.

Keywords: *Asprocottus*, systematics, morphology, phenetic relationships, diagnostic features, Lake Baikal

1. Introduction

The genus *Asprocottus* established by L.S. Berg (Berg, 1906), and originally included only one species: *A. herzensteini* (Berg, 1906; 1907; 1933; 1949). Then, D.N. Taliev (1955) extended its composition by moving the species from other genera *A. gibbosus* (from the genus *Abyssocottus*), *A. pulcher* (from *Cottinella*) and *A. megalops* with subspecies *A. m. eurystomus* and *A. kozovi* (from *Limnocottus*). Moreover, representatives of *A. herzensteini*: *A. herzensteini abyssalis*, *A. herzensteini intermedius*, *A. herzensteini parmiferus*, and *A. herzensteini platycephalus* were described as subspecies, but later this status was elevated to species (Sideleva, 1982). Subsequently, new species *A. korjakovi* and *A. korjakovi minor* were described, and *A. intermedius* was indicated as a synonym of *A. herzensteini* (Sideleva, 2001).

Currently, the genus is usually considered to consist of eight species: *A. herzensteini*, *A. abyssalis, A. intermedius*, *A. korjakovi, A. minor, A. parmiferus, A. platycephalus*, *and A. pulcher* (Bogutskaya and Naseka, 2004; Eschmeyer et al., 2018). However, there are doubts about the validity of *A. intermedius* and the taxonomic rank of *A. minor / A. korjakovi minor*. In this regard, it is necessary to conduct a study aimed at clarifying the taxonomic boundaries of species and the development of a new key for their determination.

2. Material and methods

The study was carried out on the material collected by the author in 2000 – 2004 as well as archival materials of Laboratory of ichthyology of LIN SB RAS collected by V.G. Sidelyova, A.N. Telpukhovsky, P.N. Anoshko, I.V. Khanaev, and S.V. Kirilshik in 1977 – 2009. Fishes were caught with gill nets and beam-trawl. In total, we examined 22 specimens of *A. herzensteini*, 14 – *A. abyssalis,* 17 – *A. intermedius*, 20 – *A. korjakovi,* 38 – *A. minor,* 14 – *A. parmiferus,* 68 – *A. platycephalus*, and 30 – *A. pulcher*. Species were identified by meristic features, peculiarities of coloration and morphology of the seismosensory system organs specified in the original descriptions and subsequent revisions (Berg, 1906; 1949; Taliev, 1955; Sideleva, 1982; 2001; 2003). The nomenclature is shown in accordance with the provisions of the International Code of Zoological Nomenclature (1999).

The morphometric examination was carried out by 11 meristic and 28 plastic characters. We analyzed: number of neuromasts in the lateral (*l.l.*), supraorbital (*lso*), infraorbital (*lio*), temporal (*lt*), preopercular-mandibular (*lpm*) and occipital (*lo*) sensory lines; number of rays in the first (D_1) and second (D_2) dorsal, pectoral (*P*), and anal (*A*) fins, number of gill rakers (*sp.br*); head length (*c*), length (*l*), height (*H*) and width (*w*) of the trunk; length (*lpc*) and height (*h*) of caudal peduncle; antedorsal (*aD*), postdorsal (*pD*), anteventral (*aV*), anteanal (*aA*), pectroventral (*P-V*) and ventro-anal (*V-A*) distances; length of insertions of the first (lD_1) and second (lD_2) dorsal and anal (*lA*) fins; length of maximum rays in the first (hD_1) and second (hD_2) dorsal, anal (*hA*), pectoral (*lP*), and ventral (*lV*) fins; snout length (*ao*); longitudinal eye diameter (*o*); postorbital distance (*po*); head height near occiput (*cH*) and

*Corresponding author.
E-mail address: bakhtiar.bogdanov@mail.ru (B.E. Bogdanov)

near vertical of the eye middle (*ch*); interorbital distance (*io*); and length of upper (*lmx*) and lower (*lmd*) jaws. Statistical processing of the material was performed by the generally accepted methods (Plokhinskiy, 1980). Table 1 shows the variability of meristic and plastic characters. Selections were compared by factor analysis methods (PCA) using SPSS 8.0 software. For assessment of the degree of differences, *CD* coefficient was used (Mayr, 1969).

3. Results and discussion

The following features characterize sculpins of the genus *Asprocottus*. Each pelvic fin has three soft rays. The anal fin is equal or slightly shorter than the second dorsal one. The pectoral fins are fan-shaped with a wide base. The dorsal fins are located separately or adjoin the bases. The eyes are round, and their diameter coincides with or slightly smaller than the size of the orbit.

There are crests on the infraorbital and supraorbital bones. A degree of their development in different species is unequal. On *preoperculum* there are 4-5 spines, of which the first three, rarely two, upper ones are well developed, and the lower ones can be rudimentary.

The body is completely or partially covered with bony spinelets. They can be seated separately or accreted at the base.

The external neuromasts located on the skin processes, papillae, represent the sensory system. Normally, there is an additional row of neuromasts on the body above the lateral line reaching the vertical of the posterior margin or the middle of the second dorsal fin. In the anterior part of the body, groups of neuromasts, rudiments of the second and third additional rows, can be located above or below the lateral line.

Analysis of differences by *CD* (Table 2) showed taxonomically significant differences between all species, except for *A. korjakovi* and *A. minor*. Discrete differences were determined in 13 of 27 pairwise comparisons by one – four characteristics. *A. parmiferus* having discrete differences with all other species differed the most.

Multidimensional analysis (PCA) of the variability of the meristic and plastic characters of all eight species indicated that the first and second principal components explain 34.9% of total dispersion. The maximum positive loads on the first principal component yield the number of neuromasts in supraorbital, infraorbital and preopercular-mandibular lines, and the negative one – interorbital distance. The maximum positive load on the second principal component is the head length, and the negative one – the number of neuromasts in the lateral line.

On the diagram of the species dispersion in the space of the first two principal components (Fig. 1a), *A. parmiferus* and *A. platycephalus* occupied a separate position. Other species formed three pairs of phenetically similar forms: *A. herzensteini* – *A. abyssalis, A. intermedius* – *A. pulcher*, and *A. korjakovi* – *A. minor* (Fig. 1b). The multidimensional analysis of these pairs

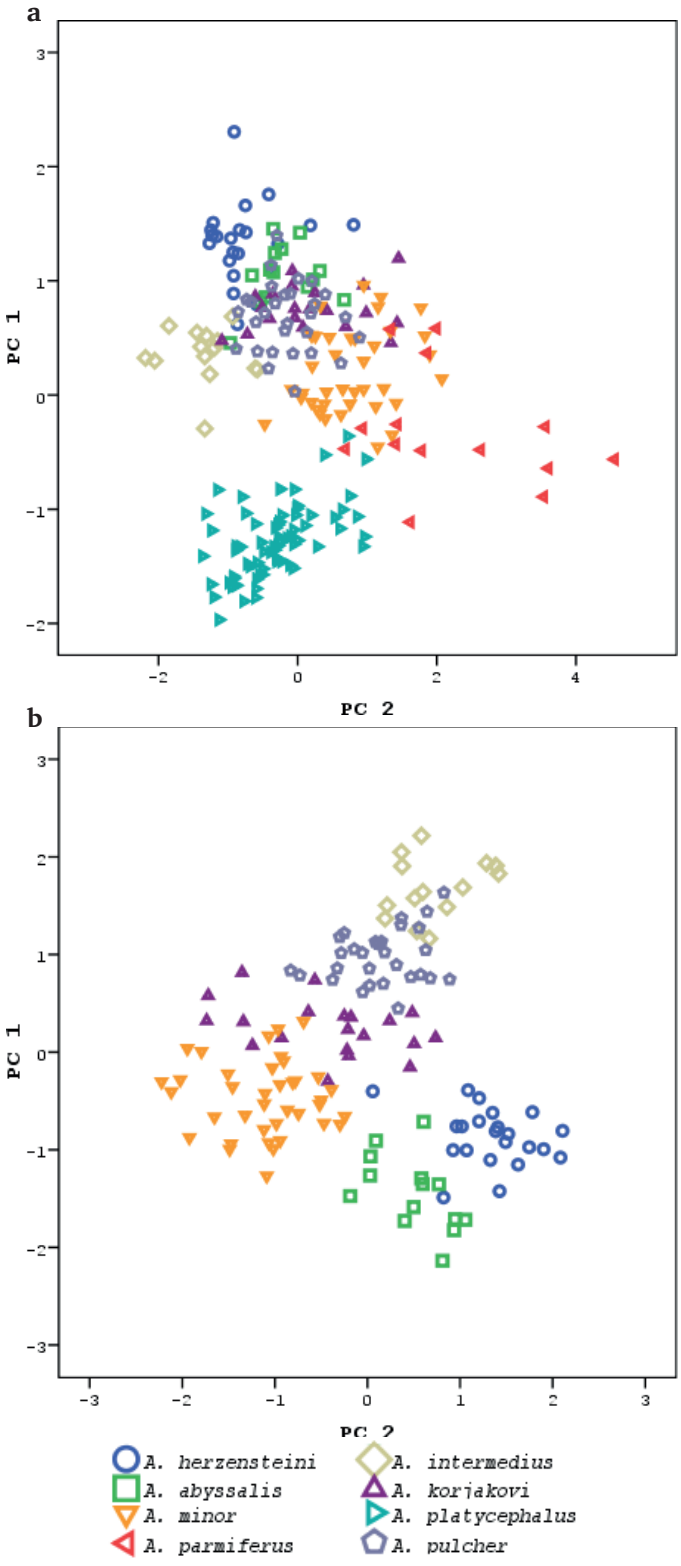

Fig. 1. Distribution of species of genus *Asprocottus* in the space of a first (PC1) and second (PC2) principals components by meristic and plastic characters: a – all species; b – the same thing, without *A. parmiferus* and *A. platycephalus*

(Fig. 2), like the analysis of the differences by *CD* (Table 2), has shown that in the pairs *A. herzensteini* – *A. abyssalis* and *A. intermedius* – *A. pulcher* the compared forms belong to different population sets, in this case – to different species, even though they do not have discrete differences. In the pair *A. korjakovi* – *A. minor*, such differences have not been identified, which indicates the conspecificity of these forms.

Table 1. The total length (*TL*), standard length (*SL*) and morphometric characters of the species of the genus *Asprocottus*

	A. herzensteini (*n*=22)	*A. abyssalis* (*n*=14)	*A. intermedius* (*n*=17)	*A. korjakovi* (*n*=20)	*A. minor* (*n*=38)	*A. platycephalus* (*n*=68)	*A. parmiferus* (*n*=14)	*A. pulcher* (*n*=29)
TL (mm)	100.9 77.9-116.0	66.4 61.0-71.9	80.8 73.6-87.2	104.8 86.2-123.2	75.5 68.3-87.7	94.3 80.2-109.5	63.2 44.2-77.1	96.9 86.7-108.3
SL (mm)	84.8 65.3-98.2	54.7 51.2-60.3	69.1 62.4-75.0	89.2 72.7-104.6	62.6 55.5-74.0	80.0 65.9-93.0	52.3 35.9-64.8	80.6 71.6-90.9
Meristic characters								
D_1	6.4 ± 0.10 6-7; 0.49	6.5 ± 0.20 5-8; 0.73	6.1 ± 0.10 5-7; 0.42	5.0 ± 0.15 3-6; 0.67	5.2 ± 0.08 4-6; 0.49	6.1 ± 0.07 5-7; 0.60	5.4 ± 0.19 4-7; 0.73	6.0 ± 0.12 5-7; 0.64
D_2	15.4 ± 0.14 14-16; 0.64	14.6 ± 0.17 14-16; 0.62	16.3 ± 0.16 15-17; 0.67	14.9 ± 0.13 14-16; 0.57	14.7 ± 0.14 13-17; 0.88	15.6 ± 0.10 14-17; 0.84	14.6 ± 0.22 13-16; 0.82	16.1 ± 0.11 15-17; 0.57
P	15.9 ± 0.11 15-17; 0.51	14.1 ± 0.21 13-15; 0.80	13.7 ± 0.18 13-16; 0.75	15.0 ± 0.05 14-15; 0.22	14.9 ± 0.08 13-16; 0.52	14.5 ± 0.07 13-15; 0.55	15.4 ± 0.28 14-17; 1.05	14.8 ± 0.11 14-16; 0.59
A	13.5 ± 0.15 12-15; 0.72	13.1 ± 0.17 12-14; 0.64	15.5 ± 0.17 14-17; 0.70	14.8 ± 0.09 14-15; 0.40	14.4 ± 0.13 13-16; 0.81	15.1 ± 0.09 14-17; 0.73	13.6 ± 0.31 12-15; 1.18	14.8 ± 0.13 14-16; 0.73
sp.br.	6.5 ± 0.17 5-8; 0.78	7.0 ± 0.23 6-8; 0.85	5.4 ± 0.20 4-7; 0.84	6.2 ± 0.09 6-7; 0.40	5.9 ± 0.12 4-7; 0.72	5.8 ± 0.08 4-8; 0.69	5.1 ± 0.22 4-6; 0.83	6.1 ± 0.15 5-9; 0.83
l.so.	10.4 ± 0.15 9-12; 0.98	9.5 ± 0.15 8-12; 0.78	10.4 ± 0.26 9-12; 0.98	9.6 ± 0.16 8-12; 1.02	7.8 ± 0.10 6-11; 0.87	7.4 ± 0.15 6-10; 0.94	7.5 ± 0.20 6-10; 1.01	9.7 ± 0.13 8-12; 0.98
l.io.	19.7 ± 0.16 17-22; 1.04	17.1 ± 0.25 14-20; 1.33	16.1 ± 0.22 14-18; 0.83	17.9 ± 0.16 16-20; 1.03	16.5 ± 0.16 14-20; 1.35	14.6 ± 0.14 13-17; 0.86	13.7 ± 0.37 11-19; 1.87	17.8 ± 0.16 15-20; 1.22
l.t.	3.3 ± 0.10 2-4; 0.62	4.3 ± 0.10 4-6; 0.51	4.6 ± 0.19 4-6; 0.73	2.4 ± 0.11 1-5; 0.70	2.3 ± 0.11 1-4; 0.91	3.1 ± 0.10 2-4; 0.56	3.4 ± 0.14 2-4; 0.69	4.6 ± 0.08 4-6; 0.65
l.oc.	1.8 ± 0.08 1-3; 0.53	1.6 ± 0.19 1-4; 0.88	2.1 ± 0.16 1-3; 0.59	1.2 ± 0.07 1-2; 0.42	1.1 ± 0.04 1-3; 0.33	1.0 ± 0.03 1-2; 0.18	1.3 ± 0.11 1-3; 0.55	1.3 ± 0.07 1-3; 0.53
l.pm.	22.0 ± 0.23 19-25; 1.52	20.7 ± 0.28 18-23; 1.47	21.9 ± 0.53 19-26; 1.99	21.8 ± 0.22 19-24; 1.37	19.3 ± 0.16 16-23; 1.43	16.7 ± 0.17 15-19; 0.99	15.8 ± 0.54 11-21; 2.78	21.8 ± 0.24 17-26; 1.83
l.l.	41.2 ± 0.62 34-50; 4.04	36.5 ± 0.59 31-43; 3.10	51.0 ± 2.52 42-61; 6.65	40.4 ± 0.54 34-48; 3.29	34.8 ± 0.22 31-42; 1.95	35.8 ± 0.43 32-42; 2.30	31.7 ± 1.10 20-38; 5.59	43.6 ± 0.61 37-58; 4.62
Plastic characters in % *SL*								
c	31.7 ± 0.22 29.9-33.9; 1.04	32.1 ± 0.31 29.3-33.9; 1.16	31.0 ± 0.27 29.2-33.0; 1.13	33.0 ± 0.30 30.2-35.5; 1.35	33.9 ± 0.16 32.3-36.9; 1.01	32.7 ± 0.13 30.4-36.3; 1.11	35.7 ± 0.35 33.6-38.7; 1.31	34.0 ± 0.20 31.2-36.7; 1.06
L	71.2 ± 0.34 68.6-74.3; 1.59	71.8 ± 0.35 67.6-73.8; 1.33	72.9 ± 0.35 69.9-75.7; 1.45	71.9 ± 0.32 69.7-74.8; 1.41	70.9 ± 0.25 67.4-74.7; 1.56	69.9 ± 0.18 65.7-72.8; 1.47	69.3 ± 0.67 64.3-73.0; 2.49	70.5 ± 0.36 65.8-73.7; 1.92

	A. herzensteini (*n*=22)	*A. abyssalis* (*n*=14)	*A. intermedius* (*n*=17)	*A. korjakovi* (*n*=20)	*A. minor* (*n*=38)	*A. platycephalus* (*n*=68)	*A. parmiferus* (*n*=14)	*A. pulcher* (*n*=29)
H	16.3 ± 0.30 14.5-21.0; 1.39	17.3 ± 0.34 15.4-19.2; 1.29	17.4 ± 0.33 13.9-19.4; 1.37	20.4 ± 0.46 15.9-23.4; 2.05	19.4 ± 0.27 15.5-22.7; 1.69	15.8 ± 0.22 12.4-20.3; 1.82	22.1 ± 0.55 18.3-25.6; 2.07	18.9 ± 0.22 16.5-21.3; 1.18
h	5.7 ± 0.08 5.1-6.9; 0.36	6.5 ± 0.09 6.1-7.3; 0.32	5.4 ± 0.11 4.5-6.2; 0.44	6.0 ± 0.13 5.3-7.4; 0.57	6.1 ± 0.08 5.2-7.2; 0.48	5.6 ± 0.06 4.6-6.9; 0.53	6.7 ± 0.21 5.2-8.2; 0.78	5.9 ± 0.07 5.0-6.8; 0.38
w	15.2 ± 0.29 12.4-18.4; 1.35	15.8 ± 0.36 13.4-18.3; 1.34	16.7 ± 0.26 14.9-18.4; 1.09	18.3 ± 0.37 14.3-21.2; 1.68	15.6 ± 0.21 13.3-18.9; 1.28	15.2 ± 0.15 12.5-17.7; 1.20	18.1 ± 0.44 14.8-20.4; 1.66	15.8 ± 0.15 14.0-17.2; 0.79
aD	36.7 ± 0.31 32.0-39.5; 1.43	36.3 ± 0.41 33.3-38.7; 1.54	37.4 ± 0.41 34.3-40.7; 1.68	38.4 ± 0.32 35.2-40.4; 1.44	39.8 ± 0.34 32.2-42.7; 2.07	37.9 ± 0.25 29.8-40.9; 2.08	41.6 ± 0.51 40.0-46.2; 1.91	39.2 ± 0.40 31.1-42.8; 2.14
pD	15.0 ± 0.26 12.2-17.6; 1.20	15.5 ± 0.64 11.3-20.2; 2.39	12.9 ± 0.33 10.2-15.1; 1.35	13.5 ± 0.24 11.7-15.5; 1.09	13.4 ± 0.22 10.1-16.1; 1.37	11.9 ± 0.17 8.3-15.2; 1.40	11.7 ± 0.41 8.9-14.6; 1.54	11.4 ± 0.23 8.7-14.9; 1.26
aV	28.2 ± 0.23 26.4-31.0; 1.08	27.3 ± 0.39 25.0-29.6; 1.47	29.7 ± 0.28 27.5-32.2; 1.16	30.5 ± 0.39 27.3-33.9; 1.73	29.3 ± 0.30 26.6-37.0; 1.87	28.7 ± 0.18 25.3-31.9; 1.52	29.7 ± 0.52 26.5-33.4; 1.95	30.8 ± 0.22 28.3-32.8; 1.19
aA	56.5 ± 0.32 54.4-60.0; 1.52	54.7 ± 0.34 52.8-57.1; 1.27	54.6 ± 0.36 52.5-58.5; 1.50	55.8 ± 0.40 53.0-59.3; 1.81	55.0 ± 0.21 51.7-58.4; 1.28	54.6 ± 0.19 50.8-58.2; 1.60	57.0 ± 0.67 52.7-62.1; 2.51	56.2 ± 0.26 53.9-59.7; 1.39
lpc	16.1 ± 0.33 13.4-19.8; 1.56	16.9 ± 0.24 15.4-18.5; 0.88	12.5 ± 0.29 10.3-14.5; 1.19	12.7 ± 0.24 10.2-14.1; 1.07	13.3 ± 0.29 9.4-16.5; 1.77	11.6 ± 0.14 8.9-13.5; 1.14	11.5 ± 0.60 7.8-16.6; 2.26	12.3 ± 0.28 9.9-15.5; 1.50
PV	4.3 ± 0.14 3.2-5.7; 0.66	4.2 ± 0.18 3.0-5.4; 0.68	5.6 ± 0.16 4.5-6.8; 0.66	5.9 ± 0.19 4.3-7.5; 0.83	5.0 ± 0.09 3.9-6.2; 0.58	5.0 ± 0.08 3.6-6.4; 0.70	4.9 ± 0.14 4.1-5.9; 0.54	5.2 ± 0.15 3.7-6.8; 0.80
VA	28.1 ± 0.35 25.2-32.5; 1.63	27.6 ± 0.47 24.4-30.5; 1.77	25.7 ± 0.65 19.0-30.3; 2.68	27.0 ± 0.57 22.6-31.5; 2.55	25.6 ± 0.30 21.7-30.5; 1.87	26.3 ± 0.25 22.1-31.2; 2.08	27.6 ± 0.59 22.3-31.7; 2.20	27.3 ± 0.37 23.9-30.9; 2.00
lD_1	17.6 ± 0.25 15.5-20.1; 1.19	18.2 ± 0.45 15.4-21.1; 1.68	17.1 ± 0.29 15.2-19.7; 1.22	18.5 ± 0.27 16.5-20.6; 1.21	17.4 ± 0.25 14.0-20.3; 1.54	16.2 ± 0.18 12.9-20.2; 1.51	16.8 ± 0.42 14.3-19.9; 1.56	17.1 ± 0.32 13.3-20.7; 1.71
lD_2	30.7 ± 0.42 25.5-33.7; 1.96	31.6 ± 0.42 28.6-35.0; 1.57	33.6 ± 0.44 29.6-36.5; 1.83	29.3 ± 0.32 26.9-31.8; 1.45	30.7 ± 0.29 27.1-34.1; 1.81	32.7 ± 0.21 27.3-36.1; 1.73	32.6 ± 0.63 27.8-36.5; 2.37	32.2 ± 0.34 27.9-37.5; 1.84
hD_1	8.2 ± 0.17 6.8-10.1; 0.78	9.6 ± 0.25 7.8-11.3; 0.95	7.7 ± 0.18 6.5-9.3; 0.73	7.5 ± 0.17 6.3-9.6; 0.76	8.4 ± 0.15 6.9-10.2; 0.92	8.1 ± 0.13 5.1-11.2; 1.06	8.3 ± 0.37 6.4-10.9; 1.39	7.4 ± 0.16 5.9-9.1; 0.86
hD_2	13.0 ± 0.23 11.5-15.7; 1.07	13.1 ± 0.33 10.4-15.0; 1.25	10.1 ± 0.23 8.4-11.6; 0.93	11.2 ± 0.20 9.8-13.8; 0.92	12.2 ± 0.21 9.8-15.8; 1.27	10.3 ± 0.17 8.0-14.9; 1.40	11.6 ± 0.42 9.3-15.3; 1.56	11.9 ± 0.28 9.7-14.7; 1.51
lA	27.1 ± 0.54 16.6-29.9; 2.55	28.4 ± 0.57 24.6-33.3; 2.13	34.4 ± 0.47 30.8-39.4; 1.94	31.2 ± 0.46 27.4-34.9; 2.04	31.6 ± 0.27 28.6-35.0; 1.67	33.8 ± 0.26 29.1-39.9; 2.16	32.7 ± 1.02 23.2-39.0; 3.80	32.3 ± 0.34 27.6-35.2; 1.81
hA	10.9 ± 0.18 9.3-13.3; 0.85	11.0 ± 0.38 7.2-13.1; 1.41	7.8 ± 0.12 6.7-8.7; 0.49	9.5 ± 0.22 7.7-11.9; 1.00	10.7 ± 0.21 8.0-13.9; 1.32	9.5 ± 0,17 7.3-13.3; 1.40	11.9 ± 0.32 10.0-15.2; 1.21	10.0 ± 0.22 8.2-13.3; 1.19
lP	23.4 ± 0.34 19.1-26.2; 1.61	22.3 ± 0.40 18.0-24.9; 1.51	22.1 ± 0.41 17.5-24.4; 1.69	21.2 ± 0.37 17.8-23.9; 1.65	23.1 ± 0.26 20.4-26.8; 1.59	19.6 ± 0,20 15.4-23.2; 1.64	24.5 ± 0.55 20.7-28.1; 2.07	23.5 ± 0.20 20.5-25.5; 1.06

	A. herzensteini (*n*=22)	*A. abyssalis* (*n*=14)	*A. intermedius* (*n*=17)	*A. korjakovi* (*n*=20)	*A. minor* (*n*=38)	*A. platycephalus* (*n*=68)	*A. parmiferus* (*n*=14)	*A. pulcher* (*n*=29)
lV	15.0 ± 0.24 13.7-17.1; 1.11	16.1 ± 0.43 13.7-20.1; 1.62	13.0 ± 0.14 11.6-13.7; 0.56	14.3 ± 0.17 12.9-15.8; 0.78	15.0 ± 0.19 11.8-18.0; 1.18	12.5 ± 0,14 10.0-15.7; 1.12	15.7 ± 0.60 11.1-19.8; 2.24	15.1 ± 0.17 13.2-17.1; 0.90
	Plastic characters in % *c*							
ao	26.5 ± 0.17 25.4-28.3; 0.79	25.2 ± 0.52 22.2-28.8; 1.94	26.4 ± 0.34 24.4-29.5; 1.39	26.4 ± 0.29 24.0-28.7; 1.30	26.9 ± 0.30 21.7-30.0; 1.84	25.5 ± 0.15 22.1-28.7; 1.23	29.5 ± 0.42 26.7-32.5; 1.58	28.1 ± 0.24 26.3-30.7; 1.31
o	23.4 ± 0.32 20.5-26.2; 1.52	26.9 ± 0.53 24.3-31.3; 2.00	22.6 ± 0.33 20.4-24.8; 1.38	21.0 ± 0.35 17.4-23.9; 1.58	24.1 ± 0.30 20.9-29.1; 1.87	19.5 ± 0.20 15.1-23.4; 1.68	21.9 ± 0.59 18.0-26.6; 2.20	20.9 ± 0.17 19.2-23.3; 0.94
op	43.7 ± 0.37 39.6-46.7; 1.71	43.0 ± 0.37 40.0-45.1; 1.40	46.4 ± 0.46 41.6-49.4; 1.92	45.3 ± 0.64 41.1-49.8; 2.88	45.1 ± 0.26 41.3-50.5; 1.62	44.9 ± 0.20 40.1-48.5; 1.63	47.1 ± 0.68 44.0-53.8; 2.56	46.7 ± 0.32 42.6-50.5; 1.70
cH	47.9 ± 0.70 42.4-55.3; 3.27	51.0 ± 0.94 44.3-56.9; 3.52	51.8 ± 0.73 47.3-59.3; 3.02	55.4 ± 0.93 46.6-61.5; 4.16	53.0 ± 0.53 45.8-61.0; 3.25	44.8 ± 0.41 37.6-52.0; 3.39	56.1 ± 1.20 47.5-66.2; 4.48	75.9 ± 0.68 70.2-83.0; 3.66
ch	34.5 ± 0.52 28.5-39.1; 2.44	37.6 ± 0.74 33.2-42.6; 2.77	34.8 ± 0.37 30.4-36.7; 1.51	38.6 ± 0.57 33.2-43.5; 2.57	37.0 ± 0.48 30.7-42.4; 2.94	30.7 ± 0.27 25.6-36.3; 2.20	39.5 ± 0.50 37.3-42.1; 1.86	51.1 ± 0.60 44.4-59.8; 3.21
io	14.4 ± 0.29 12.1-17.2; 1.38	17.3 ± 0.29 15.6-19.4; 1.09	9.4 ± 0.34 6.7-13.2; 1.39	14.1 ± 0.31 12.1-17.7; 1.41	13.0 ± 0.27 8.5-15.9; 1.66	17.0 ± 0.14 14.4-19.7; 1.14	20.4 ± 0.45 18.2-24.4; 1.67	36.7 ± 0.41 29.0-41.0; 2.21
lmx	35.8 ± 0.32 33.2-38.6; 1.49	35.1 ± 0.52 30.6-38.8; 1.94	42.6 ± 0.44 39.0-47.0; 1.81	37.5 ± 0.26 34.2-39.7; 1.17	36.3 ± 0.23 33.0-39.0; 1.44	38.3 ± 0.18 34.8-41.3; 1.47	41.9 ± 0.95 35.7-47.4; 3.55	11.5 ± 0.28 8.9-15.1; 1.48
lmd	46.4 ± 0.31 43.5-49.3; 1.47	46.4 ± 0.39 43.0-49.3; 1.45	48.7 ± 0.38 46.4-52.0; 1.59	48.2 ± 0.42 43.3-51.1; 1.87	48.0 ± 0.26 43.0-51.2; 1.62	49.2 ± 0.29 38.8-54.6; 2.39	49.2 ± 0.59 45.2-52.4; 2.19	42.3 ± 0.33 38.9-46.1; 1.78

Note: Above the line – mean value and its error; under the line – limits of variation of character and mean square deviation.

Table 2. Differences in the morphometric characters of species of the genus *Asprocottus* reaching a taxonomically significant level (CD > 1.28)

	A. herzensteini	*A. abyssalis*	*A. intermedius*	*A. korjakovi*	*A. minor*	*A. parmiferus*	*A. platycephalus*
A. abyssalis	*P*						
A. intermedius	*P, A, l.io., lpc, hD_2, *lA, *hA, io, *lmx*	*D_2, A, l.l., *lpc, hD_1, lA, hA, lV, *io, *lmx*					
A. korjakovi	*P, lpc*	*A, l.t., *lpc, *o, io*	*P, l.t., lD_2, io, lmx*				
A. minor	*D_1, l.so., l.io.*	*l.t., lpc, io*	*l.so., l.t., l.l., c, hA, lmx*	–			
A. parmiferus	*l.so., l.io. l.pm., c, H, *aD,* io*	*c, H, *aD, lpc*	*l.so., l.pm., *l.l., *c, H, *hA, *io*	*l.io. l.pm.,*io*	*io*		
A. platycephalus	*P, l.so., l.io, l.pm., lpc, lA*	*A, l.pm., *pl, lA, lV, *o, cH*	*l.so., l.oc., l.pm., l.l., *io, lmx*	*l.io, l.pm., cH, ch*	*o, io*	*H, lP, cH, *ch*	
A. pulcher	*pD, *lmx*	*D_2, aV, lpc, o,*io, *lmx*	*c, lA, lV*	*l.t., lmx*	*l.t., l.l., lmx*	*l.io., l.pm.,*io*	*l.io, l.pm., lP, ch, io*

Note: * - characters for which there is hiatus.

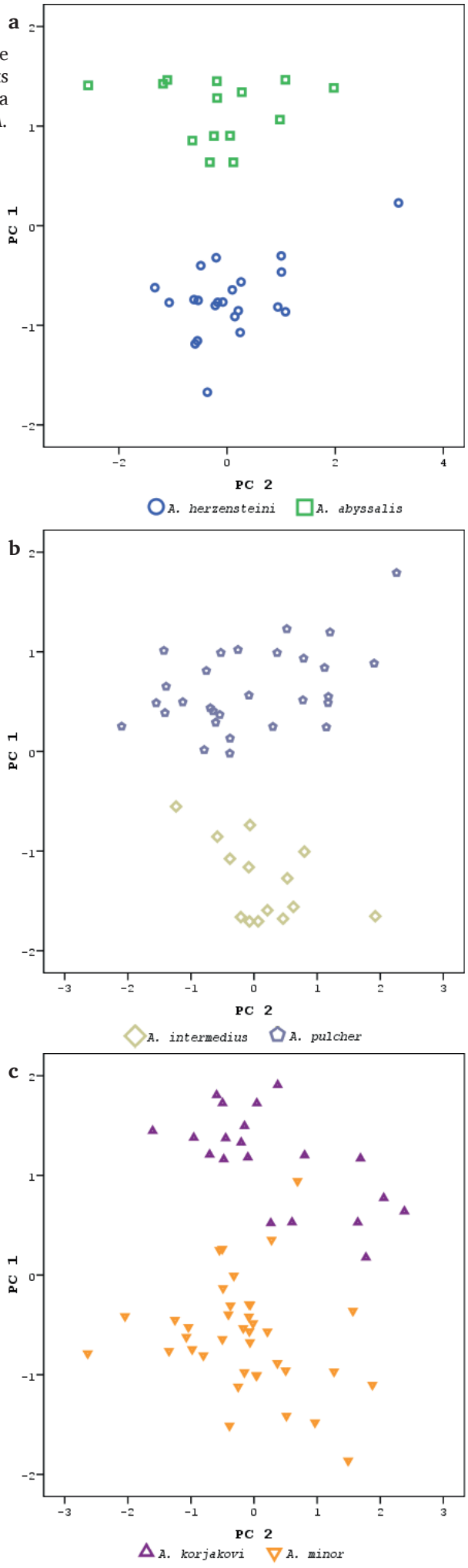

Fig. 2. Distribution of species of genus *Asprocottus* in the space of a first (PC1) and second (PC2) principals components by meristic and plastic characters in pairwise comparison: a – *A. herzensteini* and *A. abyssalis*; b – *A. intermedius* and *A. pulcher*; c – *A. korjakovi* and *A. minor*

Therefore, the genus *Asprocottus* includes seven valid species, *A. herzensteini*, *A. abyssalis, A. intermedius*, *A. korjakovi, A. parmiferus, A. platycephalus*, and *A. pulcher*, that are characterized by the following features.

Asprocottus herzensteini: (Fig 3a, 4a); D_1 6–7; D_2 13–16; *P* 15–17; *V* I 3; *A* 12–15; *sp.br.* 5–8, *l.so.* 9–12, *l.io.* 17–22, *l.t.* 2–4, *l.oc.* 1–3, *l.pm.* 19–25, *l.l.* 34–50. Body oblong. Back slightly raised above the nape. Dorsal fins separated by a small gap. Pelvic fins short, approximately half the distance to the anus. Head moderately flattened. Eyes large, oval, occupy all or most of the orbit. Interorbital distance narrow, two-three times less than the diameter of the eye. Well-defined crests on the infraorbital and frontal bones are. Four well-developed spines on *preoperculum*. Neuromasts of the sensory lines of the head are located on high papillae. Papillae of the truncal lines short. As a rule, there is one additional row above the lateral line. In addition, separate neuromasts may be located above or below the main row. Body completely covered with needle-shaped spinelets not aggregated into plates. Coloration pale yellow of grey; juveniles are pale yellow or pink. The upper part of the body and head darker; belly and fins lighter.

Asprocottus abyssalis: (Fig 3b, 4b); D_1 5–8; D_2 13–16; *P* 13–16; *V* I 3; *A* 12–14; *sp.br.* 6–8, *l.so.* 8–12, *l.io.* 14–20, *l.t.* 4–6, *l.oc.* 1–4 (or absent), *l.pm.* 18–23, *l.l.* 31–46. Body oblong. Back slightly raised above the nape. Dorsal fins separated by a small gap. Pelvic fins short, approximately half the distance to the anus. Head moderately flatted. Eyes large, oval, occupy all or most of the orbit. Interorbital distance narrow, two-three times less than the diameter of the eye. Crests on the infraorbital and front bones are not defined. Two well-developed spines on *preoperculum*. Neuromasts of the sensory lines are located on high papillae. Papillae of the truncal lines short. As a rule, there is one additional row above the lateral line. In addition, separate neuromasts may be located above or below the main row. Body completely covered with needle-shaped spinelets not aggregated into plates. Coloration pale yellow or pink. The upper part of the body and head darker; belly and fins are lighter.

Asprocottus intermedius: (Fig 3c, 4c); D_1 5–7; D_2 15–17; *P* 13–17; *V* I 3; *A* 14–17; *sp.br.* 4–7, *l.so.* 9–12, *l.io.* 14–18, *l.t.* 6–6, *l.oc.* 1–3, *l.pm.* 19–26, *l.l.* 42–61. Body oblong. Back slightly raised above the nape. Dorsal fins separated by a small gap. Pelvic fins short, approximately half the distance to the anus. Head flattened. Eyes large, oval, occupy the entire orbit. Interorbital distance narrow, two-tree times less than the diameter of the eye. Infraorbital and front bones have crests. Neuromasts of the sensory and truncal lines are located on short papillae. As a rule, there is one additional row above the lateral line. In addition, separate neuromasts

may be located above or below the main row, which are rudiments of the second and third additional rows. Spinelets on the body rudimentary, separately seated or accreted into the plates. They are located behind the nape and at the base of dorsal and anal fins. The separately located spinelets can be also found on the sides. The upper part of the body and head pale yellow or grey. Belly and fins light.

Asprocottus korjakovi: (Fig 3d, 4d); D_1 3–7; D_2 13–17; *P* 13–16; *V* I 3; *A* 13–16; *sp.br.* 4–7, *l.so.* 6–12, *l.io.* 14–20, *l.t.* 1–5, *l.oc.* 1–3, *l.pm.* 16–24, *l.l.* 31–48. Body short. Back raised above the nape. Dorsal fins separated by a small gap. Pelvic fins short, approximately half the distance to the anus. Head large, moderately flattened. Eyes round, of medium size, occupy the entire orbit. Interorbital distance narrow, twice less than the diameter of the eye. Well-defined crests on the infraorbital and front bones. Neuromasts of the sensory lines of the head are located on high papillae. Papillae of the truncal lines short. As a rule, there is one additional row above the lateral line. In addition, separate neuromasts may be located above or below the main row. The body completely covered with spinelets accreted into bony plates on the back and nape. The upper part of the body and head pale yellow or grey, with dark spots on the sides. The belly and fins light.

Asprocottus parmiferus: (Fig 3e, 4e); D_1 4–7; D_2 13–16; *P* 14–17; *V* I 3; *A* 12–15; *sp.br.* 4–6, *l.so.* 6–10, *l.io.* 11–19, *l.t.* 2–4, *l.oc.* 1–3, *l.pm.* 11–21, *l.l.* 20–40. Body short. Back raised above the nape. Dorsal fins separated by a small gap. Pelvic fins short, less than half the distance to the anus. Head large, slightly flattened. Eyes round, of medium size, occupy the entire orbit. Interorbital distance wide, approximately equal to the diameter of the eye. Crests on the infraorbital and front bones. Neuromasts of the sensory lines of the head are located on high papillae. Papillae on the body short. There is one additional row above the lateral line. Sides, back and nape completely covered with bony plates of accreted spinelets. The upper part of the body and head as well as fins are of red and brown colors. Sides, back and fins have numerous dark spots. Belly light.

Asprocottus platycephalus: (Fig 3f, 4f); D_1 4–7; D_2 13–17; *P* 13–15; *V* I 3; *A* 12–17; *sp.br.* 4–8, *l.so.* 6–10, *l.io.* 13–17, *l.t.* 2–4, *l.oc.* 1–2 (or absent), *l.pm.* 15–19, *l.l.* (30) 32–42. Body oblong. Back slightly raised over the nape. Dorsal fins separated by a small gap. Pelvic fins short, approximately half the distance to the anus. Head much

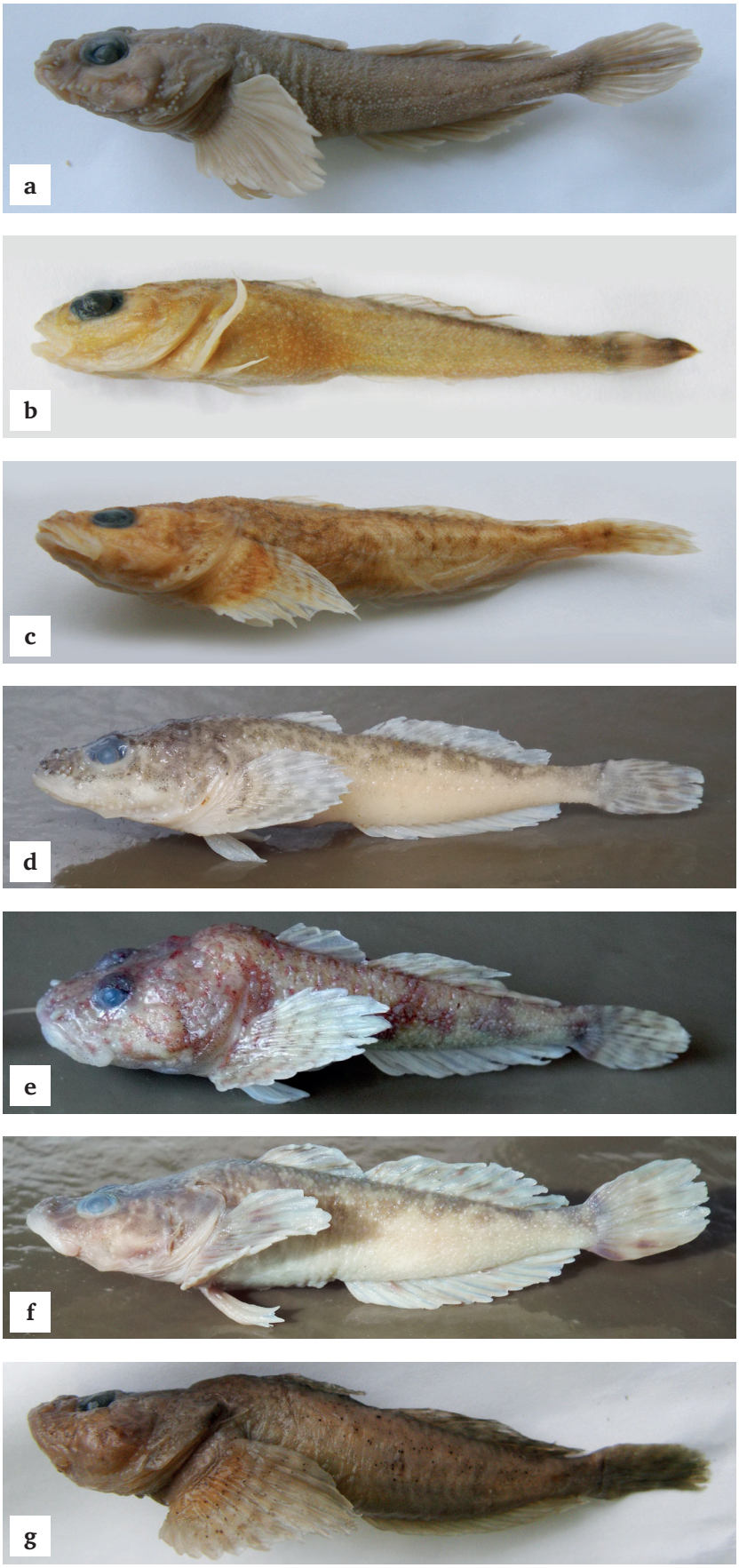

Fig. 3. The appearance (lateral) of sculpins of genus *Asprocottus*: a – *A. herzensteini*, b – *A. abyssalis,* c – *A. intermedius*, d – *A. korjakovi,* e – *A. parmiferus,* f – *A. platycephalus*, g – *A. pulcher*

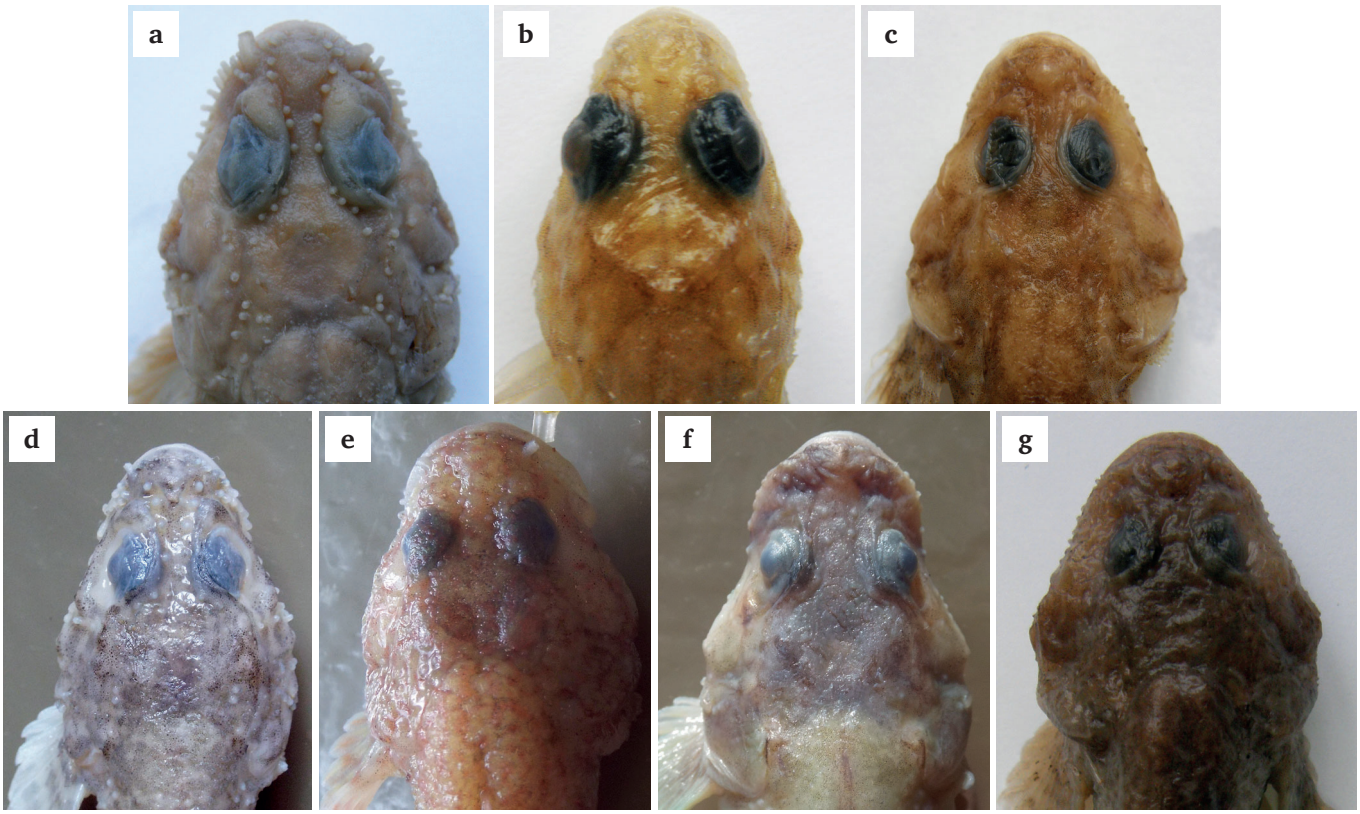

Fig. 4. The head appearance (dorsal) of sculpins of genus *Asprocottus*: a – *A. herzensteini*, b – *A. abyssalis,* c – *A. intermedius*, d – *A. korjakovi,* e – *A. parmiferus,* f – *A. platycephalus*, g – *A. pulcher*

flattened. Eyes round, small, substantially smaller than the orbit. Interorbital distance approximately equal to the diameter of the eye. Poorly defined crests on the infraorbital and front bones. Neuromasts of the sensory lines of the head and body are located on short papillae. On the body, as a rule, there is one additional row of the lateral line. In addition, separate neuromasts may be located above or below the main row, which are rudiments of the second and third additional rows. Body completely covered with small needle-shaped spinelets. The upper part of the body and head pale yellow or grey. Belly and fins light.

Asprocottus pulcher: (Fig 3g, 4g); D_1 5–7; D_2 15–17; *P* 14–16; *V* I 3; *A* 14–16; *sp.br.* 5–9, *l.so.* 8–12, *l.io.* 15–20, *l.t.* 4–6, *l.oc.* 1–3 (or absent), *l.pm.* 17–26, *l.l.* 32–67. Body short. Back behind the nape is sharply raised in the form of a hump. Dorsal fins adjoin or are separated by a mall gap. Pelvic fins short, approximately half the distance to the anus. Head moderately flatted. Eyes large, oval, occupy all or most of the orbit. Interorbital distance narrow, twice smaller than the diameter of the eye. Poorly defined crests on the infraorbital and front bones. Neuromasts of the sensory lines of the head and body are located on shirt papillae. There are three additional rows on the body. Body is bare or looks like bare. Bony needle-shaped spinelets rudimentary, located at the base of the dorsal and pectoral fins. Coloration spotty. Belly light. Fins have rows of dark stripes.

4. Conclusion

Results of the study have confirmed the phenotypic isolation and diagnosability of seven species in the genus *Asprocottus*: *A. herzensteini*, *A. abyssalis, A. intermedius*, *A. korjakovi, A. parmiferus, A. platycephalus*, and *A. pulcher*. It seems appropriate to consider *A. minor* as a small form of *A. korjakovi.* Both, the external similarity and vicarious nature of these forms, indicate this fact. Revision of diagnostic features suggests the following key to determine the species:

1(10) Body is completely or partially covered with well-developed bony spinelets or plates. On the body, as a rule, there is one additional row of the lateral line. In addition, separate neuromasts can be located above or below the main row, which are rudiments of the second and third additional rows.

2(5) Spinelets are needle-shaped, not accreted by bases.

3(4) Head is moderately flatted; the size of the eye corresponds to the size of the orbit, and its diameter is approximately equal to the length of the snout and two-three times more than the interorbital distance.

Infraorbital and supraorbital crests are well developed. There are four well-developed spines on preoperculum: *A. herzensteini*

Infraorbital and supraorbital crests are not developed. There are two well-developed spines on preoperculum: *A.abyssalis*

4(3) Head is very flattened; eye is substantially less than the orbit, its diameter is less than the length

of the snout, and it is approximately equal to the interorbital distance: *A. platycephalus*

5(2) Spines are short with a thickened base, single or accreted into plates.

6(7) Body is completely covered with plates from the accreted spinelets: *A. parmiferus*

7(6) Plates are located only behind the nape and at the base of dorsal fins; the rest of the integument has singly located spines.

8(9) Spinelets are well developed and cover the whole body and the top of the head: *A. korjakovi*

9(8) Spinelets and bony plates are rudimentary, located mainly behind the nape and at the base of the dorsal and anal fins: *A. intermedius*

10(1) Bony spinelets are rudimentary, invisible with the naked eye, simple, needle-like, and located at the base of the dorsal and pectoral fins. There are three additional rows of the lateral line on the body: *A. pulcher*

Acknowledgements

The study was performed within the framework of LIN SB RAS State Task No. 0345–2016–0002: Molecular Ecology and Evolution of Living Systems of Central Asia under Global Ecological Changes.

The author thanks V.V. Pastukhov (Baikal Museum ICS SB RAS), S.V. Kirilchik and I.V. Khanaev (Limnological Institute SB RAS) for assistance in organizing the fieldworks and collecting the material.

References

Berg L.S. 1906. Overview of Cataphracti (Fam. Cottidae, Cottocomephoridae and Comephoridae) of Lake Baikal. Zoologischer Anzeiger [Zoological Bulletin]. 30: 906–911. (in German)

Berg L.S. 1907. The Cataphracti of Lake Baikal (Fam. Cottidae, Cottocomephoridae and Comephoridae). Contributions to the osteology and systematics. In: Scientific results of the zoological expedition to Lake Baikal under the direction of professor Alexis Korotneff in 1900-1902. 3rd ed. St. Petersburg and Berlin, pp. 1–75. (in German)

Berg L.S. 1933. Freshwater fishes of the USSR and adjacent countries. V. 2. Leningrad: Academy of Sciences USSR Publ. (in Russian)

Berg L.S. 1949. Freshwater fishes of the USSR and adjacent countries. V. 3. Moscow, Leningrad: Academy of Sciences USSR Publ. (in Russian)

Bogutskaya N.G, Naseka A.M. 2004. Catalogue of agnathans and fishes of fresh and brackish waters of Russia with comments on nomenclature and taxonomy. Moscow: KMK Scientific Press Ltd. (in Russian)

Catalog of fishes: genera, species, references. 2018. In: Fricke R., Eschmeyer W. N., van der Laan R. (Eds.). [http://researcharchive.calacademy.org/research/ichthyology/catalog/fishcatmain.asp]

International code of zoological nomenclature: fourth edition. 1999. In: Ride W.D.L., Cogger H.G., Dupuis C. et al. (Eds.). [http://www.iczn.org/iczn/index.jsp]

Mayr E. 1969. Principles of systematic zoology. New York: McGraw-Hill.

Plokhinskiy N.A. 1980. Biometric algorithms. Moscow: Moscow University Press. (in Russian)

Sideleva V.G. 1982. Sensory systems and ecology of the Baikal sculpins (Cottoidei). Novosibirsk: Nauka. (in Russian)

Sideleva V.G. 2001. List of fishes from Lake Baikal with descriptions of new taxa of cottoid fishes. Proceedings of the Zoological Institute 287: 45–79.

Sideleva V.G. 2003. The endemic fishes of Lake Baikal. Leiden: Backhuys Publishers.

Taliev D.N. 1955. Sculpin fishes of Lake Baikal (Cottoidei). Moscow, Leningrad: Nauka. (in Russian)

Limnology and Freshwater Biology 2018 (2): 122-134 DOI:10.31951/2658-3518-2018-A-2-122

Original Article

ISSN 2658-3518
LIMNOLOGY FRESHWATER BIOLOGY
www.limnolfwbiol.com

Microevolution processes are detected in symbiotic microbiomes of Baikal sponges by the methods of fractal theory

Feranchuk S.I.[1,2,*], Potapova U.V.[1], Chernogor L.I.[1], Belkova N.L.[1,3], Belikov S.I.[1]

[1] *Limnological Institute, Siberian Branch of the Russian Academy of Sciences, Ulan-Batorskaya Str., 3, Irkutsk, 664033, Russia*
[2] *Department of Informatics, National Research Technical University, Lermontov Str., 83, Irkutsk, 664074, Russia*
[3] *Scientific Centre for Family Health and Human Reproduction Problems, Timiryaseva Str., 16, Irkutsk, 664033, Russia*

ABSTRACT. In recent years, a large scale ecological crisis has been observed in the Lake Baikal ecosystem. It is clearly shown by several signs, including the mass disease of sponges in the coastal zone. To investigate the causes of the crisis, the composition of symbiotic communities in sponges was investigated in 2015 by sequencing of the 16S rRNA gene in three locations of the lake. The methods of fractal theory were adopted in order to detect a fractal structure in the distribution of the sequencing reads, being considered as fragments of the 16S rRNA gene for individual bacteria within the collected samples. The fractal-like distributions were constructed for the seven most abundant phylotypes, and the observed properties of the distributions reflect microevolution processes within the selected genera and species. The values of the fractal dimension, evaluated for the distributions, are observed to correlate with an anthropogenic load at the place of sample collection, for the *Flavobacterium* and *Synechococcus* genera. The sampling sites were also observed to be associated with the properties of the distributions for chloroplasts of Trebouxiophyceae algae, the endosymbiont of *Lubomirskia baicalensis* sponge.The long-scale time dependency of fractal dimension was also evaluated for the data from temperature detectors in four locations of Lake Baikal. The values of the fractal dimension for fluctuations of temperature are also observed to be associated with an anthropogenic load in the place of measurement. The consistency of both approaches validates the usefulness of fractal-based methods in the interpretation of the experiments designed to study the ecological crisis in Lake Baikal.

Keywords: Lake Baikal, sponges, f fractals, microbiome

1. Introduction

1.1 Motivation

Lake Baikal is a unique example of a large-scale and self-sustaining ecosystem, and the ecological crisis on Lake Baikal observed in recent years needs substantial efforts just to investigate the causes and consequences of the changes in this ecosystem. Endemic sponges in Lake Baikal are clearly vulnerable in this crisis (Bormotov, 2011; Timoshkin et al., 2016; Khanaev et al., 2018). The sponges in Baikal, like all species of the phylum Porifera, always develop in symbiosis with bacterial and micro-algae species (Taylor et al., 2007; Chernogor et al., 2013; Webster and Thomas, 2016). So, the experiments intended to evaluate the composition of microbial communities in sponges from Baikal is one of the most direct ways to investigate processes in the whole lake.

Precedents where disease of sponges or corals were investigated using modern methods of molecular biology are known (Stabili et al., 2012; Prinzón et al., 2015). And there is a number of studies when a single pathogen which caused the disease was identified (Webster et al., 2002; Luter et al., 2010; Choudhury et al., 2015). But the investigations of microbial communities of diseased sponges in Lake Baikal using similar approaches just demonstrated the complexity of the problem under study (Denikina et al., 2016; Kulakova et al., 2018). So, other wider views of the processes in the Baikal ecosystem and, in particular, in the analysis of microbial communities in sponges, are required.

So-called fractal theory is based on several mathematical notions rooted in geometry and statistics. The approaches of fractal theory can be applied to describe many complex phenomena of different scales, in physics and biology. As counterbalance to this universality, the results obtained by fractal-based methods do not have solid foundations down at microscopic scales. Unlike conventional methods of molecular biology, they can give only hints in the attempts to interpret it in an applied system. And the methods from fractal theory are not very often used in the applied mole-

*Corresponding author.
E-mail address: feranchuk@gmail.com (S.I. Feranchuk)

cular biology and microbiology, partly for the reasons mentioned above.

But in the case of the symbiotic microbiomes of Baikal sponges, even hints would be useful in attempts to explain the causes and consequences of the crisis. So, the presented research has the purpose of applying the methods of fractal theory to the comparative analysis of microbial communities of sponges collected in Lake Baikal in a time of crisis. It was partly based on the methodological study by Feranchuk et al. (2018a) where several features of fractal structure were detected in the rank-abundance distributions of custom microbial communities. Also, the fine-grained temperature measurements in several locations of Lake Baikal were analyzed using methods of fractal theory, and some connections were found with the results obtained from the analysis of microbiomes.

1.2 Fractal theory, advantages and disadvantages

The term 'fractal structure' was introduced in the years 1960-1970 by B. Mandelbrot; in his paper "How Long Is the Coast of Britain" (Mandelbrot, 1967) he applied the concept of non-integer dimension to describe the so-called 'coastline paradox' noticed by L.F. Richardson (1961). The 'coastline paradox' which makes it difficult to measure the length of a coastline in any units of length is demonstrated in Fig. 1. The definitions of the Hausdorff dimension or Minkovski dimension, introduced to mathematics in the early XX-th century, allow the estimation of a non-integer value of dimension for certain specific geometrical objects. And similar methods can be applied to objects arising as natural phenomenons. Citing B. Mandelbrot, "Clouds are not spheres, mountains are not cones, coastlines are not circles, and bark is not smooth, nor does lightning travel in a straight line".

Fig. 1. The coast of the Britain measured on several scales
left: Unit = 200 km, length = 2400 km (approx.)
right: Unit = 50 km, length = 3400 km
Reprinted from Wikipedia project page

Objects which can be described as fractals arise from many specific development mechanisms; the precise details of these mechanisms cannot be explained by fractal theory. The features of fractal structure can be detected in any complex real word object if linear dependency is observed in the distribution of the geometrical properties of the object, using logarithmic coordinates, as in the example shown in Fig. 2. In linear coordinates, this dependency would have a form of the so-called "power law" ($y = Ax^D$); the value of D, with negative sign, would be the value of the fractal dimension.

The advantage of the fractal representation of complex geometrical objects is that it provides a way to describe complex structures with a single parameter D, the value of fractal dimension. The exact value of the fractal dimension can be different for the same object, depending on the methods used to calculate this value. But within the frames of any method, the estimates of the value D can be of significance, sufficient to allow this value to be used to compare several objects. There is robust statistical support for the conclusions derived from this comparison (Jelinek and Fernandez, 1998). An alternative interpretation is that the methods of fractal theory provide an efficient way to estimate the number of independent variables in high-dimensional data (Karbauskaite and Dzemuda, 2016).

The features of power-law dependency can be detected in other distributions, not only in geomet-

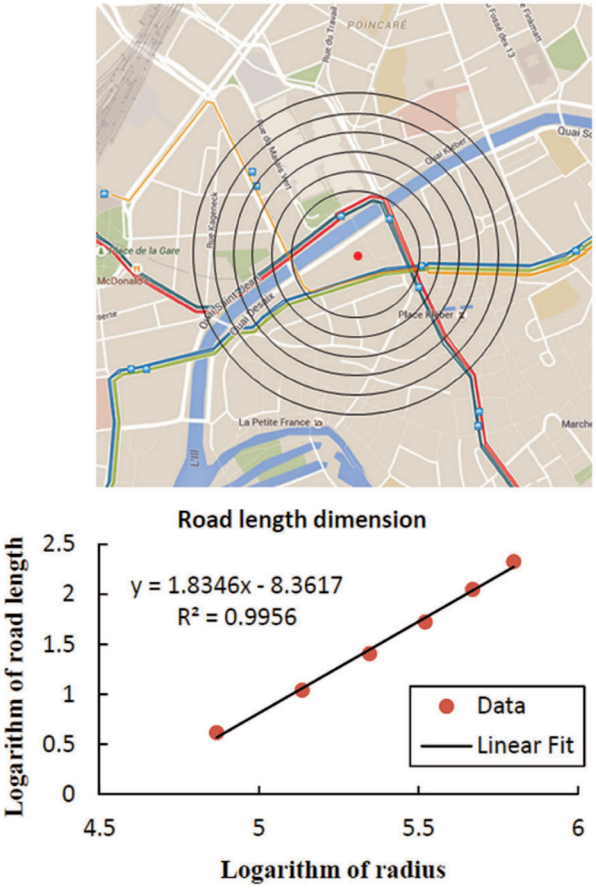

Fig. 2. Detection of fractal structure for the road network in Strasbourg, France. Adopted from (Wang et al., 2017)

rical objects. The probability distribution known as Zipf's law, which was observed for the frequencies of words in the texts in natural languages, is also a case of power-law distribution. In Zipf's law, the frequency of a word in some text corpus is inversely proportional to its rank in the frequency table.Another case of power-law distribution, the Pareto distribution used in economics, was derived from an observation by Vilfredo Pareto that 80% of Italy's land was owned by 20% of the population. This observation was then generalized to any kind of property, and in its expanded form, it expresses the power-law dependency in the wealth distribution of society.

The limitations of fractal theory follow from the fact that these methods are almost never supported by a detailed description of the system under study, and any predictions based on these methods are a 'risky business' (Seuront, 2015). In certain cases when the power law is insufficient to explain the distributions obtained by applying fractal techniques to the system under study, a continuous spectrum of exponents can be used; this approach is known as 'multi-fractal analysis' (Harte, 2001). Another more simple expanded form of the power law dependency describing the distributions of income and wealth in the economy, is developed in a series of studies known as econophysics (Yakovenko and Rosser, 2009; Banerjee and Yakovenko, 2010; Xu et al., 2017).

In the discussions proposed by B. Mandelbrot (Mandelbrot, 1960), the cases of power-law distribution were opposed to statistical physics, where the Boltzmann-Gibbs exponential probability distribution is normally applied. But in econophysics it was demonstrated on several simple models that both distributions can be described within a single framework. And this description can be fitted to the two parts of the distributions which are derived from income statistics in a real-word economy (Fig. 3A).

To explain briefly the models used to derive the unified framework, the Pareto distribution is valid for the higher class of a society where income is proportional to the assets of a household, and the Boltzmann-Gibbs distribution is valid when income is proportional to efforts and time invested in the economic activity. In the first group, but not in the second, the logarithm transformation should be applied to the values of income; this separation can unify the two models for a better description of observed income distributions.

As a result of the fit, two coefficients would consistently describe a power law (Pareto) dependency for the higher class, and an exponential (Boltzmann-Gibbs) dependency for the lower class in the income distributions of a population. Here, an exponent in power law dependency has a meaning similar to fractal dimension, and a factor in exponential dependency has a meaning similar to a temperature parameter in a classical thermodynamics. In this way the income distributions can be explained using only two parameters, but not a continuous spectrum of exponents as in a multifractal approach applied to the same kind of data.

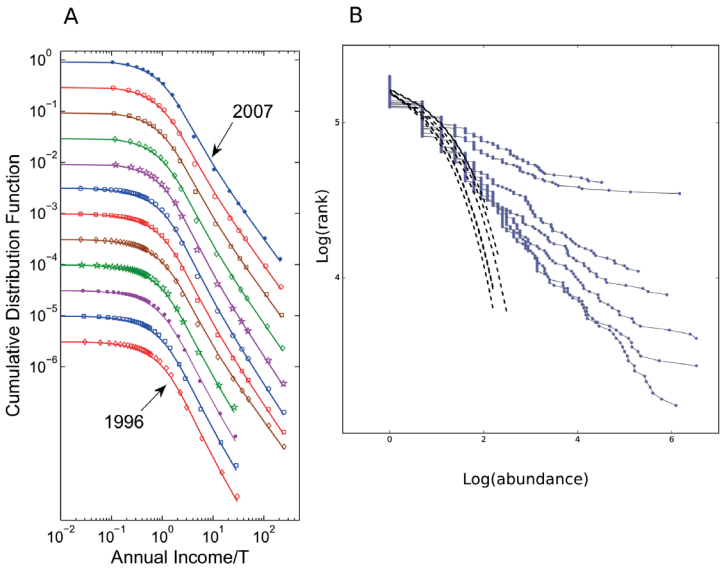

Fig. 3. Cases of dependencies where a description combined from power-law and exponential models could be applied.

A. Cumulative probability distributions of tax returns for USA.

Distributions were constructed from the IRS data (symbols) and their fits with the theoretical distribution, shown in the log–log scale versus the normalized annual income r/T . Plots for different years are shifted vertically for clarity. Reprinted from Banerjee and Yakovenko, 2010.

B. Rank-abundance distributions for sediment microbial communities at a level of genus, shown in the log–log scale. Adopted from Feranchuk et al., 2018a.

2 Methods

2.1 Processing of 16S rRNA gene sequencing reads of sponge symbionts in Lake Baikal

The results of this study are based on a 16S rRNA microbiome survey of Baikal sponges collected in June 2015 in three locations of the Lake. Several biological replicates of the *L.baicalelenis* sponges, some healthy in appearance, and some diseased, were collected in all three locations; the raw sequencing reads obtained using 454 technology for the V4-V6 region of the 16S rRNA gene are available at NCBI BioProject database under the accession number PRJNA369024. A summary of the archives used in the analysis is shown in Table 1.

All the reads were quality trimmed using the Mothur package (Schloss et al., 2009) and short reads (<200 nt) were filtered. The composition of sponge microbiomes is presented in Fig. 4 as a heatmap chart, for the 25 most abundant phylotypes of bacteria and chloroplasts. The matrix of abundances was calculated using closed-reference OTU picking, implemented in the QIIME1 package (Caporaso et al., 2010), with a database gg_13_7 and Greengenes version of bacterial taxonomy. All environmental sequences were aligned and phylogenetically assigned up to the species level. The taxon identification for phylotype was done according to the degree of similarity at the level of genus (94–97.5%), family (90–94%), order (85–90%), class (80–85%) or phylum (75–80%).

Table 1. Integral properties and biodiversity estimates of 23 samples used in the study

Sample	SRA ID	Raw reads	Reads in OTU	OTU Number	Ace	Chao1	Shannon	Simpson	Gini	Singletons	Doubletons
1	2	3	4	5	6	7	8	9	10	11	12
L1	SRR5208569	5253	3833	129	293	248	3.07	0.79	0.93	73	21
L2	SRR5208568	6200	4528	46	82	79	1.47	0.54	0.96	22	6
L3	SRR5208567	7269	4364	107	256	203	2.59	0.72	0.95	61	18
L4	SRR5208566	2762	1454	262	486	477	5.7	0.93	0.73	138	43
L5	SRR5208565	3560	1911	240	359	362	4.86	0.85	0.78	104	43
L6	SRR5208564	3713	1969	235	360	340	4.61	0.85	0.8	103	49
L7	SRR5208563	3888	2145	79	148	135	3.36	0.81	0.89	37	11
L8	SRR5208562	6528	3513	98	208	185	3	0.78	0.93	55	16
OV1	SRR5208561	4445	3747	131	228	202	2.74	0.67	0.93	59	23
OV2	SRR5208560	3338	2783	192	367	345	3.42	0.74	0.89	101	32
OV3	SRR5208559	4787	2019	148	236	231	3.94	0.85	0.86	66	25
OV4	SRR5208558	3484	1830	131	240	229	3.86	0.82	0.87	66	21
OV5	SRR5208557	2970	1277	186	264	276	6.18	0.97	0.66	69	25
OV6	SRR5208556	3068	1757	175	281	285	4.75	0.89	0.81	79	27
OV7	SRR5208555	5062	2687	265	399	359	6.07	0.96	0.76	101	53
OV8	SRR5208554	2584	1003	220	362	375	6.63	0.98	0.62	103	33
T1	SRR5208553	5095	4477	272	582	619	3.34	0.72	0.91	154	33
T2	SRR5208552	5063	4387	282	515	500	3.7	0.75	0.89	142	45
T3	SRR5208551	4912	2011	332	553	509	6.23	0.95	0.73	157	68
T4	SRR5208550	3102	1744	174	350	334	4.7	0.9	0.82	90	24
T5	SRR5208549	5487	2727	252	420	423	5.54	0.95	0.81	116	38
T6	SRR5208548	8843	4822	265	432	423	5.05	0.93	0.86	113	39
T7	SRR5208547	6581	3067	475	764	781	7.31	0.98	0.69	209	70

Collection sites are notated as follows:
L -Listvyanka area, southern Baikal (51.862 N 104.8475 E); OV - Olkhon Gate area, central Baikal (53.0175 N 106.9297 E); T - Turali cape area, northern Baikal (55.2877 N 109.7586 E).
Samples with signs of disease are shown with gray background. Estimates of biodiversity are shown in columns 6-10

2.2 Detection of power-law distributions in microbiology data, for 16S rRNA sequencing of sponge symbionts in Lake Baikal

It has been assumed that the features of fractal structures are present in the patterns of community ecology (Saravia, 2015; Våge and Thingstad, 2015). Cases of power law dependency have been detected in rank-abundance distributions of microbial communities (Feranchuk et al., 2018a), as it is shown in Fig. 3B. The features of fractal structure are expected to be observed in the object under study, whatever the scale. For microbial communities, the fractal structure should be present at all levels of taxonomic hierarchy, even for bacteria within the same species or genus. In the latter case, the properties of the fractal-like patterns should give hints not only about features of microbial community as an ecosystem, but also about micro-evolution processes within the selected species.

The environmental sequences assigned to the same phylotype, as shown on Fig. 4, are close to each other and may even belong to the same species of bacteria, but no-one expects that genomes of individual bacteria in these species be completely identical. Instead, the distributions of proximity between individual bacteria can be investigated using the available sequencing data, attempting to detect a fractal structure in these distributions. So, several microbial genera with different adaptation strategies could be chosen to study in deep the fractal-like properties of symbiotic communities of Baikal sponges.

Seven abundant components of microbiome which were selected for further precise analysis, from the 25 shown on Fig. 4, are specified below. These integral description of these phylotypes are presented in Table 2; the Genbank ID of the 16S rRNA gene sequence selected as a reference for a most abundant OTU within each phylotype, is included in the Table 2.

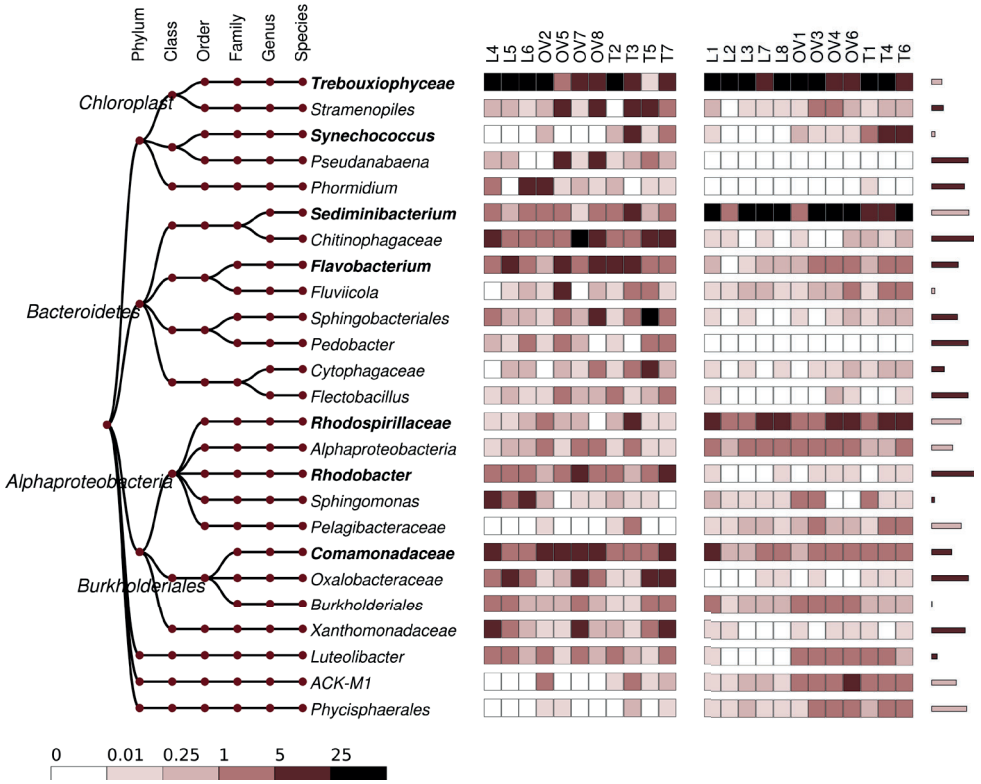

Fig. 4. A composition of microbiomes for healthy and diseased sponges, for the 25 most abundant genera of bacteria and chloroplast. Bars on the right show the significance of difference in abundances between healthy and diseased samples, for each genera. Collection sites are notated as follows: L - Listvyanka, OV - Olkhon Gate, T - Turali cape.

The phylotype annotated to Trebouxiophyceae class represents 16S rRNA gene of chloroplast from unicelluar algae, endosymbiont of *L. baicalensis* sponges (Chernogor et al., 2013). The phylotypes identified at the genus level as *Sediminibacterium* (Chitinophagaceae, Chitinophagales, Chitinophagia, Bacteroidetes) and *Synechococcus* (Synechococcaceae, Synechococcales, Cyanobacteria), as well as the phylotype identified at the level of family and belonged to *Rhodospirillaceae* (Rhodospirillales, Alphaproteobacteria, Proteobacteria) are typical for microbiomes of Baikal sponge. Reference sequences for these representatives were previously described in the sponge samples collected in Lake Baikal (Kaluzhnaya et al., 2011; Gladkikh et al., 2014). Some species of Synechococcus was reported in association with the harmful algal blooms and eutrophication (O'Neil et al., 2012; Berry et al., 2015) and the growth of these representatives of cyanobacteria was detected in several recent measurements in Baikal (Timoshkin et al., 2016). The representatives of family *Comamonadaceae* (Burkholderiales, Betaproteobacteria, Proteobacteria) and F*lavobacterium* (Flavobacteriaceae, Flavobacteriales, Flavobacteriia, Bacteroidetes) are typical for freshwater environments (Bernardet and Bowman, 2006; Willems, 2014) and have been observed in metagenomic surveys on Baikal (Kadnikov et al., 2012; Gladkikh et al., 2014). Some species from both groups were characterized as opportunistic bacteria and pathogens (Horňák and Corno, 2012; Brown et al., 2015; Walsh et al., 2017). The phylotype identi-

Table 2. The specifications of bacterial genera selected for a detailed analysis

Annotation	gg_13_5 ID	Genbank ID	h/d	p-value	% diseased	% healthy	Pareto	Boltzmann (b0)	P/B
1	2	3	4	5	6	7	8	9	10
Trebouxiophyceae	1118847	GU936925.1	h	0.085	31.8	49.4	1.21	10.7	3.1%
Sediminibacterium	840888	FJ800528.1	h	< 0.001	3.2	27.2	1.16	4.9	1.8%
Rhodospirillaceae	848608	FJ800529.1	h	0.001	1.1	5.4	0.86	7.32	3.3%
Synechococcus	550168	GU305759.1	~		0.9	2.0	0.80	8.2	1.8%
Flavobacterium	4324048	JX221823.1	d	0.002	6.8	1.2	0.59	22.0	2.5%
Comamonadaceae	72607	AF289156.1	d	0.008	6.4	2.1	0.92	28.3	2.3%
Rhodobacter	217320	DQ676416.1	d	< 0.001	2.7	< 0.1	1.08	10.7	3.1%

The significant increase of bacteria in healthy (h) or diseased (d) samples is shown on column 4
Columns 8, 9, 10 describe properties of distance-based distributions described below:
column 8 - slope of regression line in power-law part of the distribution;
column 9 - slope of regression line in exponential part of the distribution;
column 10 - threshold of identity which separate power-law part and exponential part in the distribution.

fied as *Rhodobacter* (Rhodobacteraceae, Rhodobacterales, Alphaproteobacteria, Proteobacteria) family was significantly abundant in the diseased samples, in contrast to the other phylotypes from the class Alphaproteobacteria identified as Rhodospirillaceae which was detected preliminary in healthy sponges and described as typical to Baikal. The reference sequence for this genus was obtained from samples in freshwater pond (Briée et al., 2007).

The approach, intended to detect power law distributions for the sequencing reads which are allocated to the same species, is inspired by an algorithm for calculating a Hausdorff-like dimension. One can think about individual sequencing reads as being points in a certain multidimensional space. If the dimension of this space was known, it would be possible to construct a system of multidimensional spheres around each of the points and to count the number of points within each sphere. The average point count within each sphere could be then transformed to a distribution as a function of sphere radius. Then power law dependency might be observed, and used to evaluate the Hausdorff dimension of this object.

Alternatively, it is possible to calculate a matrix of distances between the points and to count the number of cells in this matrix, where the distances between points are below some threshold. This threshold value is similar in meaning to the sphere radius in the Hausdorff-like approach. So, in the matrix the count of paired distances below the threshold, as a function of threshold value, should provide a distribution where the presence of power law dependency might be expected.

To use the proposed approach in the distributions of individual 16S rRNA genes within each of the selected phylotypes, an Usearch algorithm with 95% identity threshold was applied to screen the sequencing reads in the bulk archives, for each reference. Paired alignments generated in this screening were used to construct the multiple alignments. In these multiple alignments, paired distances between aligned sequencing reads were calculated. These distances might vary from 0 (completely identical) to 5% mutations (the identity threshold in the screening). In the distance matrix, the fraction of paired distances below some threshold was plotted against the value of the threshold; the maximal threshold being 5%, where 100% of distances are included. The obtained distributions are presented in Fig. 5, at both linear and logarithmic scales for threshold of identity.

In the distributions in Fig. 5, the linear dependency is clearly visible in the logarithmic coordinates on both axes, and the presence of linear dependency is strongly confirmed by the statistical tests (p-value $< 10^{-7}$). Also, for several phylotypes, in the right tail of the distribution, a part can be observed which looks like it could be approximated by the Boltzmann-Gibbs model. It can be seen on the right chart of Fig. 5, as a near-linear dependency in appropriate scaling

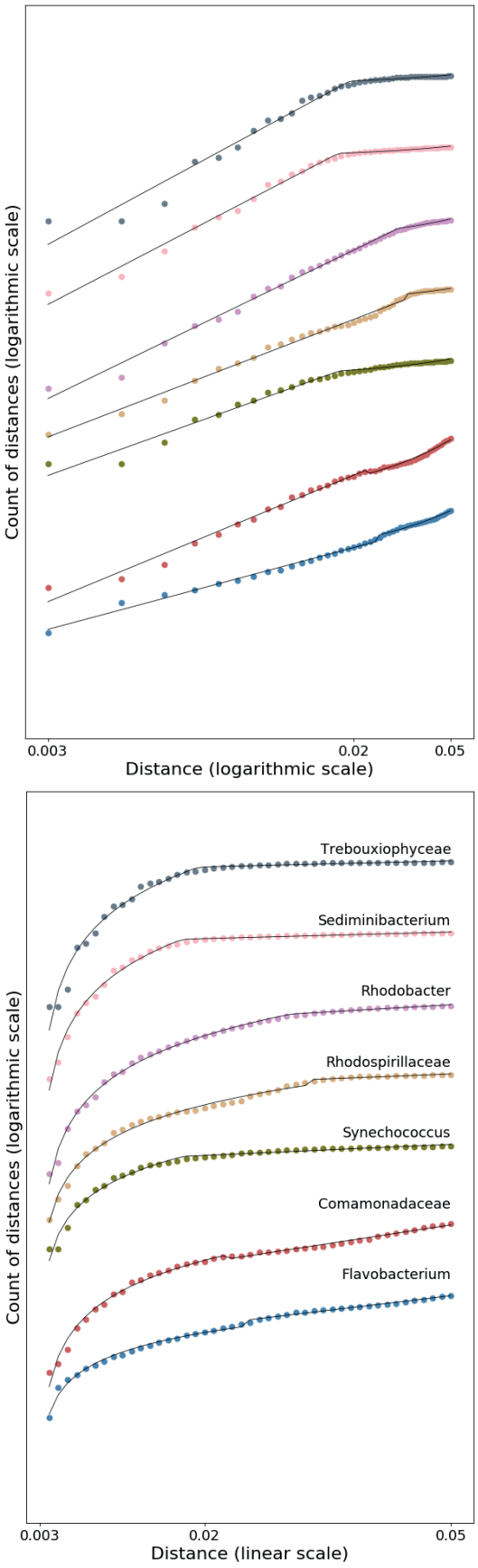

Fig. 5. The distributions of paired distances between fragments obtained by the sequencing of the V4-V6 region of the 16S rRNA genes. The distributions for fragments which have identity >95% to the reference annotated sequences are shown for 7 selected genera. The same distributions are shown in both parts of the chart, at different scales.
X axis - the threshold values of distances, at logarithmic scale (top) and at linear scale (down).
Y axis - the relative count of paired distances below the threshold, at logarithmic scale. The scatter plots are biased along the Y axis to a fixed offset value for each genus.
The thin solid lines show the fit of the combined model used to approximate the distributions.

of the axes. To evaluate the slope of the linear dependency in both parts, the same algorithm was applied to all the distributions. In this algorithm, the point which separates the parts described by the Pareto and by the Boltzmann-Gibbs distributions was selected using as criteria a total mean-square deviation in both parts of the distributions. The pairs of optimal regression lines for each phylotype are also shown in Fig. 5. The slopes of the lines in both parts of the distribution, and in the value of the optimal threshold which separates the two parts, are presented in Table 2.

Applications of fractal theory can provide only some hints about the properties of a complex system. But, as discussed above, the same methodology from fractal theory allow one to compare and interpret the distributions for several objects where a fractal-like structure is observed with sufficient significance. So, the distributions for the seven abundant phylotypes presented in Fig. 5 can be visually separated into three groups. For the Trebouxiophyceae, *Sediminibacterium.* and *Synechococcus* phylotypes, a gradual steady increase of count values is observed in the distributions, with a nearly constant right part for the high identity thresholds. For *Flavobacterium* and *Comamonadacease* phylotypes, an uneven but visible increase can be observed in the right part of the distributions. The phylotypes *Rhodospirillaceae* and *Rhodobacter* can be described as a third group with an intermediate form of the distributions.

These observed “fractal groupings” of the abundant phylotypes can most easily be interpreted in terms of the adaptation strategy of the microorganisms’ species and genera. The *Trebouxiophyceae* and *Sediminibacterium* are endemic to Baikal and expected to have a long-term adaptation to their conservative ecological niches. In contrast, the representatives of phylotypes *Flavobacterium* and *Comamonadaceae* have been observed to have highly adaptive survival strategies (Pulkkinen et al., 2009; Jezberová et al., 2017). Cyanobacteria are known to have a stable lineage with consistent survival strategy (Marsac and Houmard, 1993); this hints at the reason behind the observation that the distribution for phylotype *Synechococcus* is close to those of the conservative *Trebouxiophyceae* and *Sediminibacterium*. The *Rhodospirillaceae* and *Rhodobacter* phylotypes belonged to Alphaproteobacteria, their representatives described as phototrophic bacteria, can be expected to have an intermediate rate of adaptation flexibility (Baldani et al., 2014).

These observed “fractal groupings” of the abundant phylotypes can most easily be interpreted in terms of the adaptation strategy of the microorganisms’ species and genera. The Trebouxiophyceae and Sediminibacterium are endemic to Baikal and expected to have a long-term adaptation to their conservative ecological niches. In contrast, the representatives of genera *Flavobacterium* and *Comamonadaceae* have been observed to have highly adaptive survival strategies (Pulkkinen et al., 2009; Jezberová et al., 2017). Cyanobacteria are known to have a stable lineage with consistent survival strategy (Marsac and Houmard, 1993); this hints at the reason behind the observation that the distribution for phylotype Synechococcus is close to those of the conservative Trebouxiophyceae and *Sediminibacterium*. The *Rhodospirillaceae* and *Rhodobacter* phylotypes belonged to Alphaproteobacteria, their representatives described as phototrophic bacteria, can be expected to have an intermediate rate of adaptation flexibility (Baldani et al., 2014).

2.3 Estimates of the fractal dimension for the fluctuations of temperature in Baikal water

Temperature detectors were placed in four locations in Baikal; in Listvyanka, in Baykalsk town (South Baikal), near Uzur village (Olkhon island), and near Bolshye Koty village (direction to the north from Listvyanka). From 2010, the year when the crisis on Baikal was just beginning, detectors have recorded temperatures every two minutes. The collected data from the temperature detectors is certainly valuable in suggesting a clue as to the explanation of the processes in Baikal in time of crisis.

To interpret time series data, methods for time series analysis of various kinds have been developed for many specific applications. Estimates of fractal dimension can also be applied in time series analysis. There are several approaches which can be used to estimate fractal dimensions from time series data (Higuchi, 1988; Peng et al., 1994); the so-called ‘Higuchi dimension’ is the first and most straightforward of these approaches. It was applied to time series data from the temperature detectors in Baikal.

The method used to estimate fractal dimension proposed by Higuchi (Higuchi, 1988) is shown in Fig. 6, for time series data from Listvyanka. The total length of the lines which connect the data points has been changed when the time interval between the points is doubled. If a time series can be interpreted as a fractal object, the total length of the lines plotted against the interval between the points using logarithmic coordinates, should looks like a linear dependency, as in the classical case of coastlines described in the introduction section.

In the Fig 6, two fragments of temperature measurements are presented as test cases; June 2010 and September 2010. The higher variations of temperature in daytime in September lead to lower variations of difference in the total length of the lines constructed following the Higuchi methodology.

2.4 Specifications and availability of software

The heatmap in Fig. 4 with the results of the closed-reference pipeline was generated using the d3 javascript library (v.3 and v.4) within an interactive framework developed in-house for data visualization; the source scripts of the interactive system are available at https://github.com/sferanchuk/d3b_charts. The Scikit_bio python package (v. 0.4.2) was used to estimate biodiversity values for the samples which are presented in Table 1.

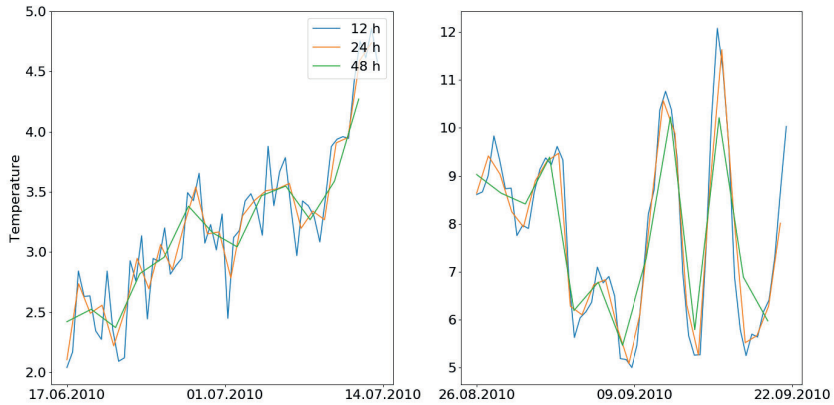

Fig. 6. Two test cases of fractal dimension estimates for fluctuations of temperature in Baikal water.
X axis - time of observations; Y axis - values of temperature, in degrees centigrade. The data from the temperature detector in Listvyanka are used. Three lines on each part of figure present the variations of temperature at different scales.

The libraries of raw sequencing reads identical to the archives available at NCBI (BioProject PRJNA369024) were preprocessed using the Mothur package v. 1.39.5 following conventional setup for filtering unreliable and short oligonucleotides; trim.seq function was applied to raw data files, with parameters ' maxambig = 0, maxhomop = 8, flip = T, bdiffs = 1, pdiffs = 2, qwindowaverage = 35, qwindowsize = 50').

The Usearch alogorithm (Edgar, 2010) implemented in the Uclust software (v. 10.0.240_i86), with the options '-id 0.95 -strand both -maxaccepts 0 -maxrejects 0 -top_hit_only', was used to align the sequencing reads to the database, constructed from the seven 16S rRNA reference sequences listed in Table 2. Paired alignments produced by the Usearch algorithm, in Sam format, were used to generate multiple alignments, by a custom software implemented in c++ programming language. The distance matrices were constructed from multiple alignments; for paired distances, the convention that a string of gaps is counted as a single gap was used, which is the default way to calculate paired distances between 16S rRNA gene fragments accepted in the Mothur package. The distributions of distances were calculated using a custom software in c++. The source codes for the newly developed software utilities are available at https://github.com/sferanchuk/bsponge_fractalmodels.

In the processing of data from temperature detectors, only the portions of the measurements which were continuous for at least 11 days were plotted. Measurements with shorter continuous periods were ignored. Statistical outliers (any value larger or smaller than the average temperature by more than 10SD, within a 16 hour interval) were changed to the value of the average temperature. The time interval used to calculate the Higuchi dimension was between two minutes and 16 hours. The values of the Higuchi dimension were obtained using a Higuchi Fractal Dimension python package; the package was modified to include a check for significance in the estimates of the dimension.

A functionality of the Matplotlib python package (v. 1.5.1) was used to present the results in figures 5, 6, 7 and 8, from the distributions of distances and the data files with records from temperature detectors. In Python, a procedure was developed to separate the two parts of the distance distributions (Fig. 5, 7), based on a linear regression function implemented in the Scipy package (v. 0.17.0) .

3. Results

3.1 The features of fractal dimension for selected microbial phylotypes evaluated separately in each sample

The main applied question, which the present research tries to answer, is to detect and interpret the separation of sponge samples by signs of disease and by geographic location. The separation of samples by disease state can easily be detected by conventional microbiological methods and is observed in the heatmap chart on Fig. 4. The microbiome of diseased sponges is more heterogeneous, and this is supported by the indicators of biodiversity like the Shannon index. But separation by location is difficult to detect, and, if it is detected by advanced statistical methods, it is difficult to interpret the observed separation.

The charts in Fig. 7 present the properties of the distributions, constructed from the alignments of sequencing reads in the same way as described above, but in the latter case the data from each of the samples was processed separately. And, in the same way, two regression lines were used to describe two parts of each of the distributions. As a result, one could use the slope coefficients of two regression lines to obtain two values which describe a sample, for all of the selected microbial phylotypes.

A comparison of the generic slope coefficients for the distributions in Table 2, with the values for separated samples in Fig. 4, suggests that combining several portions of the sequences into one alignment could change the properties of the distributions. The observed distributions are changed in multiple ways, and this problem could be the subject of a further

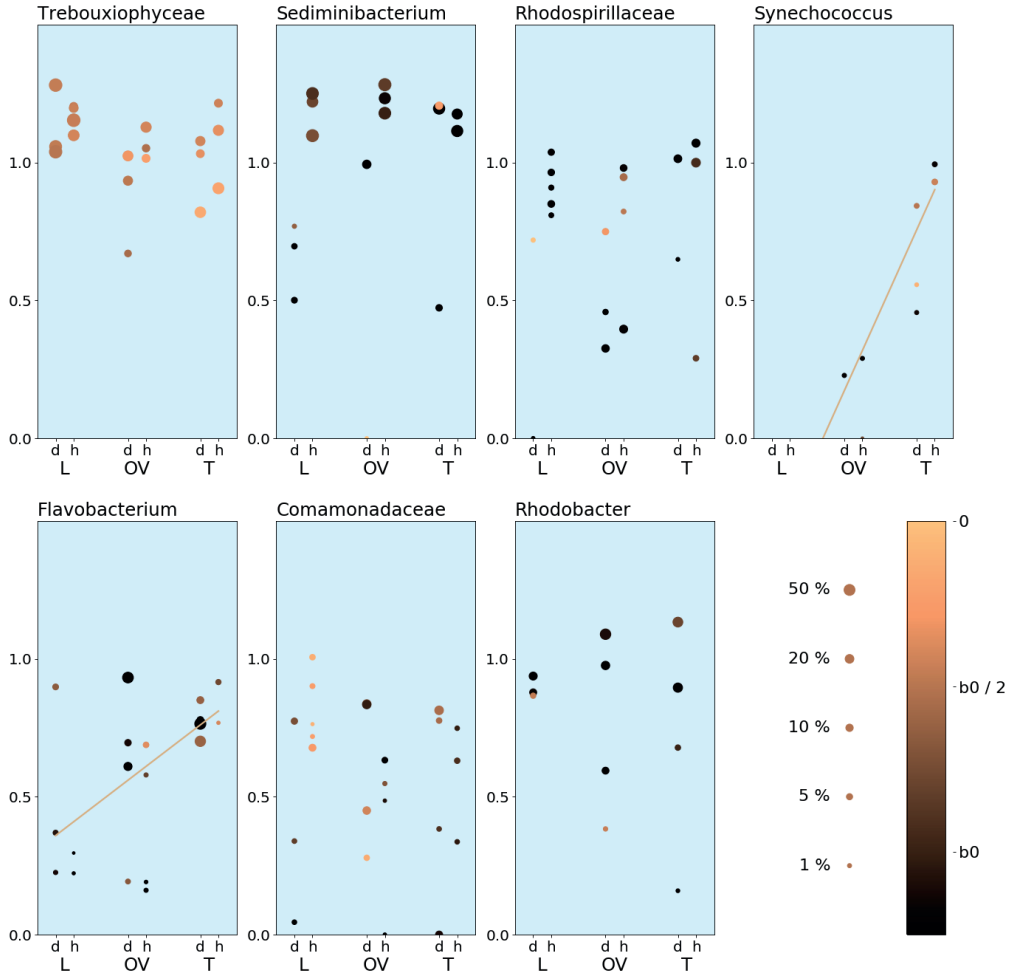

Fig. 7. Values of fractal dimension (Pareto coefficient) and a coefficient in the Boltzmann-Gibbs part of distance-based distributions for selected genera, estimated in separated samples. The separate samples are shown as circles in each part of the chart. The slope of the first part of the distribution (the fractal dimension part), defines the Y-coordinate of each sample. The size of the circle reflects the relative abundance of the selected genus in the microbial community, and color notations are used to show the slope of the regression line in the second part of the distributions (a coefficient for the Boltzmann-Gibbs model).
The X axis is used to separate the places of collection and the disease states of the samples. The scales for sample size and for the Boltzmann-Gibbs coefficient are shown at the bottom right of the chart. The values for the Boltzmann-Gibbs coefficient are scaled separately for each part of the chart, relatively to reference value b0 specific for each genera and listed in Table 2.

study. However, the generic coefficients are comparable by value with the coefficients for the separated samples, and the interpretation of the observed relative variation of coefficients is expected to be meaningful.

The area of Listvyanka at the south of Baikal is the region with high anthropogenic load; in contrast, Turali cape at the north of Baikal is the region without any kind of human activity; the Olkhon Gate area in middle Baikal is an intermediate region both by location and by anthropogenic load. For two phylotypes, *Flavobacterium* and *Synechococcus*, a significant ($pv < 0.02$) correlation is observed between the place of sample collection and the estimated fractal dimension, as is demonstrated by straight lines in two parts of Fig. 7.

The description of macroscopic systems using the Boltzmann-Gibbs distribution is developed less than a description with fractal dimension; and the slope coefficients for the a second part of the distribution, shown by color notations in Fig. 7, are harder to interpret. But anyway it should be noticed that for phylotypes belonged to chloroplast of class Trebouxiophyceae, a clear North-South gradient ($pv < 0.02$) is observed in Fig. 7 for this parameter.

3.2 The fractal dimension for the fluctuations of temperature in Baikal water

The integral representation of temperature measurements in four locations, processed using the Higuchi approach, is shown in Fig. 8. The temperature time series definitely have a fractal structure; the presence of power-law dependency is confirmed with p-value below 10^{-20}. The variations in the estimated fractal dimensions are stressed using a curve constructed as moving average for 50 data points. These variations indicate the uncertainty in the values of the Higuchi dimension. The plots contain gaps and incomplete parts, because, to apply the estimates of fractal dimension in a uniform way, continuous measurements collected every two minutes during at least 11 days were required.

The fractal dimensions shown in Fig. 8 have lowest values in late summer and highest values

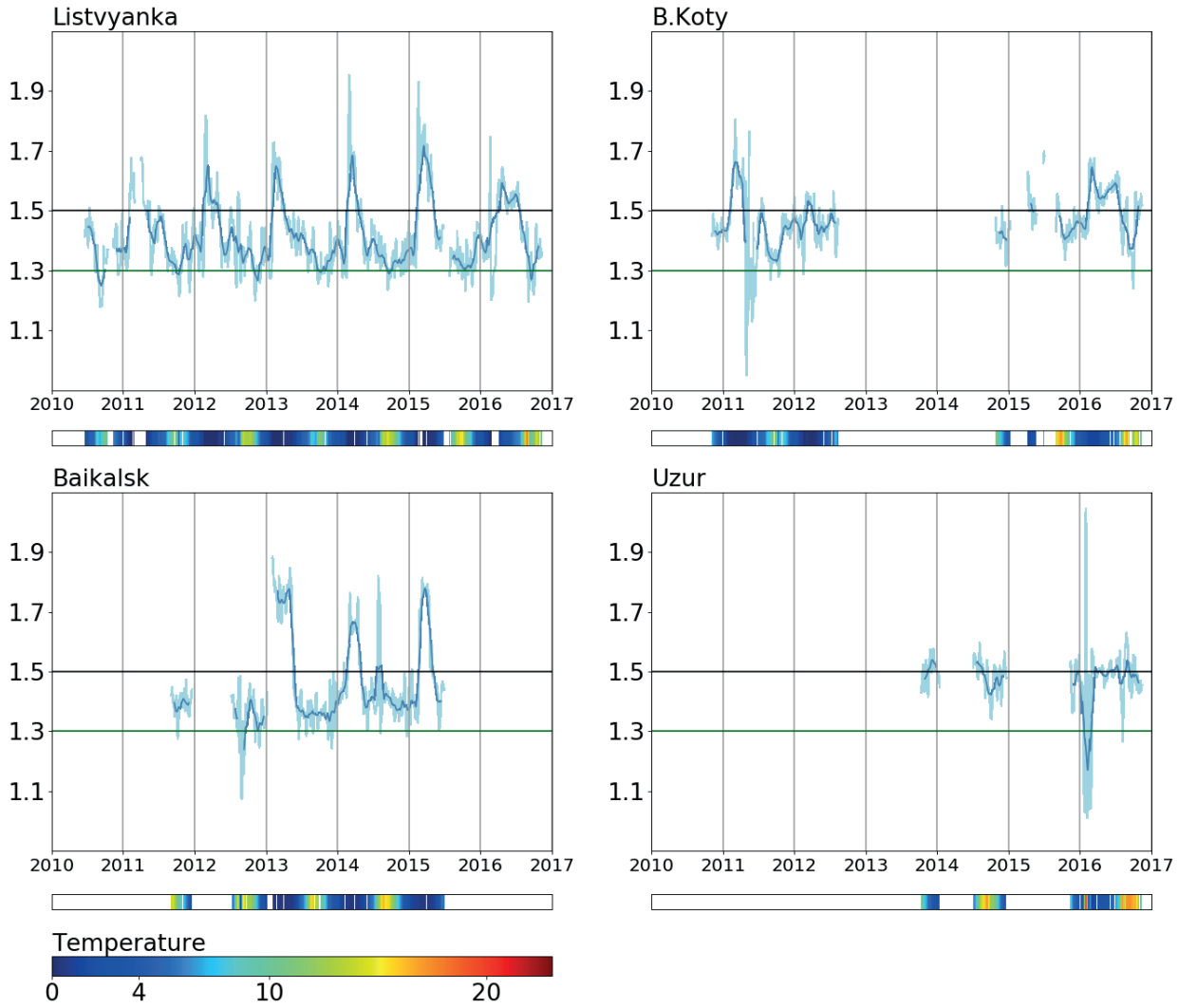

Fig. 8. The fractal dimension calculated for fluctuations of water temperature, in four locations in Lake Baikal. The fractal dimension (Y axis) was calculated at 16-hour intervals, using the Higuchi approach. The X axis shows the dates of measurement. The color bars at the bottom part of each subplot directly show the measured values of temperature. A light-blue line directly shows an estimated time dependency of the Higuchi dimension, and a dark blue line shows the same dependency smoothed using moving average with window size equal to 50 data points.

between February and April. Qualitative explanations can be suggested for these features; early spring in Baikal is the time when water is mixing in the near-shore zone beyond the ice, due to an increase in density caused by radiative heating. And, the high variations of temperature in late summer can lead to lower values of the Higuchi dimension, as was discussed above for the test cases in Fig. 6.

But, despite that, in this analysis it must be stressed that, in summer time in Listvyanka the values of the Higuchi dimension are consistently the lowest when compared to other locations and other seasons. And, the late summer in Listvyanka is the season and the place where the anthropogenic load is highest in all Baikal. Associations between the Higuchi dimension and the anthropogenic load can be extended; e.g. Baikalsk town is second after Listvyanka by anthropogenic load, and this can be observed in the distributions of Fig. 8. However, the limited completeness and precision of the measurements and the uncertainty of the estimated values, make these kinds of associations less sure.

4. Discussion

The methods applied to the sequencing data described above, are not intended to reconstruct specific metabolic processes or food chains in a sponge holo-genome. The whole of fractal theory is founded mostly on empirical observations, and therefore, so are the applied results presented in this study, since they are based of fractal theory. As discussed above in comments to the distributions of distances shown in Fig. 5, the differences observed for the selected microbial phylo-types can be interpreted in terms of evolution theory. Anyway, the microevolution processes of bacteria in Baikal sponges are too complex to reconstruct precisely at the molecular level from the available data. So, the presented methods are the most straightforward way which can be used to detect the events of microevolu-tion on Baikal in times of crisis.

It can be concluded from the presented results that microevolution processes do certainly exist in

bacterial species in Baikal sponges. Most of the events in this microevolution remains uncertain, but several facts can be derived with a sufficient confidence. For the representatives of two bacterial phylotypes from the *Flavobacterium* and *Synechococcus*, a connection is detectable between the fractal dimension and the anthropogenic load at the place of collection. And, the variations of temperature at several locations in Baikal also provide a connection between values of the fractal dimension and the anthropogenic load.

In the terms of econophysics, the lower values of the fractal dimension mean that the inequality in the society, measured using the Gini index, would be lower, and the economy would be more robust in this society. Both bacterial phylotypes mentioned above have verified associations with sponge disease and with the contamination of freshwater ecosystems, so it can be interpreted that the development of opportunistic bacteria in the regions with high anthropogenic load is more extensive. Supporting this hypothesis, a slight ($pv = 0.11$) gradient in the opposite direction can be seen in Fig. 7 for algae chloroplasts, which are expected to suffer in the areas with high anthropogenic load.

The Boltzman-Gibbs part of distributions in econophysics should explain the basic and stable foundations of an economy. In the presented results (Fig. 7), the properties of the Boltzman-Gibbs part in the distributions for the microbial species are mostly difficult to interpret. But anyway, the observed gradient for this slope coefficient for chloroplasts of Trebouxiophyceae algae suggests that the symbiotic algae of sponges are adapting to the terrible disease of their hosts. And the presence of rapid adaptation processes in these algae is also confirmed by the preliminary results published in (Feranchuk et al., 2018b) where the presence of mutations in the algae chloroplast were detected using the sequencing of sponge metagenomes.

In order to put the obtained results into the global and important context of the reasons for the crisis, three considerations are listed below:

- The events of the crisis are manifested in the rapid restructuring of food chains and changes in sponge hologenomes.
- The adaptive changes in bacterial genomes in response to anthropogenic load have been detected for species which are all typical to Baikal, but which have flexible survival strategies.
- Microevolution in a microbial community normally implies interactions between several species, genera or even classes of bacteria, like the exchange of genomic islands or the restructuring of metabolic processes.

Three possible reasons should be considered to explain the beginning of the crisis on Baikal :

- contamination by toxic agents,
- contamination by alien microorganisms,
- events of macroscopic scale.

All three reasons have probably contributed to the crisis, but the above results stress the role of alien microorganisms in the processes as perhaps the most important.

5. Conclusions

The tools from fractal theory provide a level of abstraction which is high. Too high to be certain about any interpretation in molecular terms. This level of abstraction in natural sciences becomes close to that of subjects like history or social sciences. Such reasoning allowed Mandelbrot to entitle the basic conclusions of fractal theory as the “Noah effect” and the “Joseph effect”, names borrowed from proverbs in the Bible. At this level of abstraction, one can say that the ecosystem of Baikal is strong and self-sustaining, but nevertheless any system of this kind is fragile and vulnerable. Once the processes of crisis have started, any kind of human intervention is unlikely to prevent the crisis continuing to develop.

But, one may hope that the ecosystem of Baikal, the greatest and most ancient lake on the planet, will remain self-sustaining at a deeper level. The observed signs of the adaptation of algae species to the severe situation of sponge disease give a hint as to how this resurrection of the ecosystem will take place in the near or distant future. Human intervention can be successful only if it is consistent with the processes of recovery which will anyway be continued naturally in the Lake.

And lastly, the methods used in this study are a case when a strategic question, the choice between global reasons for a crisis, can be partly resolved by the use of an experimental tools from molecular biology. But the qualitative analysis provided is obviously not precise enough to provide any suggestions about possible measures to minimize the scale and the damage of the crisis. It can only narrow the areas of interest and suggest some biological objects as a primary targets for a deeper and more extensive study at molecular level.

Acknowledgments

We thank Dr. N.G. Granin for his help with a collection and interpretation of time series data from temperature detectors, and Dr. Colin H Brown for a versatile support of our research activity.

This study was funded by budget projects of Federal Agency of Scientific Organizations number 0345-2016-0002 and Russian Foundation for Basic research (RFBR) grant numbers: 16-23 04-00065; 16-54-150007; 18-04-00224

References

Baldani J.I., Videira S.S., dos Santos Teixeira K.R. et al. 2014. The family Rhodospirillaceae. In: Rosenberg E., DeLong E.F., Lory S. et al. (Eds.), The Prokaryotes: Alphaproteobacteria and Betaproteobacteria. Berlin: Springer-Verlag, pp. 533–618. DOI:10.1007/978-3-642-30197-1_300.

Banerjee A., YakovenkoV.M. 2010. Universal patterns of inequality. New Journal of Physics 12. DOI:10.1088/1367-2630/12/7/075032

Bernardet J.F., Bowman J.P. 2006. The genus *Flavobacterium*. In: Dworkin M., Falkow S., Rosenberg E. et al. (Eds.), The Prokaryotes. Volume 7: Proteobacteria, Delta, Epsilon, subclass. New York: Springer, pp. 481–531.

Berry D.L., Goleski J.A., Koch F. et al. 2015. Shifts in cyanobacterial strain dominance during the onset of harmful algal blooms in Florida Bay, USA. Microbial Ecology 70: 361–371. DOI: 10.1007/s00248-014-0564-5.

Bormotov A.E. 2011. What has happened to Baikal sponges? Science First Hand 32: 20–23. (In Russian).

Briée C., Moreira D., López-García P. 2007. Archaeal and bacterial community composition of sediment and plankton from a suboxic freshwater pond. Research in Microbiology 158: 213–227. DOI: 10.1016/j.resmic.2006.12.012

Brown B.L., LePrell R.V., Franklin R.B. et al. 2015. Metagenomic analysis of planktonic microbial consortia from a non-tidal urban-impacted segment of James River. Standards in Genomic Sciences 10: 65. DOI: 10.1186/s40793-015-0062-5.

Caporaso J.G., Kuczynski J., Stombaugh J. et al. 2010. QIIME allows analysis of high-throughput community sequencing data. Nature Methods 7: 335–336. DOI: 10.1038/nmeth.f.303.

Chernogor L., Denikina N., Kondratov I. et al. 2013. Isolation and identification of the microalgal symbiont from primmorphs of the endemic freshwater sponge *Lubomirskia baicalensis* (Lubomirskiidae, Porifera). European Journal of Phycology 48: 497–508. DOI: 10.1080/09670262.2013.862306.

Choudhury J.D., Pramanik A., Webster N.S. et al. 2015. The pathogen of the great barrier reef sponge *Rhopaloeides odorabile* is a new strain of *Pseudoalteromonas agarivorans* containing abundant and diverse virulence-related genes. Marine Biotechnology 17: 463–478. DOI: 10.1007/s10126-015-9627-y.

Denikina N.N., Dzyuba E.V., Belkova N.L. et al. 2016. The first case of disease of the sponge *Lubomirskia baicalensis*: investigation of its microbiome. Translated in Biology Bulletin 43: 263–270. DOI: 10.1134/S106235901603002X.

Edgar R.C. 2010. Search and clustering orders of magnitude faster than BLAST. Bioinformatics 26: 2460–2461. DOI: 10.1093/bioinformatics/btq461.

Feranchuk S., Belkova N., Potapova U. et al. 2018a. Evaluating the use of diversity indices to distinguish between microbial communities with different traits. Research in Microbiology 169: 254–261. DOI: 10.1016/j.resmic.2018.03.004.

Feranchuk S., Belkova N., Chernogor L. et al. 2018b. The signs of adaptive mutations identified in the chloroplast genome of the algae endosymbiont of Baikal sponge. [version 1; referees: awaiting peer review]. F1000Research 7. DOI:10.12688/f1000research.15841.1

Gladkikh A.S., Kaluyzhnaya O.V., Belykh O.I. et al. 2014. Analysis of bacterial communities of two Lake Baikal endemic sponge species. Mikrobiology 83: 787–797. DOI: 10.1134/S002626171406006X

Harte D. 2001. Multifractals: theory and applications. London: Chapman & Hall.

Higuchi T. 1988. Approach to an irregular time series on the basis of the fractal theory. Physica D: Nonlinear Phenomena 31: 277–283.

Horňák K., Corno G. 2012. Every coin has a back side: invasion by *Limnohabitans planktonicus* promotes the maintenance of species diversity in bacterial communities. PLoS One 7. DOI: 10.1371/journal.pone.0051576.

Jelinek H.F., Fernandez E. 1998. Neurons and fractals: how reliable and useful are calculations of fractal dimensions? Journal of Neuroscience Methods 81: 9–18.

Jezberová J., Jezbera J., Znachor P. 2017. The *Limnohabitans* genus harbors generalistic and opportunistic subtypes: evidence from spatiotemporal succession in a canyon-shaped reservoir. Applied and Environmental Microbiology 83. DOI:10.1128/AEM.01530-17.

Kadnikov V.V., Mardanov A.V., Beletsky A.V. et al. 2012. Microbial community structure in methane hydrate-bearing sediments of freshwater Lake Baikal. FEMS Microbiology Ecology 79: 348–358. DOI: 10.1111/j.1574-6941.2011.01221.x.

Kaluzhnaya O.V., Itskovich V.B., McCormack G.P. 2011. Phylogenetic diversity of bacteria associated with the endemic freshwater sponge *Lubomirskia baicalensis*. World Journal of Microbiology and Biotechnology 27: 1955–1959. DOI: 10.1007/s11274-011-0654-1.

Karbauskaite R., Dzemuda G. 2016. Fractal-based methods as a technique for estimating the intrinsic dimensionality of high-dimensional data: a survey. Informatica 27: 257–281. DOI: 10.15388/Informatica.2016.84.

Khanaev I.V., Kravtsova L.S., Maikova O.O. et al. 2018. Current state of the sponge fauna (Porifera: Lubomirskiidae) of Lake Baikal: sponge disease and the problem of conservation of diversity. Journal of Great Lakes Research 44: 77–85. DOI:10.1016/j.jglr.2017.10.004.

Kulakova N.V., Sakirko M.V., Adelshin R.V. et al. 2018. Brown rot syndrome and changes in the bacterial community of the Baikal sponge *Lubomirskia baicalensis*. Microbial Ecology 75: 1024–1034. DOI: 10.1007/s00248-017-1097-5.

Luter H.M., Whalan S., Webster N.S. 2010. Exploring the role of microorganisms in the disease-like syndrome affecting the sponge *Ianthella basta*. Applied and Environmental Microbiology 76: 5736–5744. DOI: 10.1128/AEM.00653-10.

Mandelbrot B. 1960. The Pareto-Levy law and the distribution of income. International Economic Review 1: 79–106.

Mandelbrot B. 1967. How long is the coast of Britain? Statistical self-similarity and fractional dimension. Science 156: 636–638.

Manfredi R., Nanetti A., Ferri M. 1999. *Flavobacterium* spp. organisms as opportunistic bacterial pathogens during advanced HIV disease. Journal of Infection 39:146–52.

Marsac N.T., Houmard J. 1993. Adaptation of cyanobacteria to environmental stimuli: new steps towards molecular mechanisms. FEMS Microbiological Reviews 10: 119–189. DOI: 10.1016/0378-1097(93)90506-W.

O'Neil J.M., Davis T.W., Burford M.A., Gobler C.J. 2012. The rise of harmful cyanobacteria blooms: the potential roles of eutrophication and climate change. Harmful Algae 14: 313–334. DOI:10.1016/j.hal.2011.10.027.

Peng C.K., Buldyrev S.V., Havlin S. et al. 1994. Mosaic organization of DNA nucleotides. Physical Review E 49: 1685–1689.

Prinzón J.H., Kamel B., Burge C.A. et al. 2015. Whole transcriptome analysis reveals changes in expression of immune-related genes during and after bleaching in a reef-building coral. Open Science Journal 2. DOI: 10.1098/rsos.140214.

Pulkkinen K., Suomalainen L.R., Read A.F. et al. 2009. Intensive fish farming and the evolution of pathogen virulence: the case of columnaris disease in Finland. Proceedings of the Royal Society B: Biological Sciences 277: 593-600. DOI: 10.1098/rspb.2009.1659.

Richardson L.F. 1961. The problem of contiguity: an appendix to statistics of deadly quarrels. General systems: Yearbook of the Society for the Advancement of General Systems Theory 61: 139–187.

Saravia L.A. 2015. A new method to analyze species abundances in space using generalized dimensions. Methods in Ecology and Evolution 6: 1298–1310. DOI: 10.1111/2041-210X.12417.

Schloss P.D., Westcott S.L., Ryabin T. et al. 2009. Introducing mothur: open-source, platform-independent, community-supported software for describing and comparing microbial communities. Applied and Environmental

Microbiology 75: 7537–7541. DOI: 10.1128/AEM.01541-09.

Seuront L. 2015. On uses, misuses and potential abuses of fractal analysis in zooplankton behavioral studies: A review, a critique and a few recommendations. Physica A: Statistical Mechanics and its Applications 432: 410–434. DOI: 10.1016/j.physa.2015.03.007.

Stabili L., Cardone F., Alifano P. et al. 2012. Epidemic mortality of the sponge *Ircinia variabilis* (Schmidt, 1862) associated to proliferation of a *Vibrio* bacterium. Microbial Ecology 64: 802–813. DOI: 10.1007/s00248-012-0068-0.

Taylor M.W., Radax R., Steger D. et al. 2007. Sponge-associated microorganisms: evolution, ecology, and biotechnological potential. Microbiology and Molecular Biology Reviews 71: 295–347.

Timoshkin O.A., Samsonov D.P., Yamamuro M. et al. 2016. Rapid ecological change in the coastal zone of Lake Baikal (East Siberia): is the site of the world's greatest freshwater biodiversity in danger? Journal of Great Lakes Research 42: 487–497. DOI:10.1016/j.jglr.2016.02.011.

Våge S., Thingstad T.F. 2015. Fractal hypothesis of the pelagic microbial ecosystem can simple ecological principles lead to self-similar complexity in the pelagic microbial food web? Frontiers in Microbiology 6. DOI: 10.3389/fmicb.2015.01357.

Walsh K., Haggerty J.M., Doane M.P. 2017. Aura-biomes are present in the water layer above coral reef benthic macro-organisms. PeerJ 5. DOI: 10.7717/peerj.3666.

Wang H., Luo S., Luo T. 2017. Fractal characteristics of urban surface transit and road networks: Case study of Strasbourg, France. Advances in Mechanical Engineering 9: 1–12. DOI: 10.1177/1687814017692289.

Webster N.S., Negri A.P., Webb R.I. et al. 2002. A spongin-boring α-proteobacterium is the etiological agent of disease in the great barrier reef sponge *Rhopaloeides odorabile*. Marine Ecology Progress Series 232: 305–309. DOI: 10.3354/meps232305.

Webster N.S., Thomas T. 2016. The sponge hologenome. MBio 7. DOI: 10.1128/mBio.00135-16.

Willems A. 2014. The family Comamonadaceae. In: Rosenberg E., DeLong E.F., Lory S. et al. (Eds.), The prokaryotes: Alphaproteobacteria and Betaproteobacteria. 4th edition. Berlin: Springer-Verlag, pp. 777–851.

Xu Y., Wang Y., Tao X. et al. 2017. Evidence of Chinese income dynamics and its effects on income scaling law. Physica A: Statistical Mechanics and its Applications 147: 143–152. DOI: 10.1016/j.physa.2017.06.020.

Yakovenko V.M., Rosser J.B. 2009. Statistical mechanics of money, wealth, and income. Reviews of Modern Physics 81. DOI:10.1103/RevModPhys.81.1703

Limnology and Freshwater Biology 2018 (2): 135-140 DOI:10.31951/2658-3518-2018-A-2-135

Original Article

ISSN 2658-3518
LIMNOLOGY FRESHWATER BIOLOGY
www.limnolfwbiol.com

The effects of sound pollution as a stress factor for the Baikal coregonid fish

Sapozhnikova Yu.P.[1,*], Gasarov P.V.[2], Makarov M.M.[1], Kulikov V.A.[3,4], Yakhnenko V.M.[1], Glyzina O.Yu.[1], Tyagun M.L.[1], Belkova N.L.[1], Wanzenböck Jo.[5], Sullip M.K.[6], Sukhanova L.V.[1]

[1] *Limnological Institute, Siberian Branch of the Russian Academy of Sciences, Ulan-Batorskaya Str., 3, Irkutsk, 664033, Russia*
[2] *Irkutsk State University, Irkutsk 664003, Russia*
[3] *Skolkovo Institute of Science and Technology, Moscow 143026, Russia*
[4] *Institute of Automation and Electrometry, Siberian Branch of the Russian Academy of Sciences, Novosibirsk 630090, Russia*
[5] *Research Institute for Limnology Mondsee, University of Innsbruck, A-5310 Mondsee, Austria*
[6] *ICAR-National Bureau of Fish Genetic Resources, Telibagh, Lucknow 226 002, India*

ABSTRACT. We have studied morphological features of the hearing epithelium affected and unaffected by increased long-term sound (at 160 dB re 1 μPa) on the example of the Baikal omul (Coregonidae, *Coregonus migratorius*). The sensory epithelium was analyzed using the 3D confocal laser scanning techniques. We observed local epithelium damages in the rostral, central and caudal regions of the saccule, e.g. sticking stereocilia, vacuolization and round shape gaps. This article discusses the reasons for the local effects of sound on different regions of the sensory epithelium. We assume that using of morphological screening of sensory acoustic system in the artificial rearing of the Baikal coregonid fishes under the conditions of intense noise could contribute to indicating the most stress-resistant forms, which are promising for high-tech industrial aquaculture, and developing more gentle approaches to its creation.

Keywords: Lake Baikal, sound as a stress factor, hair cells, sensory epithelium, Baikal omul

1. Introduction

The study of fish hearing and their acoustic behavior is important due to increasing effects of sound pollution on fish in their natural habitat (Hastings et al., 1996; Popper and Hastings, 2009; Ladich, 2013; Sapozhnikova, 2018). Intensive production of fish in aquaculture also involves the use of equipment, such as aerators, air and water pumps, combines, blowers, and filtration systems, which increase the noise level in fish storage tanks (Wysocki et al., 2007). Constant exposure to intense noise levels can adversely affect the cultivated species. Possible consequences include impairment of hearing sensitivity, increased stress, and reduced growth rates (Popper and Hastings, 2009). As a result, the acoustic conditions of larvae maintaining during artificial reproduction of fish populations determine their further survival and population replenishment. After their release into the wildlife, they use their sensory organs in order to locate direction, select suitable habitat, settle at locations with sufficient shelter, and avoid the immediate attention of many voracious predators (Montgomery et al., 2006; Caiger et al., 2012).

Fish estimate the locomotion of their body in the acoustic field relative to the otoliths in the inner ears, the utricle, saccule, and lagena (Popper, 2011; Ladich and Schulz-Mirbach, 2016). Nevertheless, the saccule has the main auditory load in many fishes (Zhongmin and Xu, 2002). Sagitta is usually larger than other parts of the labyrinths in these fishes; the removal of both sagittae sharply reduces the auditory sensitivity (Lu and Xu, 2002). These results demonstrate that the saccule plays significant roles in hearing and frequency distinction. In addition, the largest diversity in ultrastructural features for teleosts is characteristic of the saccule (Platt and Popper, 1981; Popper and Coombs, 1982; Popper and Fay, 1999; Sapozhnikova et al., 2017).

The saccular otoliths lag in their locomotion relative to the fish body in the acoustic field and thus stimulate the sensory saccular cells by deflecting their ciliary (hair) bundles (Fig. 1). This mediated process limits the detectable frequencies to a few hundred hertz and restricts the sound intensities to higher levels (Schuijf and Hawkins, 1976; Bradbury and Vehrencamp, 2011).

Lake Baikal was previously suggested as an ideal location for investigation of the application of ocean sound propagation models and assessment of

*Corresponding author.
E-mail address: jsap@mail.ru (Yu.P. Sapozhnikova)

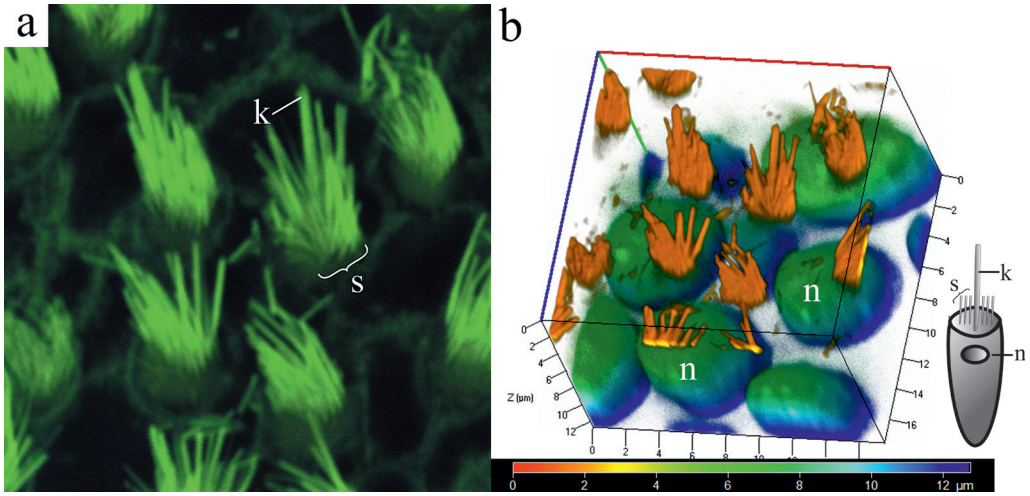

Fig. 1. Sensory epithelium of the Baikal omul (LSM 710, Carl Zeiss): a – sensory elements on the surface of the epithelium; b – 3D model of sensory epithelium. k – kinocilium, s – stereocilia, n – nucleus.

hearing adaptations in hydrobionts (Glotin et al., 2017). Although some sounds are natural for Lake Baikal (ice crackle, natural gas seepages, surf noise in the splash zone, voices of seals and birds), now, there is often a cacophony of transient and continuous man-made sound from boating, shipping, construction, nearby roadways, tunnels, etc. Thus, another question is whether these sounds potentially interfere with the behavior of fish populations. The greatest effect may result from acoustic masking which would shorten the distances over which animals can detect sounds of biological importance, for example, from potential predators (Engas et al., 1996; Hawkins et al., 2014; Hughes et al., 2014; Voellmy et al., 2014; Glotin et al., 2017).

The fish with high hearing characterstics may be affected by this noise up to a distance of several hundred meters (Amoser et al., 2004; Ladich, 2013), but fish lacking hearing characterstics, such as lacustrine and riverine coregonid fishes, would be affected predominantly at close distance, which is also typical for aquaculture cultivation.

Among Baikal coregonid fishes, omul is more popular for growing in aquaculture, particularly due to the reduction of its populations in the natural conditions and the introduction of a ban on its catch in 2017 for Lake Baikal. Omul is one of the most important species to the subsistence fisheries throughout the world, including Lake Baikal (Tallman and Reist, 1997; Smirnov et al., 2009; Sukhanova et al., 2017).

Therefore, this study was aimed at the evaluation of long-term effects of increased sound on the auditory epithelium of the Baikal omul. In previous studies, control hearing thresholds showed that coregonid fishes (on the example of broad whitefish Coregonus nasus Pallas, 1776) had far less sensitive hearing and broader bandwidth of hearing than other investigated fish (Popper et al., 2005). This was expected, since the coregonid fish is not a member of the superorder Otophysi, a group of hearing specialists that have a set of bones, the Weberian ossicles, which acoustically couple the swim bladder to the saccule of the inner ear. The initial analysis of hearing sensitivity in coregonid fish showed that they could detect sounds up to 1600 Hz (Popper et al., 2005). However, they have a very poor hearing at 1600 Hz. Therefore, in our work the specimens were exposed to the 500 and 1 kHz tones at 160 dB re 1 µPa, which are within the range of hearing of this species and are usually observed in artificial cultivation.

2. Materials and methods

The study objects were adult specimens of the artificially obtained Baikal omul (Coregonidae, *Coregonus migratorius*). Coregonid fishes was artificially inseminated under controlled conditions of the Unique Facility «Experimental Freshwater Aquarium Complex of Baikal Hydrobionts» at the Limnological Institute Siberian Branch of the Russian Academy of Sciences.

To conduct the evaluation experiments of the effects of increased sound on the auditory organs of the Baikal fish under the conditions of the Aquarium Complex, the installation consisting of two round pools with a diameter of 2 m and a height of 0.5 m was constructed. These two pools were located in separate rooms. One pool had the control fish (without the sound stimulation) and another one had sound-exposed fish (an experimental pool). In both pools, fish were maintained with daily 50% water changes. The walls of the pools were made of plastic.

Tone signals with the frequencies of 500 Hz and 1 kHz (corresponding to determined ranges of acoustic sensitivity) at 160 dB re 1 µPa were generated through a portable computer using the Sound Forge program (Fig. 2). The sound was radiated continuously for 18 days in the experimental pool. After the amplifier, the signal was fed to the UW30 Electro-Voice hydroacoustic emitter with operating frequencies of 100 Hz – 100 kHz and nameplate capacity of 120 W. The emitter was set under the water at half the depth of the experimental pool for noise-exposed fish. The form and intensity of the emitted signal were controlled using the RESON TC 4013 piezoceramic transducers. After the linear amplifier, the signal from the transducer was fed to the LCard E-440D analog-digital converter. The amplitude and frequency analysis were carried out using the specialized LCard PowerGraph software. The sensitivity of fish to the sound signal was determined visually and

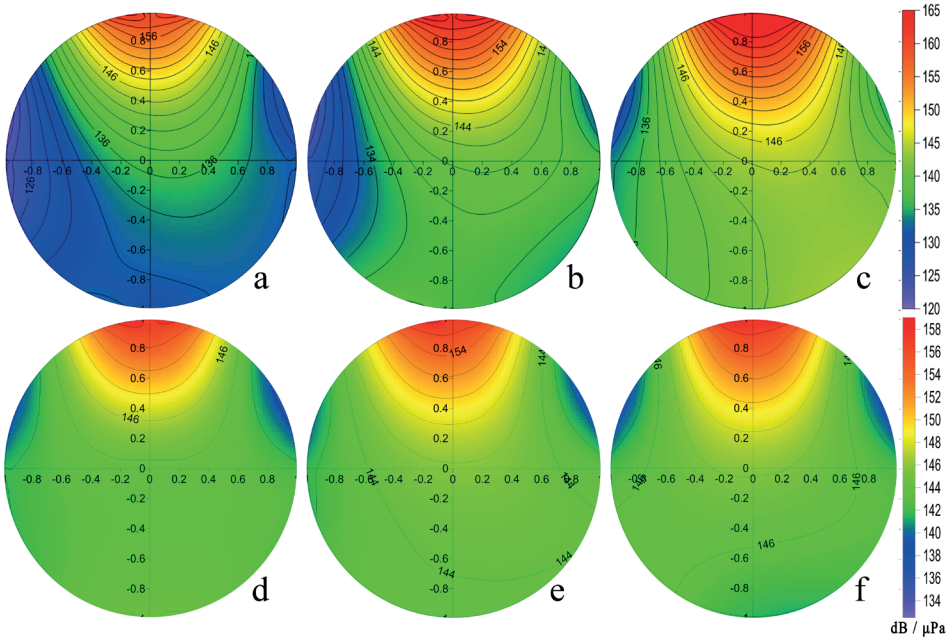

Fig. 2. Uneven sound field of 500 Hz (a, b, c) and 1 kHz (d, e, f) in the horizontal plane, scale in dB / μPa: a, d – the surface, b, e – half the depth, and c, f - the bottom.

by the EthoStudio density maps, as well as by activity of the specimens and a positive reaction to a certain acoustic signal (active movements and jerks) (Kulikov et al., 2014).

Fish from both experimental and control pools were collected with a dip-net, euthanized by using clove oil (0.02-0.05 ml / l, a sedative, contains eugenol) and killed by cutting the spine in accordance with Guidance on the use of clove oil as an anesthetic in aquaculture (Mikodina et al., 2011) and the American Veterinary Medical Association (AVMA) Guidelines for Euthanasia (2013).

Immediately prior to the preparation of the auditory organ samples, the cranium was opened from the ventral side, the brain was removed, the ear capsules were uncovered, the right and left labyrinths were extracted, and the saccule was removed together with the sagitta (otolith). Hair cell bundle loss was determined using laser confocal scanning microscopy LSM 710 (Carl Zeiss).

Histological processing of the samples with sensory epithelium was performed according to the standard technique (Klimenkov et al., 2018). The sensory epithelium was fixed for 30 min in a 2% paraformaldehyde (Sigma-Aldrich Co. LLC, USA, Cat. No. 158127) solution in 0.1 M phosphate buffer (pH 7.4) and permeabilized for 20 min in 0.25% Triton™ X-100 (Sigma-Aldrich Co. LLC, USA, Cat. No. T8787). Actin microfilaments were stained for 40 min with FITC-Phalloidin (Sigma-Aldrich Co. LLC, USA, Cat. No. P5282). The nuclei were stained for 15 min with DAPI (Sigma-Aldrich Co. LLC, USA, Cat. No. D9542). Functionally active mitochondria were stained with MitoTracker® Orange CMTMRos (Termo Fisher Scientifc Inc., USA, Cat. No. M7510) by 25-min incubation in medium 199 with Hank's salts (Kompaniya PanEko, Russia, Cat. No. S230p); the medium contained 100–500 nM dye at 37 °C. After each step, the samples were washed three times in Hank's solution without phenol red (PanEko, Russia, Cat. No P020p). The stained samples were mounted on glass slides in ProLong® Gold Antifade Mountant (Termo Fisher Scientifc Inc., USA, Cat. No. P36930) and covered with a coverslip. The slides were analyzed using a Carl Zeiss LSM 710 laser confocal microscope; Plan-Apochromat 20 × /0.8 and 63× /1.40 Oil DIC M27; lasers: track 1, 405 nm: 3.0%; track 2, 488 nm: 3.0%; track 3, 561 nm: 3.0%.

The morphometric analysis yielded 10-50 images of each macula along the length and depth (depending on the length of the epithelium) at an interval of 30 μm. The density of hair cells on the macula, the length of sensory elements (kinocilium and stereocilia) and hair cell bundle loss were measured using program Image-Pro Plus.

To classify hair cells, cluster analysis was used, in particular, k-means and hierarchical clustering, using the Statistica 8.0 program. Quantitative similarity indicator of hair cells belonging to the same cluster was calculated from the lengths of the kinocilia (k) and the maximum length of the stereocilia (s). Statistical processing of the obtained data was carried out using the single-factor analysis of variance in the R Project. The Kruskal-Wallis test was used for the verification of the null hypothesis.

3. Results and discussion

Confocal scanning microscopy revealed regional distinctions in native hair cells of fish based on the different density of hair cells in central and caudal regions of the epithelium, as well as the presence of different types of cells in these regions. The mean density of the intact hair cells in the rostral region was 571500 ± 8975 cells/mm2, M ± m in the Baikal omul. In the central region of the macula, hair cells were considerably distant from each other. The hair cells of the caudal region were located more densely.

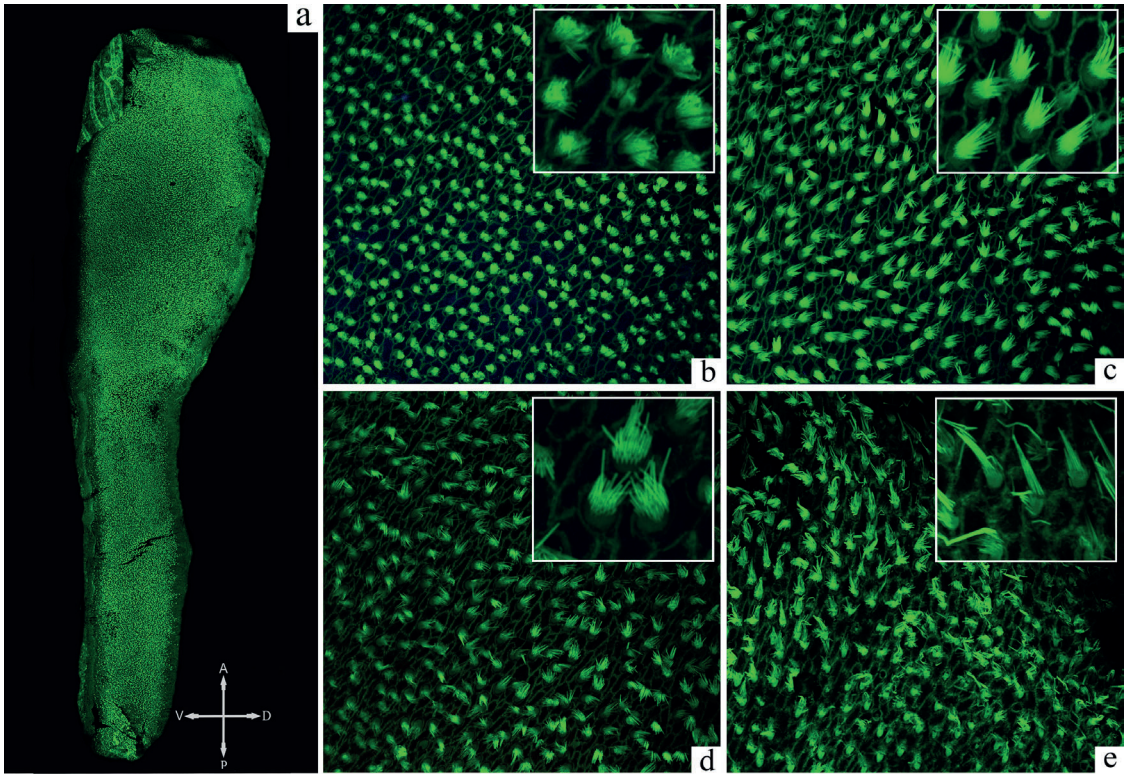

Fig. 3. Different types of the sensory saccular cells in Baikal omul: a – general view of the saccule; b – k3s2 type; c – k6s5 type; d – k7s2 type; e – k11s4 type. k – kinocilium, s – stereocilia. Orientation of the saccule: V – ventral, D – dorsal, A – anterior (rostral), P – posterior (caudal). LSM 710, Carl Zeiss.

Cluster analysis combined sensory cells into classes (types) in such a way that similar cells were included in one class. The length of kinocilium (k) and maximum length for stereocilium in one sensory bundle (s) were the most significant characteristics for the integration of sensory cells into different clusters (designation for cilia was used by Platt and Popper (1981)). These most variable characteristics were regarded as criteria for identification of types of sensory saccular cells. Four cell morphotypes were identified in the Baikal omul, k3s2, k6s5, k7s2, and k11s4 (Fig. 3).

These hair cell types vary across the peripheral, rostral, central and caudal areas of the saccule. The cell types k3s2, k6s5, k7s2, and k11s4 were the most typical for the peripheral and caudal areas of the saccule. The type k7s2 was found in the rostral region of the saccule. Finally, in the central region of the saccule, we identified the cell types k3s2 and k7s2. Thus, in the Baikal omul cells, stereociliar and kinociliar length varies by location: shorter stereocilia are more characteristic of the central and rostral regions of the saccule, longer stereocilia were found in the peripheral and caudal regions of the saccule.

In the course of the experiment on the increased acoustic stimulation of the Baikal omul, there were no exposure effects on mortality. The swim bladders were intact in all experimental and control specimens. But after confocal scanning of sensory hearing epithelium, we found varieties of local epithelial damages: rounded ruptures emerging on the surface of the epithelium, the coalescence of stereocilia described previously for other animals damaged by highly intense sound or ototoxic antibiotics (Wysocki et al., 2007). Damage of various parts of the sensory epithelium of the inner ear occurs unevenly. The hair cell bundle loss in the Baikal omul was individual and varied in different parts of the rostral, central, and caudal regions, at the saccule of each fish. In some specimens, the damages are represented by small foci, in other ones significant areas were injured. However, there were some patterns: the damaged areas were localized and usually varied as a function of exposure sound frequency. The cell damages were minimal at 1 kHz. The small areas of damaged hair cells were observed throughout the epithelium, and, primarily, in the central and rostral areas.

Visible changes in the epithelium occurred only on the 10th day of the experiment at 500 Hz, and then gradually depending on the day of stimulation: evident vacuolization was registered on the 10th day; obvious ruptures of the sensory epithelium were observed on the 18th day after the onset of sound stimulation (Fig. 4).

The zones of saccular hair cell loss were larger for fish exposed to 500 Hz (up to 44% in the different parts of the peripheral area on the 10th day after the onset of sound stimulation). This tone destroyed hair cells predominantly in the peripheral part with the largest cell injuries occurring in the caudal region (Fig. 4g-i). The destructive changes occurred in the hair cells on the 18th day after the onset of sound stimulation (up to 60% in the different parts of the peripheral area) (Fig. 4j-l). Thereby, there was a hypothesis about the tone selectivity in different areas of the auditory epithelium with the different cell types (Hawkins and Sand, 1977; Smith et al., 2011; Sapozhnikova et al., 2016). The changes in cells of the different saccular

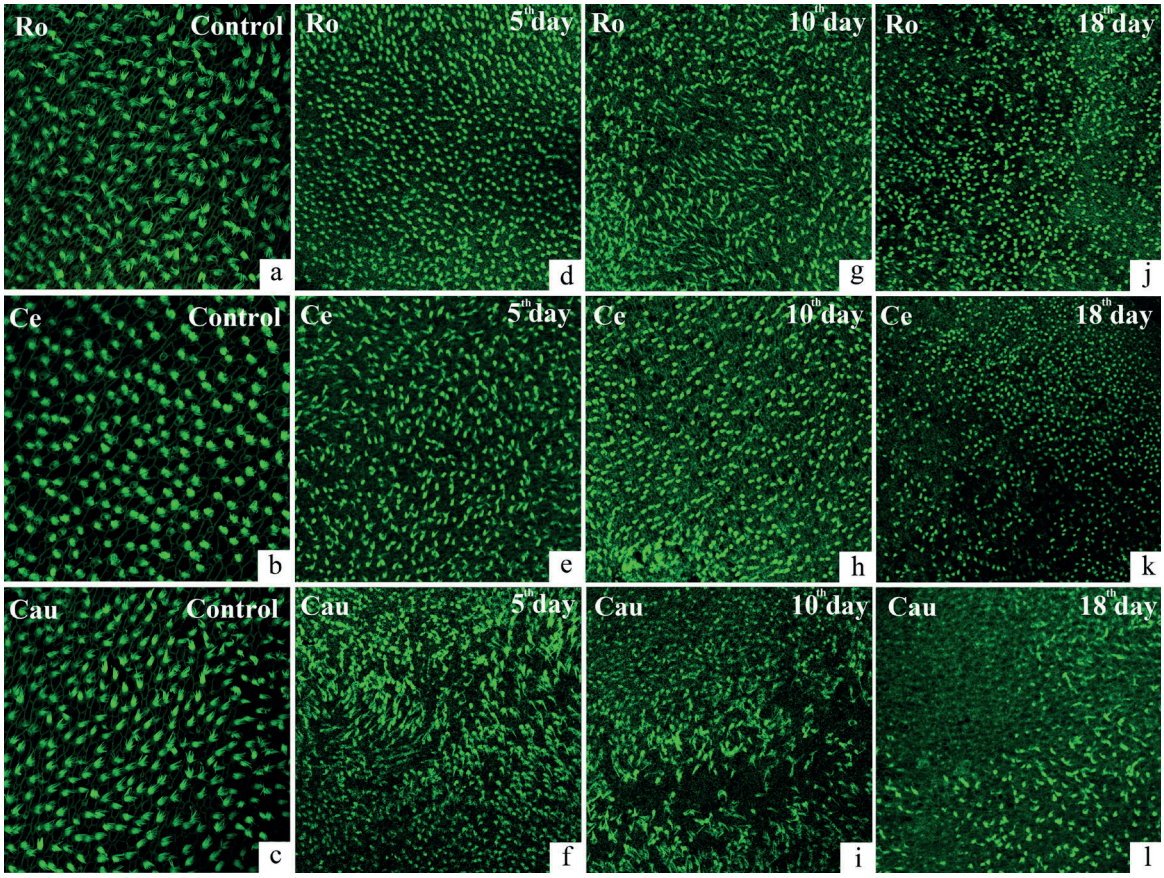

Fig. 4. Images obtained by LSM 710 (Carl Zeiss) showing hair cells destructive changes in the Baikal omul due to stimulation by increased sound (500 Hz, 160 dB) in rostral (Ro), central (Ce) and caudal (Cau) regions of the saccule: a-b – control; d-f – epithelium after 5 days of sound exposure; g-i – epithelium after 10 days of sound exposure; j-l – epithelium after 18 days of sound exposure.

regions are likely to be a result of their damages due to the increased stimulation by various sounds, which confirms the involvement of these regions in the perception of relevant frequency sound oscillations.

4. Conclusions

The obtained results can be used for further study of the acoustic communication of the Baikal fishes, including conditions of acoustic pollution. Unfortunately, anthropogenic increased sound under natural conditions may dramatically reduce acoustic communication of fish reducing their ability to acoustically detect incoming hazards (Hastings et al., 1996; Popper and Hastings, 2009; Ladich, 2013). As it was previously shown, 50% of aquatic noise is generated by 15% of ships, and in some coastal and other high-traffic areas, ship noise has reached levels that degrade habitat for endangered species (Glotin et al., 2017). In particular, prolonged exposure to noise leads to stress, which may affect the nervous and immune systems of hydrobionts (Popper and Hastings, 2009).

The conducted experiment allows us to successfully record the response of specimens to the presence of sensitivity to a particular sound signal, including increased sound evoking anxiety. Moreover, the experiments, in which the increased acoustic stimulation caused a different degree of hair cell damages in different regions of the macula, presumably showed the existence of the regions with different tonal specialization in the auditory maculae of the Baikal omul. So far, we can make only preliminary conclusions about the presence of tonotopic specialization in different regions of the epithelium in coregonid fishes. However, a better understanding of the physiological processes causing cell damage and regeneration, which affect the behavior and lead to stress under the influence of different acoustic effects, requires additional studies. This work may be ultimately used to mitigate the effects of increased sounds on fish in aquaculture or in the natural environment, and contribute to the development of new approaches for the management of lake environment.

Acknowledgements

We are grateful to Yuliya Vitushenko (LIN SB RAS) for her valuable assistance in preparing the manuscript. Ethological and morphological screening of coregonid fish was performed at the LIN SB RAS Collective Instrumental Center (http://www.lin.irk.ru/copp/eng/) using the Unique Facility «Experimental Freshwater Aquarium Complex of Baikal Hydrobionts» supported by RFBR and the Government of the Irkutsk Region, projects Nos. 17-44-388081 r_a and 17-44-388106 r_a, and within the framework of the State Task No. 0345-2016-0002 (AAAA-A16-116122110066-1) «Molecular Ecology and Evolution of Living Systems ...». Aquaculture of coregonid fish was obtained within the framework of the project of the Government of the

Irkutsk Region «Obtaining a High-Tech Aquaculture of Whitefish ...» (Youth Forum Baikal-2020).

References

Amoser S., Wysocki L.E., Ladich F. 2004. Noise emission during the first powerboat race in an Alpine lake and potential impact on fish communities. Journal of the Acoustical Society of America 116: 3789–3797. DOI: 10.1121/1.1808219

Bradbury J.W., Vehrencamp S.L. 2011. Principles of animal communication. 2nd Edn. Sunderland: Sinauer Associates Inc. Publishers.

Caiger P.E., Montgomery Jo.C., Radford C.A. 2012. Chronic low-intensity noise exposure affects the hearing thresholds of juvenile snapper. Marine Ecology Progress Series 466: 225–232. DOI: 10.3354/meps09933

Engas A., Lokkeborg S., Ona E. et al. 1996. Effects of seismic shooting on local abundance and catch rates of cod (Gadus Morhua) and haddock (*Melanogrammus aeglefinus*). Canadian Journal of Fisheries and Aquatic Sciences 53: 2238–2249. DOI: 10.1139/f96-177

Glotin H., Poupard M., Marxer R. et al. 2017. Big data passive acoustic for Baikal Lake soundscape and ecosystem observatory [B2O]. Toulon: DYNI CNRS LSIS team. (in Russian)

Hastings M.C., Popper A.N., Finneran J.J. et al. 1996. Effect of low frequency underwater sound on hair cells of the inner ear and lateral line of the teleost fish *Astronotus ocellatus*. Journal of the Acoustical Society of America 99: 1759–1766. DOI: 10.1121/1.414699

Hawkins A.D., Sand O. 1977. Directional hearing in the median vertical plane by the cod. Journal of Comparative Physiology A 122: 1–8. DOI: 10.1007/BF00611244

Hawkins A., Roberts L., Cheesman S. 2014. Responses of free-living coastal pelagic fish to impulsive sounds. Journal of the Acoustical Society of America 135: 3101–3116. DOI: 10.1121/1.4870697

Hughes A.R., Mann D.A., Kimbro D.L. 2014. Predatory fish sounds can alter crab foraging behavior and influence bivalve abundance. Proceedings of the Royal Society B 281. DOI: 10.1098/rspb.2014.0715

Klimenkov I.V., Sudakov N.P., Pastukhov M.V. et al. 2018. Rearrangement of actin microfilaments in the development of olfactory receptor cells in fish. Scientific Reports 8. DOI: 0.1038/s41598-018-22049-7

Kulikov V.A., Sapozhnikova Yu.P., Kirilchik S.V. et al. 2014. Algorithms for quantitative analysis of the behavior of the Baikal omul under experimental conditions. In: V All-Russian Conference Fish Behavior, pp. 131–136. (in Russian)

Ladich F. 2013. Effects of noise on sound detection and acoustic communication in fishes. In: Brumm H. (Ed.), Animal communication and noise. Berlin: Springer, pp. 65–90.

Ladich F., Schulz-Mirbach T. 2016. Diversity in fish auditory systems: one of the riddles of sensory biology. Frontiers in Ecology and Evolution 4. DOI: 10.3389/fevo.2016.00028

Lu Z., Xu Z. 2002. Effects of saccular otolith removal on hearing sensitivity of the sleeper goby (*Dormitator latifrons*). Journal of Comparative Physiology A 188: 595–602. DOI: 10.1007/s00359-002-0334-6

Mikodina E.V., Sedova M.A., Pyanova S.V. et al. 2011. Aquaculture. Issue 6. Guidance on the use of an anesthetic “clove oil” in aquaculture. Moscow: VNIRO Publishing House. (in Russian)

Montgomery J.C., Jeffs A.G., Simpson S.D. et al. 2006. Sound as an orientation cue for the pelagic larvae of reef fishes and decapod crustaceans. Advances in Marine Biology 51: 143–196. DOI: 10.1016/S0065-2881(06)51003-X

Platt C., Popper A.N. 1981. Fine structure of the ear. Hearing and sound communication in fishes. New York: Springer-Verlag, pp. 3–38.

Popper A.N. 2011. Auditory system morphology. In: Farrell A.P. (Ed.), Encyclopedia of fish physiology: from genome to environment. Amsterdam: Academic Press, pp. 252–261.

Popper A.N., Coombs S. 1982. The morphology and evolution of the ear in actinopterygian fishes. American Zoologist 22: 138–143.

Popper A.N., Fay R.R. 1999. The auditory periphery in fishes. In: Fay R.R., Popper A.N. (Eds.), Comparative hearing: fish and amphibians. New York: Springer Verlag, pp. 43–100.

Popper A.N., Hastings M.C. 2009. The effects of anthropogenic sources of sound on fishes. Journal of Fish Biology 75: 455–489.DOI: 10.1111/j.1095-8649.2009.02319.

Popper A.N., Ramcharitar J., Campana S.E. 2005. Why Otoliths? Insights from inner ear physiology and fisheries biology. Marine and Freshwater Research 56: 497–504. DOI: 10.1071/MF04267

Sapozhnikova Yu.P. 2018. Fish hearing. Science First Hand 80: 80–91. (in Russian)

Sapozhnikova Yu.P., Belous A.A., Makarov M.M. et al. 2017. Ultrastructural correlates of acoustic sensitivity in Baikal coregonid fishes. Fundamental and Applied Limnology 189: 267–278. DOI: 10.1127/fal/2017/0810

Sapozhnikova Yu.P., Klimenkov I.V., Khanaev I.V. et al. 2016. Ultrastructure of saccular epithelium sensory cells of four sculpin species (Cottoidei) of Lake Baikal in relation to their way of life. Journal of Ichthyology 56: 289–297. DOI: 10.1134/S0032945216010136

Schuijf A., Hawkins A.D. 1976. Sound reception in fish. Amsterdam, Oxford, New York: Elsevier Scientific Publishing Company.

Smirnov V.V., Smirnova-Zalumi N.S., Sukhanova L.V. 2009. Microevolution of Baikal omul: *Coregonus autumnalis migratorius* (Georgi). Novosibirsk: Publishing House of the SB RAS. (in Russian)

Smith M.E., Schuck J.B., Gilley R.R. et al. 2011. Structural and functional effects of acoustic exposure in goldfish: evidence for tonotopy in the teleost saccule. BMC Neuroscience 12: 1–16. DOI: 10.1186/1471-2202-12-19

Sukhanova L., Politov D., Wanzenbock Jo. et al. 2017. Biology and management of Coregonid fishes. Fundamental and Applied Limnology 189: 177–179. DOI: 10.1127/fal/2017/1028

Tallman R.F., Reist J.D. 1997. Information requirements for fishery management and overview of scientific approach. Canadian Technical Report of Fisheries and Aquatic Sciences 2193: 53–62.

Voellmy I.K., Purser J., Simpson S.D. et al. 2014. Increased noise levels have different impacts on the anti-predator behavior of two sympatric fish species. PLoS ONE 9: e102946. DOI: 10.1371/journal.pone.0102946

Wysocki L.E., Davidson III J.W., Smith M.E. et al. 2007. Effects of aquaculture production noise on hearing, growth, and disease resistance of rainbow trout *Oncorhynchus mykiss*. Aquaculture 272: 687–697. DOI: 10.1016/j.aquaculture.2007.07.225

Zhongmin L., Xu Z. 2002. Effects of saccular otolith removal on hearing sensitivity of the sleeper goby (*Dormitator latifrons*). Journal of Comparative Physiology 188: 595–602. DOI: 10.1007/s00359-002-0334-6

Limnology and Freshwater Biology 2018 (2): 141-143 DOI:10.31951/2658-3518-2018-A-2-141

Short communication

ISSN 2658-3518
LIMNOLOGY FRESHWATER BIOLOGY
www.limnolfwbiol.com

Phytoplankton assemblages of the Southern Baikal in 1990-1995 and 2016-2018

Vorobyeva S.S.

Limnological Institute, Siberian Branch of the Russian Academy of Sciences, Ulan-Batorskaya Str., 3, Irkutsk, 664033, Russia

ABSTRACT. At present, the littoral zone of the Southern Baikal is under anthropogenic impact. The negative changes in underwater vegetation landscapes most dramatically appeared near the Listvyanka settlement. In this study, we compare phytoplankton assemblages from the surface layer (ca. 1.5 m depth) near the Listvyanka settlement collected during 1990-1995 and 2016-2018. We have compared phytoplankton data with solar irradiance and air temperatures. Phytoplankton community was represented by 70 taxa, where Bacillariophyta and Cryptophyta dominated the biomass. In 2016-2018, there were no significant differences in biomass or abnormal seasonal vegetation of the studied phytoplankton taxa compared to 1990-1995

Keywords: phytoplankton assemblage, species-dominant, Lake Baikal

1. Introduction

Over the past decade (Timoshkin et al., 2018), negative changes take place in the littoral zone of Lake Baikal. Dramatic examples of these changes are an expansion of green algae Spirogyra and a disease of Baikal sponge (Belikov et al., 2018; Khanaev et al., 2018; Timoshkin, 2018). On the other hand, there is no clear evidence of drastic changes in chemical and hydrological condition in this zone (Khodzher et al., 2017; 2018). In this study, we compared phytoplankton from the shallow zone of the Southern Baikal collected during 1990-1995 and 2016-2018. Unlike 2016-2018, the 1990-1995 period can be characterized by a low anthropogenic impact. In addition, a solar activity also differed in these periods. In this regard, this study was aimed at the investigation of phytoplankton diversity.

2. Materials and Methods

The studied area (ca. N51˚52', E104˚49') of Lake Baikal was near the settlement Listvyanka (head of the Angara River). Phytoplankton was sampled between January-December during 1990-1995 and 5-10 June and September during 2016-2018. The samples were collected with bathometer and net (using the Juday net with a 110 μm mesh). The samples were fixed with the Utermöhl-solution and concentrated by sedimentation. The concentrate was placed into a 0.1 mL cell and examined under a Amplival (Carl Zeiss, Germany) microscope at two magnifications. At 800x magnification, net species and nanoplankton were identified, and at 2000x magnification – picoplankton. Phytoplankton was analyzed following the techniques from Starmach (1985), Round et al. (1990), Glezer et al. (1992). Cell counts were converted to algal biomass taking an average individual cell volume measured according to Makarova and Pichkily (1970) and Belykh et al. (2011).

3. Results and Discussion

3.1 Phytoplankton assemblage in 1990-1995

Phytoplankton assemblage comprised 70 taxa and their species. Amount of phytoplankton changed from 0.015 to 136 million cells L^{-1} with biomass of 0.004-2.13 g m^{-3}. Diatoms (20 taxa) were represented by *Aulacoseira baicalensis, A. islandica, Cyclotella minuta, C. baicalensis, Nitzschia graciliformis, Synedra acus* subsp. *radians* and *Stephanodiscus meyeri*. *Gyrodinium helveticum, Gymnodinium baicalense, Peridinium baicalense* and *Glenodinium* sp. dominated Dinophyta. *Rhodomonas pusilla* (up to 6064 thousand cells L^{-1}) dominated Cryptophyta. Chrysophyta were formed by *Chrysochromulina parva* (up to 6439 thousand cells L^{-1}) and *Dinobryon cylindricum* (up to 192 thousand cells L^{-1}). Chlorophyta was represented by *Monoraphidium contortum, M. arcuatum, Koliella longiseta* and *Chlamydomonas* sp.

Diatoms and Cryptophyta in biomass were dominant in phytoplankton assemblage, 23.6 and 46.2%, respectively (Fig. 1). In general, the bulk of Cyanophyta vegetation occurred during summer; however, the ratio of their biomass was almost 100 % in January-Marth 1993 (Fig. 2).

*Corresponding author.
E-mail address: lana@lin.irk.ru

3.2 Phytoplankton assemblage in 2016-2018

Diatoms and Cryptophyta were also dominant, but their species composition changed compared to 1990-1996. Thus, the cell number of *A. baicalensis, N. graciliformis* and *C. baicalensis* was minor. For example, *N. graciliformis* reduced from 53-9490 thousand cells L^{-1} to 1.1 thousand cells L^{-1}, and *R. pusilla* – from 6064 thousand cells L^{-1} to 669 thousand cells L^{-1}. On the contrary, *S. acus* subsp. *radians* and *Chlamydomonas* sp. increased up to 46 and 72 thousand cells L^{-1}. In general, species with small-sized cells dominated in 2016-2018.

3.3 Correlation with climate parameters

We have compared phytoplankton data with solar insolation and air temperatures. The first vegetation of Baikal phytoplankton occurs under ice in March-April (Bondarenko et al., 2012). The depth of snow cover on the ice also is important for plankton vegetation, since sunlight penetration depends on this parameter (Jewson et al., 2008). However, we did not find an increase in phytoplankton taxa during the ice periods. The studied periods were observed from maximum to minimum in the 22nd solar cycle and declined in the 24th cycle (Fig. 3). In addition, solar irradiance during 2016-2018 was lower than in 1996-1998. There is an obvious positive correlation between solar irradiance and ultraviolet index (Fig. 3). We assume that high phytoplankton vegetation most likely happens at high ultraviolet index. However, it was not observed in the maximum of the 22nd cycle (1990-1992). Moreover, phytoplankton biomass was minimal during this period.

Despite the changes in the diatom plankton taxa, in 2016-2018 there were no significant differences in biomass or an abnormal seasonal vegetation of the studied phytoplankton taxa compared to 1990-1995. In this regard, we have not detected current negative changes in the phytoplankton community of the Southern Baikal.

4. Conclusions

We have compared phytoplankton taxa of the Southern Baikal collected in 2016-2018 with those of 1990-1995. Spring phytoplankton in 2016-2018 was characterised by an increase in *Synedra acus* subsp. *radians* and *Dinobryon cylindricum,* while large cells of *A. baicalensis* and *A. islandica* were minor. Diatoms and Cryptophyta were dominant in the biomass of phytoplankton assemblage during these periods. Increase in phytoplankton biomass was observed at low solar irradiance. In 2016-2018, there were no significant differences in biomass or an abnormal seasonal vegetation of the studied phytoplankton taxa compared to 1990-1995.

Acknowledgements

This study was supported by the basic funding within the projects Nos. 0345–2016–0006 (AAAA-A16-116122110063-0), RFBR-17-29-05016

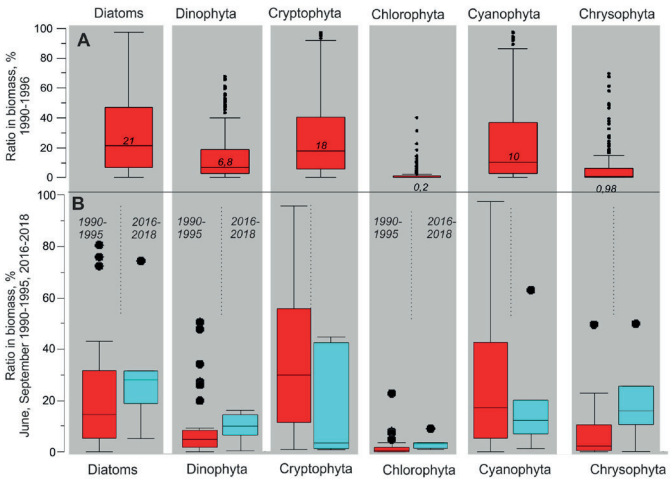

Fig. 1. Amount of phytoplankton taxa according to their biomass. The panel A (red) is the period of 1990-1995, the panel B –June and September of 1990-1995 (red) and 2016-2018 (bluish)

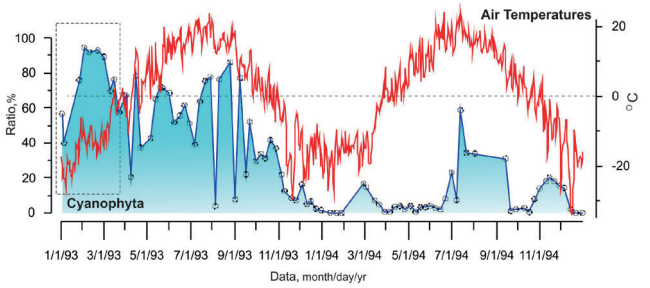

Fig. 2. Seasonal vegetation of Cyanophyta in comparison with air temperatures of 1993-1994

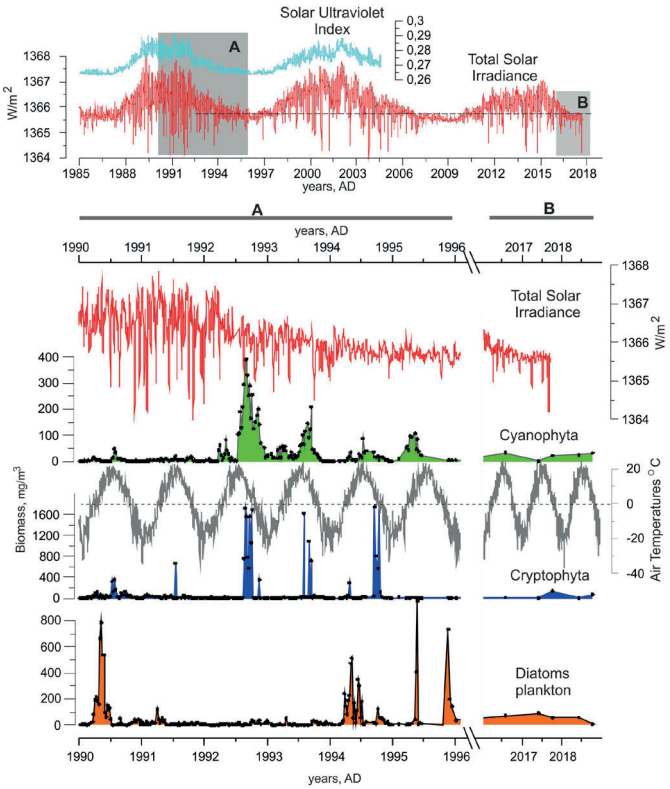

Fig. 3. Distribution of main phytoplankton taxa and changes in solar irradiance (Fröhlich, 2006), ultraviolet index (Viereck and Puga, 1999) and air temperatures during 1990-2018

References

Belikov S.I., Feranchuk S.I., Butina T.V. et al. 2018. Mass disease and mortality of Baikal sponges. Limnology and Freshwater Biology 1: 36–42. DOI: 10.31951/2658-3518-2018-A-1-36

Belykh O.I., Bessudova A.Yu., Gladkikh A.S. et al. 2011. Guidelines for the determination of biomass of species of phytoplankton in pelagic zone in Lake Baikal. Irkutsk: Irkutsk University publisher. (In Russian)

Bondarenko N.A., Belykh O.I., Golobokova L.P. et al. 2012. Stratified distribution of nutrients and extremophile biota within freshwater ice covering the surface of Lake Baikal. The Journal of Microbiology 50: 8–16. DOI: 10.1007/s12275-012-1251-1

Fröhlich C. 2006. Solar irradiance variability since 1978. Space Science Reviews 125: 53–65.

Jewson D.H., Granin N.G., Zhdanov A.A. et al. 2008. Resting stages and ecology of the planktonic diatom *Aulacoseira skvortzowii* in Lake Baikal. Limnology and Oceanography 53: 1125–1136.

Khanaev I.V., Kravtsova L.S., Maikova O.O. et al. 2018. Current state of the sponge fauna (Porifera: Lubomirskiidae) of Lake Baikal: Sponge disease and the problem of conservation of diversity. Journal of Great Lakes Research 44: 77–85. DOI: 10.1016/j.jglr.2017.10.004

Khodzher T.V., Domysheva V.M., Sorokovikova L.M. et al. 2017. Current chemical composition of Lake Baikal water. Inland Waters 7: 250–258. DOI: 10.1080/20442041.2017.1329982

Khodzher T.V., Domysheva V.M., Sorokovikova L.M. et al. 2018. Hydrochemical studies in Lake Baikal: history and nowadays. Limnology and Freshwater Biology 1: 2–9. DOI: 10.31951/2658-3518-2018-A-1-2

Makarova I.V., Pichkily L.O. 1970. To some aspects of how to measure phytoplankton biomass. Botanical Journal 10: 1488–1494. (In Russian).

Round F.E., Crawford R.M., Mann D.G. 1990. The Diatoms. Biology and morphology of the genera. Cambrige: Cambrige University Press.

Starmach K. Chrysophyceae und Haptophyceae. 1985. In: Pascher A. (Ed.) Subwasserflora von Mitteleuropa. Bd. 1 Jena: VEB Gustav Fischer Verlag. (In German)

The diatoms of the USSR (fossil and recent). II (2). 1992. In: Glezer S.I., Makarova I.V., Moisseeva A.I., Nikolaev V.A. (Eds.). SPb: Nauka. (In Russian).

Timoshkin O.A. 2018. Coastal zone of the world's great lakes as a target field for interdisciplinary research and ecosystem monitoring: Lake Baikal (East Siberia). Limnology and Freshwater Biology 1: 81–97. DOI: 10.31951/2658-3518-2018-A-1-81

Timoshkin O.A., Moore M.V., Kulikova N.N. et al. 2018. Groundwater contamination by sewage causes benthic algal outbreaks in the littoral zone of Lake Baikal (East Siberia). Journal of Great Lakes Research 44: 230–244. DOI: 10.1016/j.jglr.2018.01.008

Viereck R., Puga L. C. 1999.The NOAA Mg I1 core-to-wing solar index: Construction of a 20-year time series of chromospheric variability from multiple satellites. Journal of Geophysical Research 104: 9995-10005.

Limnology and Freshwater Biology 2018 (2): 144-149 DOI:10.31951/2658-3518-2018-A-2-144

Original Article

ISSN 2658-3518
LIMNOLOGY FRESHWATER BIOLOGY
www.limnolfwbiol.com

Population monitoring of *Epischura baikalensis* Sars, 1900 in Maloye More Strait (Lake Baikal)

Sheveleva N.G.[1,*], Penkova O.G.[2], Makarkina N.V.[2]

[1] *Limnological Institute, Siberian Branch of the Russian Academy of Sciences, Ulan-Batorskaya Str., 3, Irkutsk, 664033, Russia*
[2] *Irkutsk State University, Karl Marx Str., 1, Irkutsk, 664003, Russia*

ABSTRACT. The article presents the long-term observations data (1997-2017) on the population dynamics of the endemic planktonic copepod *Epischura baikalensis* in Maloye More Strait (Lake Baikal) under new environmental conditions, such as global climate warming, low water level period and increased anthropogenic load. We give a full description of the morphological features of females and males. We show that, like in the open pelagic zone of the lake, the population of *E. baikalensis* inhabiting Maloye More Strait has two generations in the year cycle. Epishura plays a leading role in the zooplankton quantitative indicators of the strait, which is typical for Lake Baikal in the whole. The values of the abundance and biomass of the epishura population in Maloye More Strait for the period of our observations fit into the amplitude of the long-term oscillations typical of open Baikal.

Keywords: morphology, biology, long-term dynamics, Epischura baikalensis, Maloye More Strait (Lake Baikal)

1. Introduction

Long-term seasonal spatial dynamics of zooplankton in the open pelagic zone of Lake Baikal is well studied. The bulk of Baikal zooplankton is rotifers and crustaceans. The endemic copepod *Epischura baikalensis* Sars is the most important representative of crustaceans, which comprises up to 80-90 % of the number and biomass of zooplankton. An analysis of the population dynamics of epishura is necessary for the sustainability of the ecological system in the lake (Kozhova, 1971; 1991; Kozhova and Pavlov, 1985). According to Kozhova (1991), zooplankton monitoring should be based on the investigations of the spatial and temporal variability of the structure populations of dominant species. Obviously, the contribution of some groups and species to the total number and their different dependence on water temperature determine the long-term dynamics of zooplankton. Endemic epishura prefers the cold waters of open Baikal, where it dominates throughout the year, and it appears in bays and sors of the lake only in the ice and spring periods. However, now, in addition to the natural environmental factors that determine the functioning of the planktonic community, there are new ones with the unknown consequences. They are global warming and low water level period (Kuimova et al., 2015). Since 2011, there has been an increase in water temperature over most of the Baikal water area (Shimaraev et al., 2015). Most current publications show a change in the structure of the Baikal zooplankton in the summer towards an increase in thermophilic species (Hampton et al., 2008; Pislegina and Zilov, 2009; Izmesteva et al., 2016; Bondarenko and Logacheva, 2017).

Since the beginning of the century, the anthropogenic load on the Baikal ecosystem has been significantly increasing, which has primarily affected the shallow zone of the lake. Maloye More Strait now exhibits the enhanced recreational pressure. According to the recent data, the ecological crisis is developing in the vast shallow waters of the strait (Timoshkin et al., 2015). In the past and this century, special studies on the state of the epishura population have been sporadic and not numerous (Afanasyeva, 1973; 1977a; Kozhov and Pomazkova, 1973; Pavlov and Pislegina, 2004; Pislegina et al., 2004; Pislegina, 2010; Sheveleva and Penkova, 2018), and, in particular, such data are not available for Maloye More Strait. In 1997, we have initiated regular studies of zooplankton in the southern part of Maloye More Strait that are still ongoing (Sheveleva and Penkova, 2005; 2018; Sheveleva et al., 2009).

This work is aimed at the analysis of long-term dynamics of quantitative indicators of the *E. baikalensis* population and the characteristics of its life cycle in Maloye More Strait under new environmental conditions.

*Corresponding author.
E-mail address: shevn@lin.irk.ru (N.G. Sheveleva)

2. Materials and methods

Studies of long-term dynamics of quantitative indicators of the *E. baikalensis* population were conducted in the open part of Maloye More Strait (53°05'20,7''N; 106°54'38,7''E) in 1997 – 2017. Samples were taken from May to October in the daytime, and only in 2002 the sampling was additionally carried out in the ice period (March). Zooplankton was collected by the Juday net (diameter of openings was 37.5 cm and mesh widths were 100μm). The upper 25-m layer was caught above a depth of more than 100 m. At the same time, the surface water temperature and transparency were measured. Laboratory investigations were carried out according to the standard method (Kozhova and Melnik, 1978). In the epishura population, all stages of development (orthonauplii, metanauplii, copepodite instars and adults) were calculated. To calculate the zooplankton biomass, individual weights shown for Baikal organisms were used (Kozhova and Melnik, 1978).

The total number and biomass of all zooplankton, as well as the epishura population, were calculated as arithmetic averages over a period of May-October for each year separately.

To study the morphology of crustaceans, a Philips SEM 525M (Philips, Holland) scanning microscope was used. Copepods were photographed on the basis of the Collective Instrumental Center "Ultramicroanalysis" at the Limnological Institute of the Siberian Branch of RAS.

3. Results and discussion

There is a species description and images of appearance, details of the structure of the fifth leg in female and male as well as the structure of the oral appendages of epishura (Sars, 1900; Garber, 1941; Afanasyeva, 1977b; 1995). There are detailed schemes of habit view and description of nauplial stages, from stage 1 to stage 6 (Afanasyeva, 1977a; 1995). Later publications discussed particular study issues: the morphology and structure of the mandibles in four epishura species, including Baikal species (Naumova et al., 2015; Zaidykov, 2016). The analysis of mitochondrial genes (COI) resolved the issue of a single population in Lake Baikal (Zaidykov et al., 2015). Our studies using scanning electron microscopy (SEM) have added a description of morphological parts of adult male and female epishura. We have shown the armament of maxillipeds and maxillules (Fig. 1D, 1E). We have also shown the armament of female spines on the exopodite II (Exp II). These spines are covered with small sensory spines located vertically and horizontally (Fig. 1G, 1H). In male, the surface of the abdomen segments 2 and 3 has a dotted pattern (Fig. 2C), below which, on segment 5, there is a rounded plate-like protuberance with five peaks (Fig. 2B). The fifth leg of male is asymmetric; the left leg (Fig. 2E 1; 2F) is much larger than the right one (Fig. 2E 2, 2D). Basipodite (Bsp) of the right leg in the distal part is wide with 3-4 small spinelets (Fig. 2D). The distal part of exopodite (Exp) of the right leg is blunt ending with a small spine (Fig. 2G, 2H, 2I) and indented plate.

According to Kozhov (1962) and Afanasyeva (1977b; 1995), during a year epishura produces two generations in the pelagic zone of Lake Baikal. Our data have shown that in Maloye More Strait epishura also has two generations in the year cycle (Fig. 3). In the ice period, nauplii represented up to 100% of the winter and spring epishura population. However, already in mid-June with a temperature of less than 5°C the copepodite instars dominated the population. Moreover, the bulk was copepodites of instars I-II (36%) and III-IV (14%). Additionally, there were copepodites of instar V and adults. In July, we observed the second peak of the nauplii number due to the summer generation (Fig. 3). Like in open Baikal, in Maloye More Strait, the summer population develops faster than the winter and spring one. Since mid-August and September, already late copepodites (72-74%) dominated plankton, and adults appeared. At the end of September and in October, the winter and spring generation began to regress. In Maloye More Strait, as in the open pelagic zone of the lake, epishura of all instars can be found at any time of the year. According to Kozhov (1962) and Afanasyeva (1995), this is due to the fact that during the year the epishura population has two generations, and females lay eggs in portions. In such conditions, copepods of several litters represent each generation. Therefore, we have shown that in Maloye More Strait, like in the open pelagic zone (Afanasyeva, 1977a; 1995), *E. baikalensis* has two generations during the year.

Based on long-term observations (1997-2017), we have shown that epishura was the bulk of zooplankton in Maloye More Strait (Fig 4). Previously, Kozhov (1962) and Afanasyeva (1977a) indicated that the optimum water temperature for epishura development is 7°C; therefore, it is rather natural to expect its maximum abundance during the colder season. Thus, during the ice and early spring periods its share was up to 75-85 % of the total number and up to 90% of the total mass. During the ice-free period (May-November), the long-term share of epishura in the abundance of zooplankton community was 19–71%. We recorded relatively maximum abundance of epishura (83%) in 2012 (Fig. 4). In the general series of observations, the exception was the usual temperature regime of 1999 as well as warm 2002 (Pislegina and Zilov, 2009). In these years, rotifers and the *Cyclops kolensis* population dominated the fauna of plankton. The share of epishura was less than 1-2% of the total zooplankton number.

The long-term dynamics of quantitative indicators of epishura in Maloye More Strait was oscillatory, which is typical for Baikal in the whole. The 1997 and 2013 observations stand out of the general series, in which the epishura abundance decreased to the minimum values (0.5-1.7 thousand individuals per m^3). At the same time, we indicated three peaks of the epishura abundance (2001, 2008 and 2012) with a maximum of 23.6 thousand individuals per m^3 in 2001. Based on the data on annual mean value of weighted average water temperature, 2001 was referred to as a cold year (Kiprushina and Izmestieva, 2009), and 2008

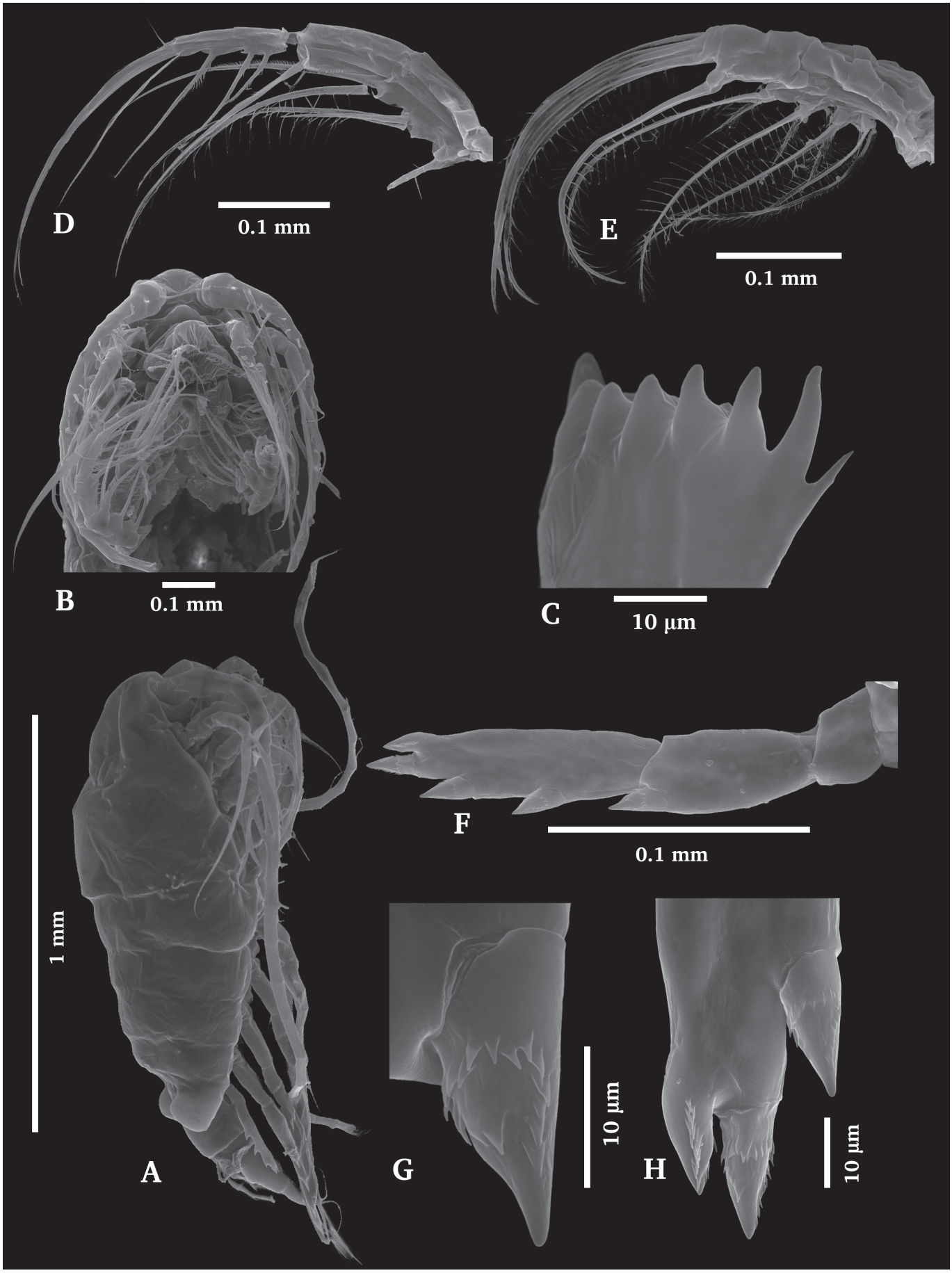

Fig. 1. *Epischura baikalensis*, female. A – lateral view; B – cephalothorax, ventral view; C – mandible; D – maxilliped; E – maxilla; F – P5 leg of female; G – armament of distal spine of Exp II of P5; H – armament of all other spines of Exp II of P5.

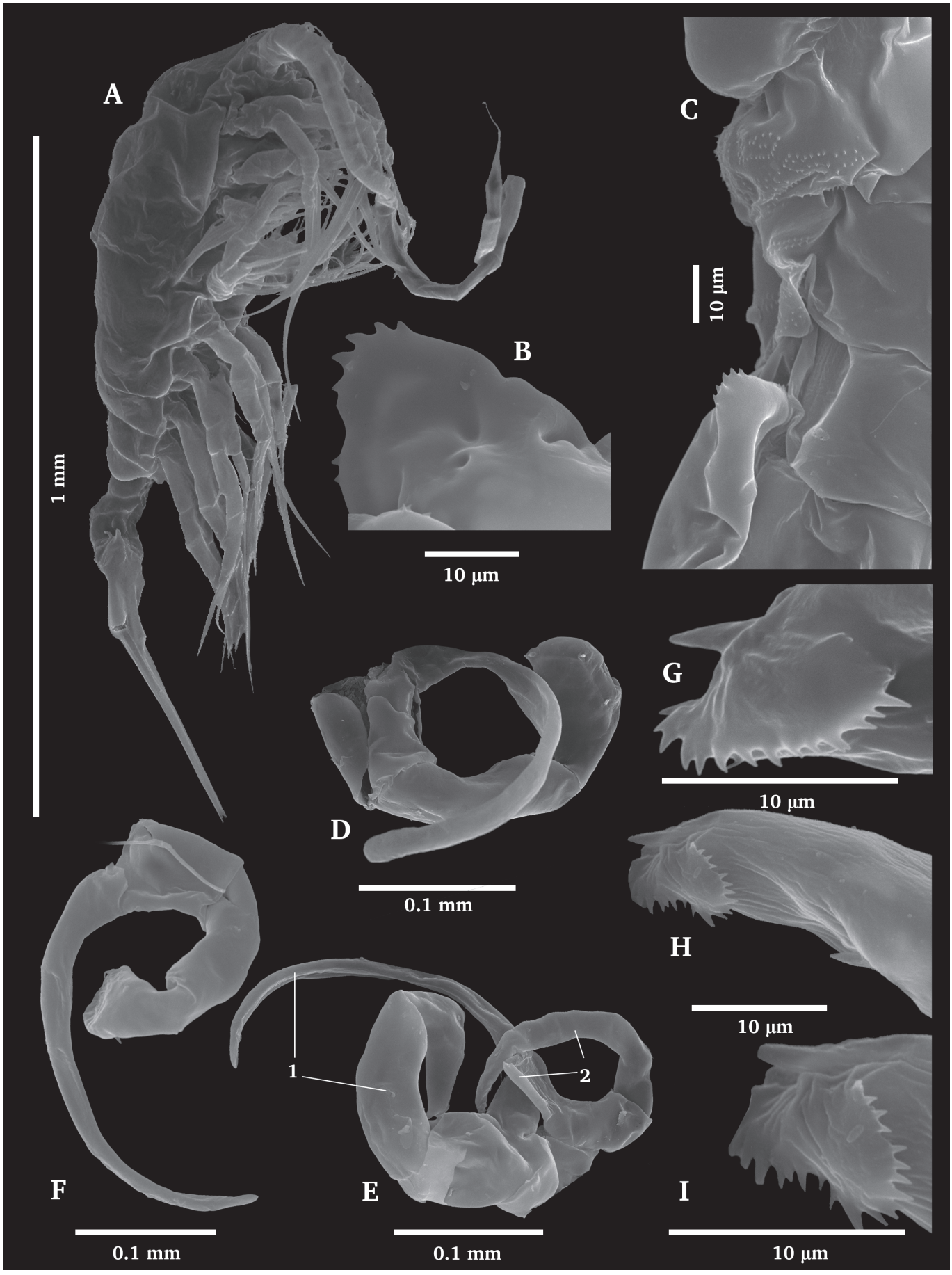

Fig. 2. *Epischura baikalensis*, male. A – lateral view; B – abdomen projection on segment 5; C – armament of abdomen segments 2 and 3 with a protuberance on abdomen segment 5; D – right P5 leg; E – P5 (1– left leg; 2 – right leg); F – left P5 leg; G, H, I – armament of the apical part of Exp of the right leg.

and 2012 were warm years (Sheveleva and Penkova, 2018). The previous statistical data proved that epishura abundance poorly depends on water temperature (Sheveleva et al., 2009). In general, the long-term dynamics of the epishura population in Maloye More Strait fully reflects the changes in the abundance of the whole zooplankton in this part of Lake Baikal and demonstrates the emerging trend of a decrease in both, the total number and the epishura population, since 2013.

The confirmation of the above assumptions requires further control of the Baikal endemic epishura.

4. Conclusions

The analysis of the long-term dynamics of quantitative data on the *E. baikalensis* population in Maloye More Strait over a period of our research (1997-2017) fits into the amplitude of the long-term indicators and is comparable with the data for 1951 (Vilisova, 1959) and 1961-1974 (Afanasyeva, 1977a). *E. baikalensis* plays a leading role in the abundance and biomass of zooplankton, which is typical for Lake Baikal in the whole.

We have shown that, like in the open pelagic zone of the lake, in Maloye More Strait, the *E. baikalensis* population has two generations in the year cycle.

Long-term studies of quantitative indicators of epishura for the ice-free period have shown three peaks in its development, which were observed in the cold (2001) and warm (2008, 2012) years. Over 20 years of observation, maximum density of epishura was indicated in 2001, when it was 23.6 thousand individuals per m^3.

Acknowledgements

The authors are very grateful to E.A. Dolid for the design of figures 1 and 2, and Yu.M. Vitushenko for the translation of the article into English.

The processing of material and preparation of this article was partially supported by the project No. 0345-2016-0010 (AAAA-A16-116122110062-3) “The Influence of Changing Natural and Anthropogenic Factors on Biochemical Processes on the Stony Littoral of Lake Baikal”.

References

Afanasyeva E.L. 1973. The abundance and biomass of zooplankton in Lake Baikal in the 0–50 m layer. In: Smirnov N.N. (Ed.), Long-term indicators of zooplankton development in lakes. Moscow, pp. 176–178. (in Russian)

Afanasyeva E.L. 1977a. Composition, number and production of zooplankton (1961-1974). In: Florence O.N. (Ed.), Biological productivity of the pelagic zone of Lake Baikal and its variability. Novosibirsk, pp. 39–61. (in Russian)

Afanasyeva E.L. 1977b. Biology of Baikal epishura. Novosibirsk: Science. (in Russian)

Afanasyeva E.L. 1995. Copepods of Copepoda subclass, suborder Calanoida. In: Timoshkin O.A. (Ed.), Guide and key to pelagic animals of Baikal. Novosibirsk, pp. 365–405. (in

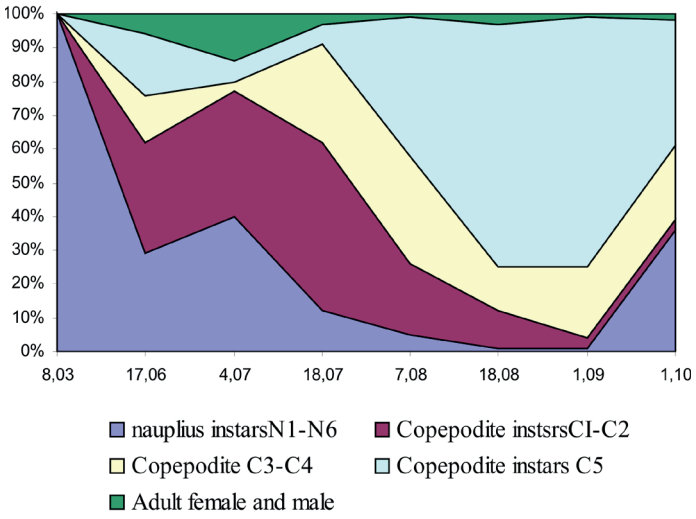

Fig. 3. Structure of population (%) of *Epischura baikalensis* in Maloye More Strait.

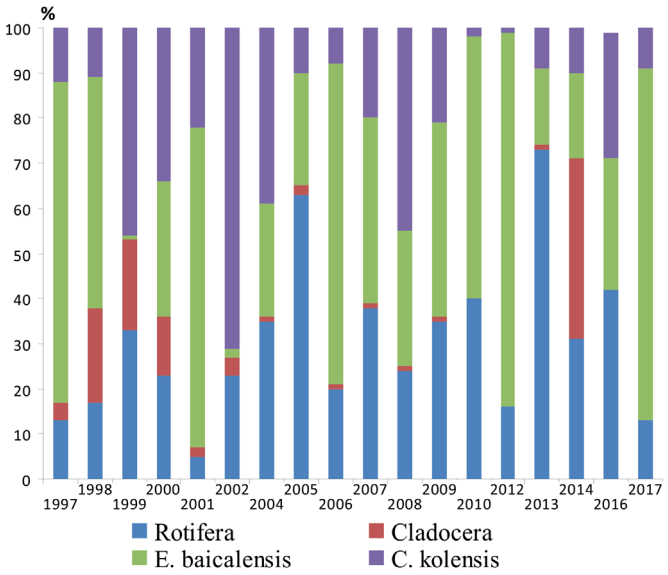

Fig. 4. Contribution (%) of some taxonomic groups (rotifers, cladocerans, copepods) and *E. baikalensis* to the total zooplankton number.

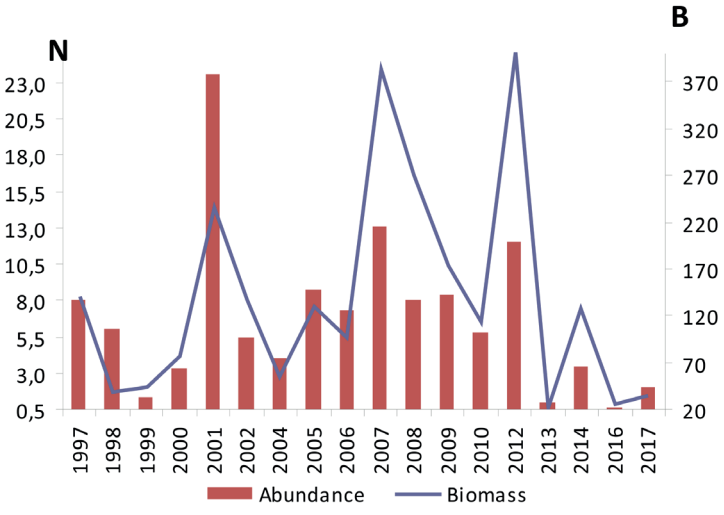

Fig. 5. Long-term dynamics of abundance (A, 10^3 ind. m^{-3}) and biomass (B, mg m^{-3}) of the *E. baikalensis* in the open part of Maloye More Strait.

Russian)

Bondarenko N.A., Logacheva N.F. 2017. Structural changes in phytoplankton of the littoral zone of Lake Baikal. Hydrobiological journal 53: 16–24. DOI: 10.1615/HydrobJ.v53.i2.20

Garber B.I. 1941. Postembryonic development of *Epischura baikalensis* Sars. Izvestiya Akademii Nauk SSSR. Seriya biologicheskaya [Bulletin of the USSR Academy of Sciences. Biological sciences] 1: 106–114. (in Russian)

Hampton S.E., Izmesteva L.R., Moore M.V. et al. 2008. Sixty years of environmental change in the world's largest freshwater lake – lake Baikal, Siberia. Global Change Biology 14: 1–12. DOI: 1365-2486.2008.01616.x

Izmesteva L.R., Moore M.V., Hampton S.E. et al. 2016. Lake-wide physical and biological trends associated with warming in Lake Baikal. Journal of Great Lakes Research 42: 6–17. DOI: 10.1016/j.jglr.2015.11.006

Kiprushina K.N., Izmestieva L.R. 2009. Long-term and seasonal dynamics of zooplankton in the open part of southern Baikal. Bulletin of Tomsk State University 327: 202–207. (in Russian)

Kozhov M.M. 1962. Biology of Lake Baikal. Moscow: Academy of Sciences USSR. (in Russian)

Kozhov M.M., Pomazkova G.I. 1973. Lake Baikal. In: Smirnov N.N. (Ed.), Long-term indicators of zooplankton development in lakes. Moscow, pp. 133–178. (in Russian)

Kozhova O.M. 1971. Some modern problems of hydrobiological study of Siberia in connection with anthropogenization of water bodies. In: Kozhova O.M. (Ed.), Studies of hydrobiological regime of water bodies in East Siberia. Irkutsk, pp. 10–16. (in Russian)

Kozhova O.M. 1991. The problem of monitoring zooplankton. In: Israel Yu.A., Anokhin Yu.A. (Eds.), Monitoring of Lake Baikal. Leningrad, pp. 209–222. (in Russian)

Kozhova O.M., Melnik N.G. 1978. Instructions for processing samples by counting method. Irkutsk: ISU. (in Russian)

Kozhova O.M., Pavlov B.K. 1985. Ecological monitoring. Principles and methods. In: Kozhova O.M. (Ed.), Improving regional monitoring of Lake Baikal. Leningrad, pp. 22–37. (in Russian)

Kuimova L.N., Yakimova N.I., Sherstyankin P.P. 2015. Trends in climatic changes in temperature and ice conditions of Lake Baikal and the Arctic according to the observed data. In: 6th International Vereshchagin Baikal Conference, p. 34. (in Russian)

Naumova E.Yu., Zaidykov I.Yu., Tauson V.L. et al. 2015. Features of the fine structure and Si content of the mandibular gnathobase of four freshwater species of *Epischura* (Copepoda: calanoida). Journal of Crustacean Biology 35: 741–746. DOI: 10.1163/1937240X-00002385

Pavlov B.K., Pislegina E.V. 2004. Population assessment of *Epischura baikalensis* Sars in Lake Baikal for the implementation of environmental monitoring. In: 1st International symposium "Baikal. Current state of surface and underground hydrosphere of mountain countries", pp. 120–123. (in Russian)

Pislegina E.V., Pavlov B.K., Zilov E.A. 2004. Temporal variability of abundance and biomass of the Baikal zooplankton edifier species *Epischura baikalensis* Sars. In: 1st International symposium "Baikal. Current state of surface and underground hydrosphere of mountain countries", pp. 123 – 127. (in Russian)

Pislegina E., Zilov E. 2009. Long-tern dynamics of Baikal zooplankton and clime change. In: 13th World Lake Conference, pp. 110–111.

Pislegina E.V. 2010. Dynamics of pelagic zooplankton in Southern Baikal for 2007–2008. In: Problems of ecology. Workshop in the memory of Professor M.M. Kozhov, p. 92. (in Russian)

Sars G.O. 1900. On *Epischura baikalensis*, a new Calanoid from Baikal Lake. Ezhegodnik Zoologicheskago muzeya Imperatorskoy akademiy nauk [Yearbook of the Zoological museum of the Academy of Sciences] 5: 226 – 238.

Sheveleva N.G., Penkova O.G. 2005. Zooplankton in the southern part of Maloye More Strait (Lake Baikal). Inland Water Biology 4: 42–49. (in Russian)

Sheveleva N.G., Penkova O.G., Kiprushina K.N. 2009. Long-term dynamics of zooplankton abundance in open part of Maloye More Strait (Lake Baikal). Izvestiya Irkutskogo Gosudarstvennogo Universiteta [The Bulletin of Irkutsk State University] 2: 18–22. (in Russian)

Sheveleva N.G., Penkova O.G. 2018. Changes of the zooplankton community in Maloye More Strait during 20 years. In: International Conference «Freshwater Ecosystems – Key Problems», pp. 331–332.

Shimaraev M.N., Sinyukovich V.N., Sizova L.N. et al. 2015. Changes in the ice-thermal and water regime of Lake Baikal in 1950-2014. In: 6th International Vereshchagin Baikal Conference, p. 34. (in Russian)

Timoshkin O.A., Malnik V.V., Sakirko V.M. et al. 2015. Ecological crisis in the coastal zone of Lake Baikal. In: 6th International Vereshchagin Baikal Conference, pp. 40–42. (in Russian)

Vilisova I.K. 1959. Zooplankton of Maloye More Strait. Trudy Baikalskoi limnologicheskoi stantsii AN SSSR [Proceedings of the Baikal Limnological Station of the Academy of Sciences of the USSR] 17: 275–312. (In Russian)

Zaidykov I.Y. 2016. Why does the cleaner of Lake Baikal need dental crowns? Science First Hand 44: 57–60.

Zaidykov I.Y., Mayor T.Y., Sukhanova L.V. et al. 2015. MtDNA polymorphism of Lake Baikal Epischura – an endemic key species of the plankton community. Russian Journal of Genetics 9: 1087–1090. DOI: 10.1134/S102279541508013X